MOLECULAR GENETICS OF USHER SYNDROME -INHERITED DEAFNESS AND BLINDNESS

HANNA VÄSTINSALO

Department of Medical Genetics
University of Helsinki
Finland

Folkhälsan Institute of Genetics
Helsinki, Finland

ACADEMIC DISSERTATION

To be presented, with the permission of the Faculty of Medicine of the University of Helsinki, for public examination in the Folkhälsan lecture hall Arenan, Topeliuksen katu 20, Helsinki, 11.11.11 at 12 noon.

Helsinki 2011

Supervisors: Eeva-Marja Sankila, MD, PhD
Department of Ophthalmology
Helsinki University Central Hospital
Helsinki, Finland
and
Folkhälsan Institute of Genetics
Helsinki, Finland
and
Department of Medical Genetics
University of Helsinki
Helsinki, Finland

Professor Anna-Elina Lehesjoki, MD, PhD
Folkhälsan Institute of Genetics
Helsinki, Finland
and
Department of Medical Genetics
and
Neuroscience Center
University of Helsinki
Helsinki, Finland

Reviewers: Professor Helena Kääriäinen, MD, PhD
National Institute for Health and Welfare
Helsinki, Finland

Docent Katarina Pelin, PhD
Division of Genetics
Department of Biosciences
University of Helsinki
Helsinki, Finland

Opponent: Professor Jaakko Ignatius, MD, PhD
Department of Clinical Genetics
Turku University Hospital
Turku, Finland

ISBN 978-952-10-7269-7 (paperback)
ISBN 978-952-10-7270-3 (PDF)
http://ethesis.helsinki.fi

Unigrafia Oy
Helsinki 2011

to my godfather

CONTENTS

LIST OF ORIGINAL PUBLICATIONS

This thesis is based on the following original publications, which are referred to in the text by their Roman numerals. In addition some unpublished data (U) are presented.

I **Västinsalo H**, Isosomppi J, Aittakorpi A, Sankila EM. Two Finnish USH1B patients with three novel mutations in *myosin VIIA. Molecular Vision* 12:1093-7. (2006)

II **Västinsalo H**, Jalkanen R, Bergmann C, Neuhaus C, Kleemola L, Jauhola L, Bolz HJ, Sankila EM. Extended mutation spectrum of Usher syndrome in Finland. *submitted*

III **Västinsalo H**, Jalkanen R, Dinculescu A, Isosomppi J, Geller S, Flannery JG, Hauswirth WW, Sankila EM. Alternative splice variants of the USH3A gene *Clarin 1* (*CLRN1*). *European Journal of Human Genetics* 19:30-5. (2011)

IV Isosomppi J*, **Västinsalo H***, Geller SF, Heon E, Flannery JG, Sankila EM. Disease-causing mutations in the *CLRN1* gene alter normal CLRN1 protein trafficking to the plasma membrane. *Molecular Vision* 15:1806-18. (2009)

*These authors contributed equally to the respective article.

ABBREVIATIONS

ANK	ankyrin domain
APEX	arrayed primer extension
arRP	autosomal recessive retinitis pigmentosa
BCIP	5-Bromo-4-chloro-3-indolyl phosphate
BHK	baby hamster kidney cells
bp	base pair
BSA	bovine serum albumin
CDH23	cadherin 23
cDNA	complementary deoxyribonucleic acid
CEPH	Centre d'Etude du Polymorphisme Humain
CLRN1	clarin 1
COS	African green monkey kidney cells
DNA	deoxyribonucleic acid
dpf	days post fertilization
Dr-Clrn1-ab	antibody against zebrafish Clrn1
ELM	external limiting membrane
ENCODE	Encyclopedia of DNA elements
E	embryonic development
ER	endoplasmic reticulum
ERG	electroretinography
EST	expressed sequence tag
FERM	protein 4.1, ezrin, radixin, moesin domain
FN3	fibronectin type III domain
GCL	ganglion cell layer
GFP	green fluorescent protein
G -protein	guanine nucleotide binding protein
GPR98	G -protein coupled receptor 98 (VLGR1/mass1)
HEK	human embryonic kidney cells
HELA	human cervical cancer cells
hpf	hours post fertilization
ILM	inner limiting membrane
INL	inner nuclear layer
IPL	inner plexiform layer
IS	photoreceptor inner segment
kb	kilobase
kD	kiloDalton
LCA	Leber congenital amaurosis
Mb	megabase
MO	morpholino oligonucleotide
mRNA	messenger RNA
MYO7A	myosin VIIA
MyTH4	myosin tail homology 4 domain
NBT	nitro blue tetrazolium chloride
NGS	normal goat serum
NMD	nonsense-mediated mRNA decay
OKR	optokinetic response
OLM	outer limiting membrane
ONL	outer nuclear layer
OPL	outer plexiform layer
ORF	open reading frame
OS	photoreceptor outer segment

P	postnatal day
PAGE	polyacrylamide gel electrophoresis
PBM	PDZ domain binding motif
PCDH15	protocadherin 15
PCR	polymerase chain reaction
PDZ	post-synaptic density, disc-large, zo-1 domain
PDZD7	PDZ domain containing 7
RACE	rapid amplification of cDNA ends
RNA	ribonucleic acid
RP	retinitis pigmentosa
RPE	retinal pigment epithelium
SAM	sterile α- motif
SANS	scaffold protein containing ankyrin repeats and SAM domain
RT-PCR	reverse transcriptase polymerase chain reaction
SH	src homology domain
SNP	single nucleotide polymorphism
src	sarcoma
UTR	untranslated region
USH	Usher syndrome
USH1	Usher syndrome type 1
USH1C	harmonin
USH2	Usher syndrome type 2
USH2A	usherin
USH3	Usher syndrome type 3
VLGR1	very large G-protein-coupled receptor 1 (GPR98/mass1)
WERI-Rb	human retinoblastoma cells
WHRN	whirlin
wt	wild type

ABSTRACT

Usher syndrome (USH) is an inherited blindness and deafness disorder with variable vestibular dysfunction. The syndrome is divided into three subtypes according to the progression and severity of clinical symptoms. Usher syndrome type 1 (USH1) is characterized by congenital severe hearing loss, vestibular dysfunction and early onset of retinal degeneration; Usher syndrome type 2 (USH2) by congenital milder hearing loss, normal vestibular function and later onset retinal degeneration; Usher syndrome type 3 (USH3) by post-verbal progressive hearing loss, variable onset of retinal degeneration and variable presence of vestibular dysfunction.

The gene mutated in USH3, clarin 1 (*CLRN1*), was identified in Finland in 2001 and two mutations were identified in Finnish patients at that time. All the Finnish USH3 patients have the main Finnish USH3 *CLRN1* mutation, p.Y176X, most often in homozygous form. Prior to this study, the two *CLRN1* gene mutations were the only USH mutations identified in Finnish USH patients. To further clarify the Finnish USH mutation spectrum, all nine USH genes (cadherin 23 [*CDH23*], *CLRN1*, G-protein-coupled receptor 98 [*GPR98*], harmonin [*USH1C*], myosin VIIa [*MYO7A*], protocadherin 15 [*PCDH15*], scaffold protein containing ankyrin repeats and SAM domain [*SANS*], usherin [*USH2A*] and whirlin [*WHRN*]) were studied in Finnish USH patients. Seven mutations were identified: one was a previously known mutation in *CLRN1,* four were novel mutations in *MYO7A* and two were a novel and a previously known mutation in *USH2A*. Several other *MYO7A* and *USH2A* sequence variants were identified in Finnish USH patients, but many of these have been classified as non-pathogenic. Our results, however, suggest that some of these variations, considered as polymorphisms, may change the function of the protein products enough to modify or cause the USH phenotype when combined with disease -causing pathogenic USH mutations in *MYO7A*, *USH2A* or *CLRN1*.

Another aim of this research was to further study the structure and function of the *CLRN1* gene, and to clarify the effects of mutations on protein function. The search for new splice variants resulted in the identification of eight novel splice variants in addition to the three splice variants that were already known prior to this study. Studies of the possible promoter regions for these splice variants showed the most active region included the 1000 bases upstream of the translation start site in the first exon of the main three exon splice variant. The 232 aa CLRN1 protein encoded by the main (three-exon) splice variant was transported to the plasma membrane when expressed in cultured cells. Western blot studies suggested that CLRN1 forms dimers and multimers. The CLRN1 mutant proteins studied (p.N48K, p.M120K, p.L150P and

p.I153_154delinsM) were retained in the endoplasmic reticulum (ER) and some of the USH3 mutations (p.N48K and p.M120K) caused CLRN1 to be unstable. During this study, two novel *CLRN1* sequence alterations were identified and their pathogenicity was studied with cell culture protein expression. CLRN1 with a p.A123D change was mislocalized and unstable, like the previously known pathological mutations, but CLRN1 with a p.L54P change had localization and stability indistinguishable from that of wild type CLRN1. Accordingly, the p.L54P change was classified as a polymorphism.

The final aim of this study was to find out more about the function of CLRN1 in retina and cochlea. Previous studies with mice had shown that *Clrn1* is expressed in mouse cochlear hair cells and spiral ganglion cells, but the expression profile in mouse retina remained unknown. The *Clrn1* knockout mice display cochlear cell disruption/death, but do not have a retinal phenotype. The zebrafish, *Danio rerio*, has been used successfully as a model for other USH subtypes, thus zebrafish larvae were used in this thesis to investigate Clrn1 retinal function. Zebrafish *clrn1* was found to be expressed in hair cells associated with hearing and balance. This expression profile was similar to that in mouse ear. *Clrn1* expression was also found in the inner nuclear layer (INL), photoreceptor layer and retinal pigment epithelium layer (RPE) of the zebrafish retina. When Clrn1 production was knocked down with injected morpholino oligonucleotides (MO) targeting Clrn1 translation or correct splicing, the zebrafish larvae showed symptoms similar to USH3 patients. These larvae had balance/hearing problems and reduced response to visual stimuli.

The knowledge this research has provided about the mutations in USH genes and the Finnish USH mutation spectrum are important in USH patient diagnostics. The extended information about the structure and function of *CLRN1* is a step further in exploring USH3 pathogenesis caused by mutated *CLRN1* as well as a step in finding a cure for the disease.

REVIEW OF THE LITERATURE

1. Human eye and ear

1.1 Vision

1.1.1 Structure and function of the human retina

The human retina is composed of seven main cell types that create a laminated structure only a few hundred micrometers thick. The sensory cells are light-sensitive photoreceptors that absorb different wavelengths. The information absorbed by photosensitive pigments is converted through chemical processes into electrical signals that are sent to the brain, where they are interpreted into what we experience as sight. The anatomy of the retina was reported as early as 1893 when Spanish histologist Santiago Ramon y Cajal published the first study of the different retinal cell types (Ramon y Cajal, 1893).

The retinal cell types are organized into functional layers (Figure 1). The light travels through the layers to the light-sensitive cells, photoreceptors. The photoreceptors have their nuclei in the outer nuclear layer (ONL) that is separated from the light-sensitive compartments located on the other side of the outer limiting membrane (OLM). The photoreceptor compartments beyond the OLM are inner segment (IS) and outer segment (OS) connected by a connecting cilium. The outer segment is actually a modified cilium. The inner segment is responsible for the maintenance of the photoreceptor, and for the synthesis and transport of proteins through the connecting cilium to the outer segment, where stacks of membranous disks are filled with light-sensitive pigments. Beyond the photoreceptor outer segment is the retinal pigment epithelium (RPE). The RPE is not involved in light detection or signal transmission, but is packed with melanin pigment granules and provides a pigmented layer that absorbs light that is not absorbed in the photoreceptor outer segments. RPE cells are also crucial in homeostasis of the photoreceptor outer segments. Photoreceptors shed older membranous disks from the RPE end of the OS which are reabsorbed through phagocytosis by RPE cells (Schraermayer and Heimann, 1999). There are two types of photoreceptors, rods and cones. Rods are more sensitive to light and function in the dark, when we don't see colours. Cones function during the daytime, and different cone subpopulations absorb different wavelengths of light, which enables our colour vision.

The light reaching the photoreceptor OS changes the conformation of light-sensitive pigments, such as rhodopsin in rod photoreceptors, and activates the G -protein (guanine nucleotide-binding protein) coupled cascade that converts the light signal to plasma membrane hyperpolarization and affects neurotransmitter release at the photoreceptor synapse (Rattner et al., 1999). This reaction to light is called the phototransduction cascade, in which the light excitation in the photoreceptor outer segment is converted into an electrical signal. This signal is then relayed through photoreceptor synapses in the outer plexiform layer (OPL) to the bipolar cells located in the inner nuclear layer (INL). The electrical signal is transferred via bipolar cells to the ganglion cells through another synaptic transfer in the inner plexiform layer (IPL). In the ganglion cell layer (GCL) the ganglion cells relay the electric signal to the optic nerve and towards the brain (Wong, 2006).

The photoreceptors, bipolar cells and ganglion cells form the primary signal relay mechanisms in the retina, but the correct function of the retina requires auxiliary cells that modify the signal received. For example, the amacrine cells connect to synapses between bipolar and ganglion cells. These connections form a larger network that modifies the signal leaving the retina. Similarly, the horizontal cells connect singular photoreceptors into networks of interconnected photoreceptors by connecting to photoreceptor synapses in the OPL.

The seventh retinal cell type originally identified by Ramon y Cajal is the Müller cell, the primary glia in the vertebrate retina. Müller cells are also the only cells that span through all the layers in the retina from the inner limiting membrane (ILM) separating the retina from the vitreus humour to the OLM separating the photoreceptor nuclei from the inner and outer segments (Newman and Reichenbach, 1996).

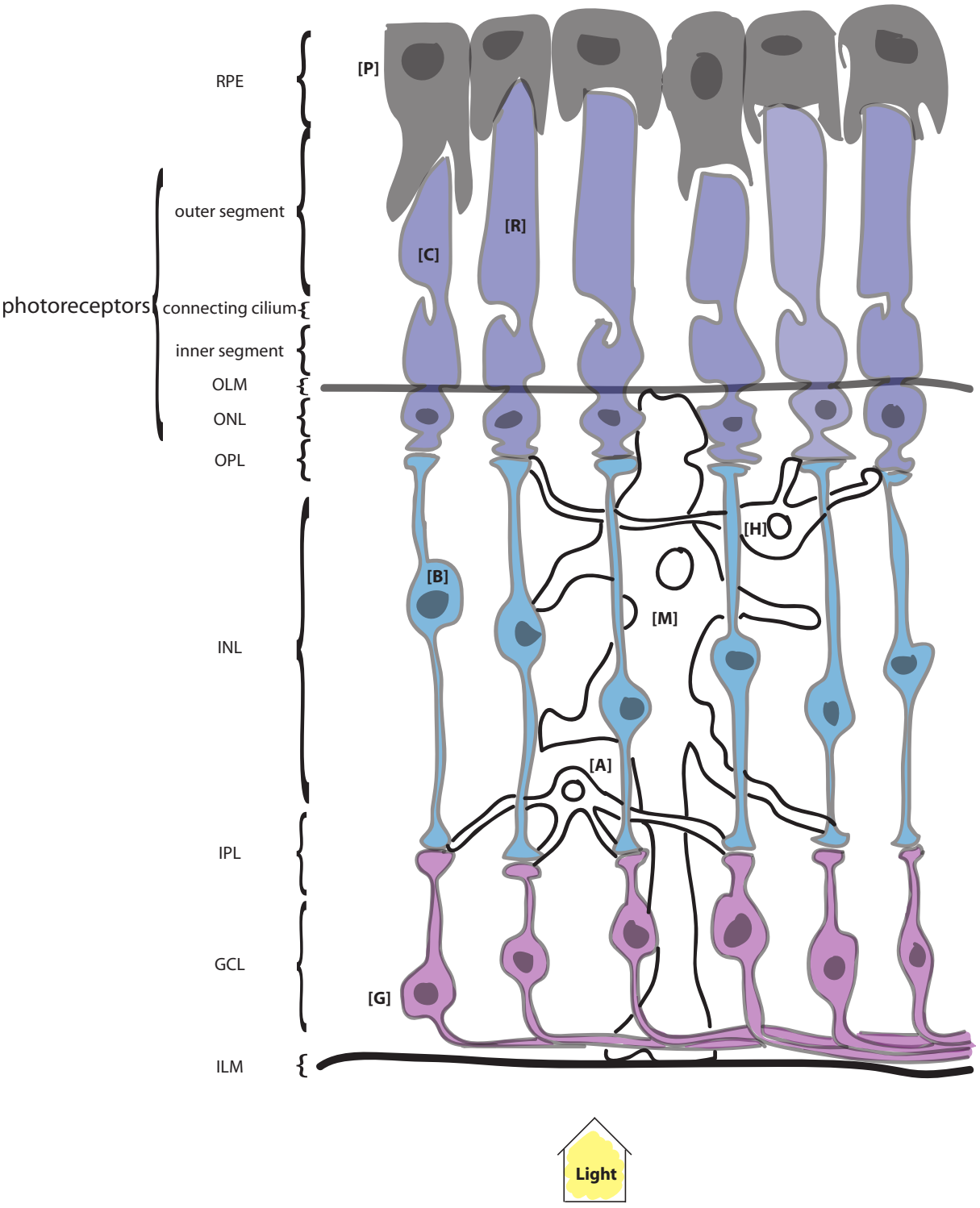

Figure 1. Anatomy of the vertebrate retina. Light hits the retina from the ganglion cell side (located at the bottom layer in the image) and is detected by photosensitive pigments in the photoreceptor outer segments. Primary retinal cell types: retinal pigment epithelium cell [P], rod photoreceptor cell (nucleus, inner and outer segment) [R], cone photoreceptor cell (nucleus, inner and outer segment) [C], Müller cell [M], horizontal cell [H], bipolar cell [B], amacrine cell [A], ganglion cell [G]. Retinal layers: retinal pigment epithelium layer [RPE], photoreceptor outer segment layer, photoreceptor inner segment layer, outer

limiting membrane (OLM), outer nuclear layer (ONL), outer plexiform layer (OPL), inner nuclear layer (INL), inner plexiform layer (IPL), ganglion cell layer (GCL) and inner limiting membrane (ILM).

1.1.2 Development of the human retina

The seven different cell types, light detectors (cone and rod photoreceptors), projection neurons (bipolar and retinal ganglion cells), circuit neurons (amacrine and horizontal cells) and the retinal glia (Müller cells) are generated in all developing retinas studied to date in similar order. From larger to smaller cells, the first to appear are ganglion cells, horizontal cells and cone photoreceptors. After the first wave of retinal cell generation amacrine cells are produced followed by bipolar cells, rod photoreceptors and Müller glia. The first layer to develop is the GCL, then the INL and finally the ONL (Rapaport, 2006). During retinal development synaptogenesis starts from the IPL and then proceeds to OPL, first progressing within the layer and then vertically between layers. In mice the photoreceptor ribbon synapses mature between postnatal days (P) P7 and P12 (Sernagor, 2006).

The Müller cells envelope the synapses on both plexiform layers during retinal development and take up glutamate released in the neuronal synapses. The glutamate is converted by glutamine synthetase into glutamine and recycled back to the neurons by the Müller cells. Müller cells also produce factors promoting neuronal survival especially in the damaged retina, but Müller cells can also produce toxic factors that can contribute to retinal degeneration (Zahs and Esguerra, 2006). The RPE is also important in controlling the photoreceptor and retinal progenitor cell developmental cell death (Sheedlo et al., 1998, 2001; Soderpalm et al., 2000).

1.2 Hearing and balance

1.2.1 Structure and function of the human cochlea

The sensory epithelium able to detect sound waves is located inside a hollow bony spiral in the inner ear called the cochlea. The sensory epithelium within the cochlea was named the organ of Corti after the man who discovered it, Marchese Alfonso Corti. He described the structure of the epithelium, including the outer and inner hair cells and tectorial membrane, in 1851 (Figure 2) (Hachmeister, 2003).

The basic sensory unit of the organ of Corti consists of hair cells, supporting cells, otic neurons and Schwann cells. The hair cells can convert sound waves moving through the cochlear

duct to electrical signals, detecting sound waves with stereocilia that move when liquid inside the cochlear duct is moved by the sound waves. The supporting cells hold the sensory hair cells in the correct pattern (Alsina et al., 2009). There are five different types of supporting cells that help to keep the hair cells functioning properly (Ashmore and Gale, 2000). The otic neurons connect the sensory cells to the brain through the spiral ganglion (the ganglion of the cochlear nerve). The glia, Schwann cells, envelope the neurons and their axons (Alsina, 2009; Becker et al., 1988). The morphology of sensory hair cells differs between cochlear and the vestibular system (Kelley, 2006a). The cochlea also has two morphologically distinct hair cells. The inner hair cells make up 95 % of the fibers in the auditory nerve, whereas the outer hair cells, functioning as signal enhancers, make up only 5 % (Ashmore and Gale, 2000; Becker et al., 1988).

The only "true" hair cell cilium is the kinocilium that disappears after functioning during development to orient the growth and shape of the graded rows of stereocilia. The kinocilium has a tubulin core whereas the stereocilia are mechanosensory organelles with F-actin cytoskeletons (Petit, 2001; Saihan et al., 2009). The stereocilia actin cytoskeletons are anchored to the actin-rich cuticular plate located at the base of the stereocilia (Hasson et al., 1997). The stereocilia are tethered together in graded rows with fibrous links (ankle links and tip links). Sound waves travelling through the inner ear move the stereocilia, this stretches the tip links between them. The movement of tip links open the mechanosensory channels. Potassium inflow from the endolymph causes hair cell depolarization which activates the ribbon synapses starting the signal to the brain (Petit, 2001; Saihan et al., 2009).

1.2.2 Development of the human cochlea

The human cochlea develops from the thickening of ectoderm, which forms the otic vesicle. The vesicle then separates into vestibular and cochlear parts. The cochlea elongates into a circular tube, the cochlear duct, by the 8th week of fetal development (E8). A week after that the organ of Corti starts to develop. At this same time, ganglion cell processes enter the base of the developing organ of Corti (Moore and Linthicum, 2007). Vestibular hair cells start to develop at E12 and cochlear hair cells around E13 (Kelley, 2006b). The maturation of the cochlea continues until the first sound waves are interpreted as sound during weeks E28-29 (Moore and Linthicum, 2007).

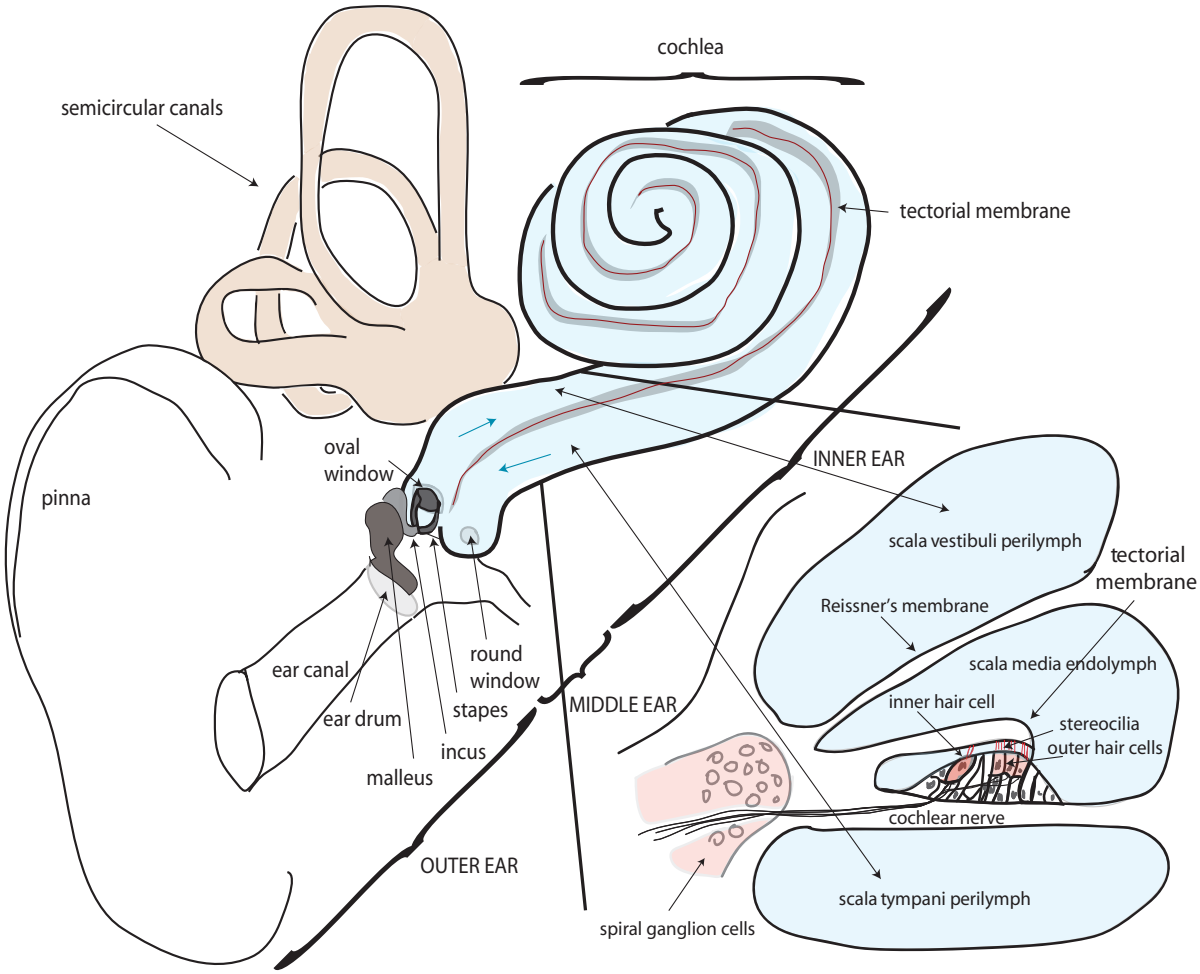

Figure 2. Schematic structure of the ear (inner, middle and outer) and a cross-section of the cochlea. The outer ear is composed of the pinna and ear canal. In the middle ear, the three ossicles (malleus, incus and stapes) transfer the sound waves moving the ear drum to the oval window and into the cochlea. The inner ear has two sensory units. In the cochlea, hair cells detect the sound waves moving in the liquid filling the cochlear duct. The vestibular system is composed of the semicircular canals containing hair cells sensing gravity and motion.

2. Usher syndrome

Usher syndrome (USH) is characterized by hereditary deafness and blindness with variable vestibular dysfunction. The simultaneous occurrence of deafness and retinal degeneration in patients was first reported in Germany by von Graefe (von Graefe et al., 1858). Scottish doctor Charles Usher was the first to report that the retinal degeneration and deafness were hereditary in several families (Usher, 1914). In Finland, Arto Nuutila studied patients with retinitis pigmentosa and deafness calling the disease dystrophia retinae pigmentosa-dysacusis (DRD) (Nuutila, 1970). The syndrome with retinitis pigmentosa (RP) and sensorineural deafness was

officially classified as USH in 1994 (Smith et al., 1994). The prevalence of USH ranges between 3.5-6.2 per 100,000 in different populations worldwide and accounts for half of all adult cases of deaf-blindness (Saihan et al., 2009; Yan and Liu, 2010).

2.1 Clinical manifestations

The blindness in USH patients is caused by progressive retinal degeneration, retinitis pigmentosa (RP) (Smith et al., 1994). RP is the most frequent cause of hereditary blindness with an incidence of 1:3,500 worldwide (Sullivan et al., 1999). RP starts with night blindness, followed by reduction of the peripheral visual field, resulting in tunnel vision and complete blindness with the loss of central vision. Vision loss in USH is caused by photoreceptor degeneration (Jacobson et al., 2008). RP first presents itself in retinal examinations with mottled pigmentation called bone spicules followed by changes of the optic nerve head and thinning of the retinal blood vessels (Figure 3). RP can be caused by mutations in over 40 genes. To date, mutations in 161 genes are known to cause retinal diseases (RetNet, http://www.sph.uth.tmc.edu/retnet/).

The hearing loss in USH is sensorineural. The main finding in the inner ear is degeneration of cochlear sensory cells and disorganization of hair cell cilia that lead to either progressive or congenital deafness (Davenport and Omenn, 1977; Fishman et al., 1983; Becker et al., 1988; Smith et al., 1994). It is estimated that congenital deafness occurs in 1 in 1,000 births. It has been approximated that half of the cases of congenital deafness are caused by mutated genes and the other half by environmental influences (Resendes et al., 2001). Mutations in 83 genes are known to cause hereditary hearing loss (Hereditary Hearing loss Homepage, http://hereditaryhearingloss.org/).

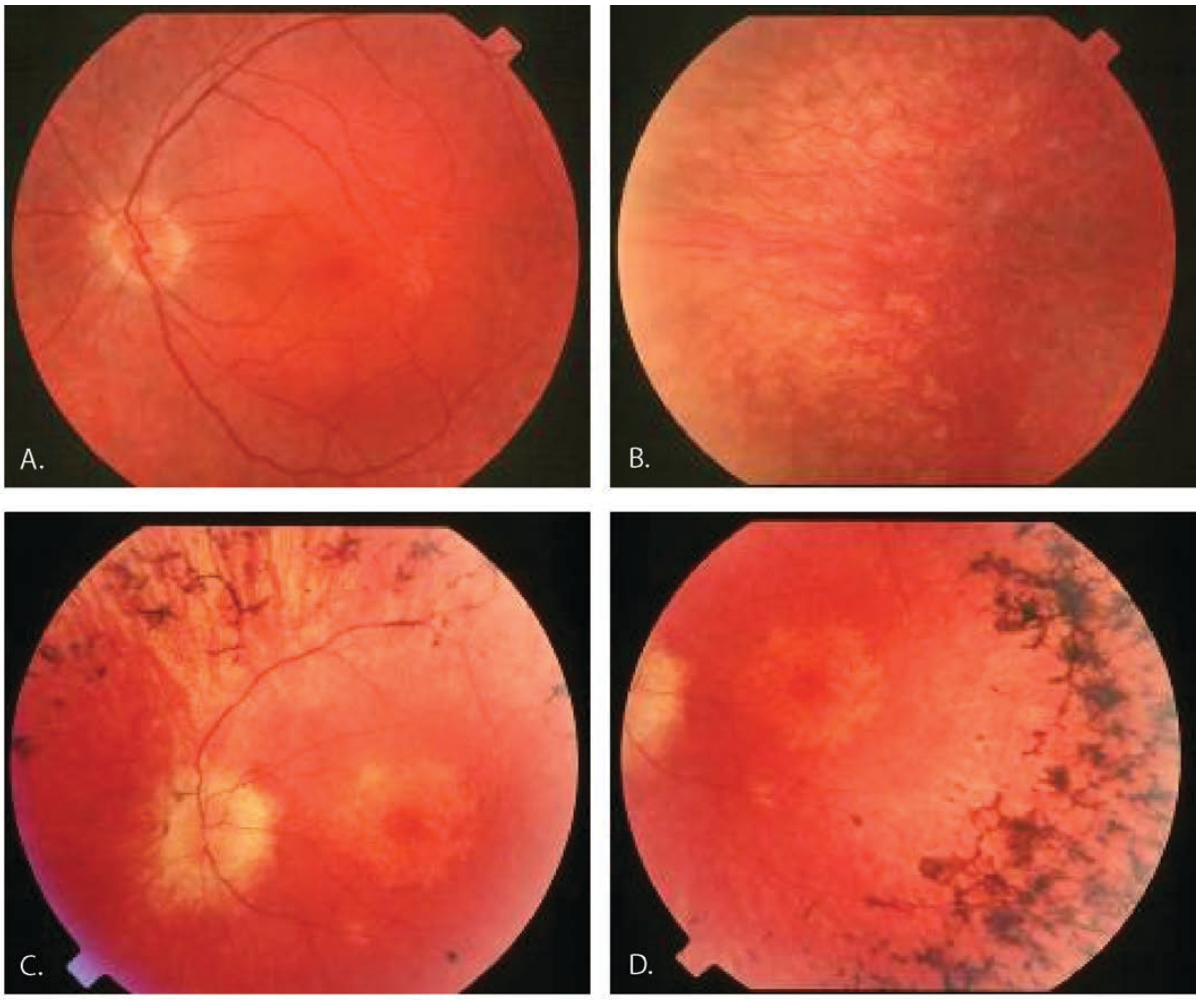

Figure 3. Progression of retinitis pigmentosa in USH patients. Funduscopic examination of a 17-year-old male USH3 patient with 40 degree visual field and visual acuity of 20/30. The retina is showing no signs of RP (A, B). Funduscopic examination of a 32-year-old female USH3 patient with 20 degree visual field and visual acuity of 20/60. The retinal vessels are thinning and mottled pigmentation (bone spicules) have formed (C, D). Images provided by Sankila EM.

2.2 Clinical subtypes

Usher syndrome has been traditionally divided according to the severity of the clinical symptoms into three subtypes (Table 1). Usher syndrome type 1 (USH1) is characterized by severe congenital deafness with prepubertal onset of RP and vestibular problems. Usher syndrome type 2 (USH2) is characterized by congenital moderate to severe deafness, RP that starts during the first or second decade of life, and normal vestibular function. Usher syndrome type 3 (USH3) is characterized by

usually post-verbal progressive hearing loss with variable onset of RP and either normal or variably affected vestibular function (reviewed in Yan and Liu, 2010).

Table 1. Clinical subtypes of Usher syndrome

USH subtype	USH1	USH2	USH3
Onset of RP	prepubertal	prepubertal/pubertal	prepubertal/pubertal
Deafness	severe congenital	severe/moderate congenital	progressive leads to severe/moderate
Vestibular function	abnormal	normal	abnormal/normal

USH2 is the most common USH subtype. Worldwide, 56-67 % of USH patients have USH2 (Keats and Savas, 2004; Petit, 2001). USH1 accounts for 30-40 % of USH cases worldwide (Espinos et al., 1998; Hope et al., 1997; Spandau and Rohrschneider, 2002). Subtypes USH1B (mutated gene myosin VIIa) and USH2A (mutated gene usherin) together account for 75-80 % of USH cases worldwide (Pennings et al., 2002). In 1994, when the official classification of USH was made, an USH subtype with progressive hearing loss was reported in rare cases (Beatty et al., 1979; Davenport and Omenn, 1977; Gorlin et al., 1979; Gröndahl and Mjöen, 1986; Karp and Santore, 1983; Merin et al., 1974) and only two subtypes, USH1 and USH2, were recognized (Smith et al., 1994). USH3, with progressive hearing loss, was eventually recognized as an official USH subtype after Sankila et al. (1995) assigned linkage for ten Finnish USH3 families to a new locus on chromosome 3q21-q25 and identified the causative gene, *USH3A* (Joensuu et al., 2001). One reason why USH3 was identified in Finland is the USH subtype distribution. In Finland, the USH3 subtype is more common than in the rest of the world because of a founder effect and subsequent enrichment of the founder mutation in the small and relatively isolated Finnish population. The proportion of different subtypes among Finnish USH patients are approximately: 34 % USH1, 12 % USH2 and 40 % USH3 while 14 % of patients have unknown USH subtype (Pakarinen et al., 1995a). A similar prevalence of USH3 patients among USH cases has also been reported in Ashkenazi Jews (Ness et al., 2003).

Symptoms of USH3 overlap with those of USH1 and USH2, making the clinical diagnosis difficult. A study of Finnish USH patients suggested differences of refractive errors between different USH types: USH3 patients have hypermetropia with astigmatism, whereas USH1 patients have hypermetropia without astigmatism, and USH2 patients have myopic refractive

errors (Pakarinen et al., 1996). USH3 patients have similar rates of deterioration in visual function compared to USH1B and USH2A patients. The USH3 patients' visual field deterioration is more severe than in USH2A patients and is similar to that in USH1B patients (Plantinga et al., 2006). In the studied USH3 patients, rod dysfunction and loss starts from the peripheral field in the first decade of life and spreads to the central retina in the second decade. The rod loss is almost complete within the first two decades of life. Some peripheral cone function is still present during the third decade. Central cone loss is gradual and can last for several decades. There is no evidence of malfunction in synaptic activity in electroretinograms (ERG) during USH3 retinal degeneration, but the ONL loss accompanied by visual symptoms suggests that photoreceptor degeneration is involved in the USH3 pathogenesis (Herrera et al., 2008). The hearing loss in USH3 patients is highly variable. The patients can have close to normal hearing thresholds or their hearing loss can be more severe than in subtype USH2, closer to the USH1 subtype level. Patients may lose their speech recognition before language development as a child, but most patients have good speech recognition to a far more advanced age. The hearing loss progresses fastest during the first two decades of life (Plantinga et al., 2005).

3. **Molecular genetics of Usher syndrome**

3.1 The definition of a gene

The estimated gene count of the human genome has changed over the years. There are approximately 20 000—25 000 protein coding genes in the human genome that is composed of 23 chromosome pairs (HUGO, 2004). Chromosomes are coiled DNA structures, where DNA is bound and packed around DNA binding proteins. Genes are traditionally thought to be composed of exons and introns. During the reading process of the gene, splicing of the intronic segments happens so that only the exons form the coding region which is translated into an amino acid sequence. This amino acid sequence folds into local three-dimensional structures (secondary structure) and finally, the locally folded amino acid sequence folds into the main three-dimensional structure (tertiary structure). After the protein is correctly folded into the final structure, it is possibly joined with other proteins into a working complex (quaternary structure). This traditional way of seeing a gene as a simple message to code a single protein has changed with recent findings about gene splicing.

Approximately 95 % of known multi-exon genes undergo alternative splicing (Pan et al., 2008). Recently, the concept of a gene has been refined according to an improved understanding of alternative splicing (Figure 4). The ENCODE project (ENCyclopedia Of DNA Elements) cataloged biologically functional elements in 1 % of the human genome. This project redefined the concept of a gene into "a union of genomic sequences encoding a coherent set of potentially overlapping functional products" (Gerstein et al., 2007). It seems that much of human complexity is not the direct result of the number of genes we have (which is relatively similar to several other mammals), but rather, the complexity of the transcripts (and thus proteins) that are generated by those genes (Johnson et al., 2003a; Matlin et al., 2005; Pan et al., 2008; Wang et al., 2008).

The transcriptional activity of a gene is controlled by the gene's promoter region. The promoter region is divided into the proximal promoter, which is usually located within 250 bp upstream of the transcription start site, and the distal promoter, which includes regulatory elements (either inhibiting or enhancing transcription) further upstream or downstream of transcription start site. Our knowledge about the promoter region has also changed over time. A simple single promoter region controlling the expression of a single, always similarly spliced variant, has changed into a complex network of alternative splice variants possibly controlled by multiple promoter regions. If a gene has an alternative 5' end which generates an alternative splice variant, there is also an alternative proximal promoter region regulating this new variant. On the other hand, a certain gene may have the same transcribed sequence in different tissues, but alternative active promoters. Approximately 18 % of genes have alternative promoters that control their expression (Landry et al., 2003).

Although the definition of a gene has evolved to be more complex and closer to reality in recent years, we cannot even now assume that we know the whole truth about what comprises a gene and influences its function.

Figure 4. Progressive understanding of gene structure. The traditional definition of a gene (1.) was one promoter controlling the transcription and splicing of the exons (A) of a single spliced transcript (B) encoding an open reading frame (ORF) (C) translated into a protein (D). The refined definition of a gene (2.) is that a gene can have multiple splice variants with several exon combinations (E). The original gene (A) was in fact five different genes intertwined with three alternative promoter regions sharing the same exons but in alternative combinations (F).

1. Traditional definition of a gene:

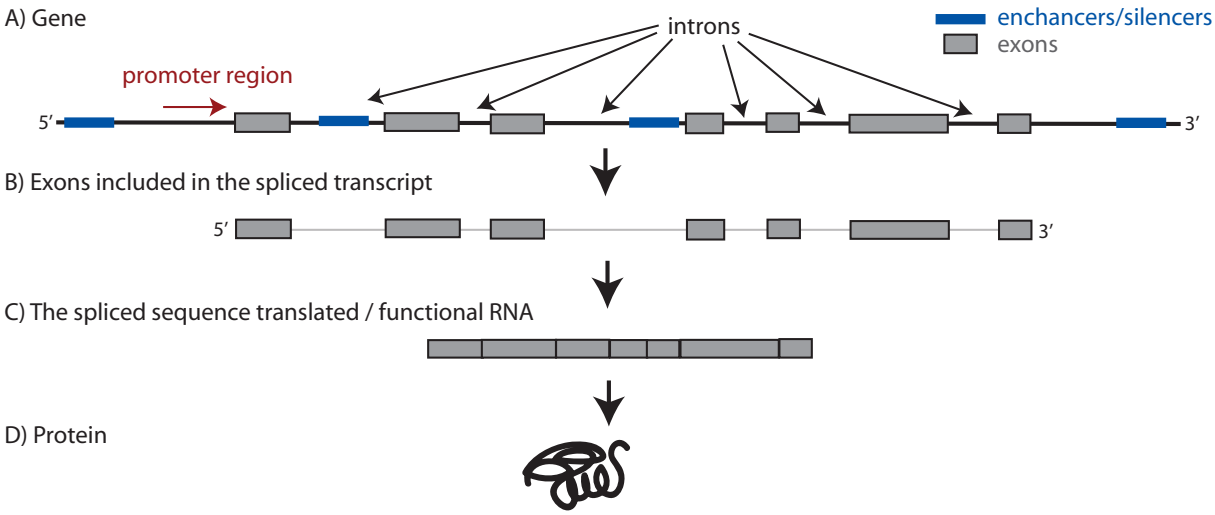

2. Refined definition of a gene:

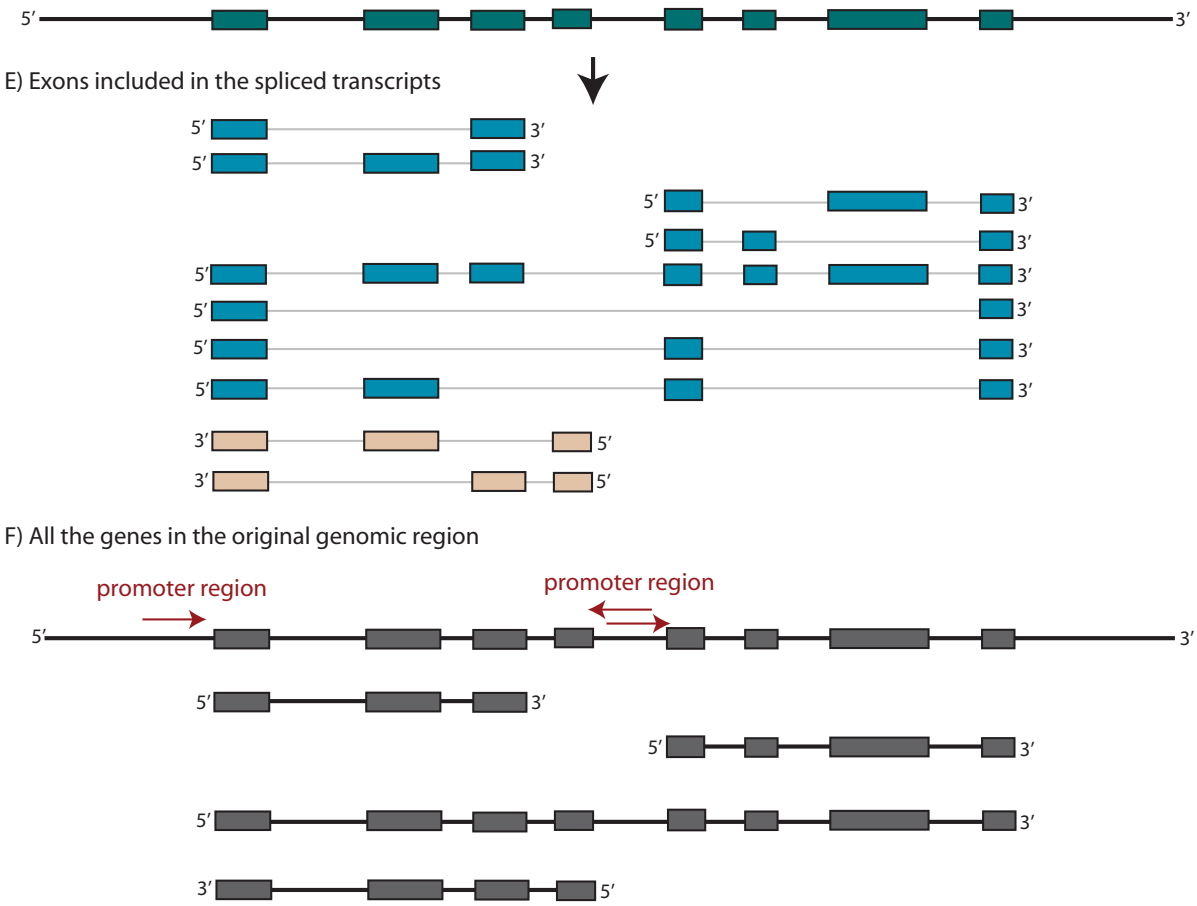

3.2 Genes behind USH subtypes

The genes that cause USH when mutated range in size from the three exon clarin 1 (*CLRN1*) causing USH3 to "G -Protein coupled Receptor 98" (*GPR98*) with 90 exons causing USH2C (Table 2) (Adato et al., 2002; Weston et al., 2004).

Eight different chromosomal loci (*USH1B-H*) have been mapped in families with USH1. To date, five genes have been reported with mutations in these five genes causing different USH1 subtypes. USH1B is caused by mutated *MYO7A* (encodes protein myosin VIIa) (Kimberling et al., 1992; Smith et al., 1992; Weil et al., 1995), USH1C by mutated *USH1C* (harmonin) (Bitner-Glindzicz et al., 2000; Smith et al., 1992; Verpy et al., 2000), USH1D by mutated *CDH23* (cadherin 23) (Bolz et al., 2001; Bork et al., 2001; Wayne et al, 1996), USH1F by mutated *PCDH15* (protocadherin 15) (Ahmed et al., 2001; Wayne et al., 1997) and USH1G by mutated *USH1G* (scaffold protein containing ankyrin repeats and SAM domain [SANS]) (Kikkawa et al., 2003; Weil et al., 2003). There are also two additional loci (*USH1E* and *USH1H*) in which no USH1 gene has yet been identified (Ahmed et al., 2009; Saihan et al., 2009; Yan and Liu, 2010). The *USH1A* locus reported in 1992 (Kaplan et al., 1992) was later found to be a linkage artifact (Gerber et al., 2006). Of the USH1 subtypes, USH1B is the most common and mutated *MYO7A* accounts for one third to half of the USH1 cases in the UK and USA (Astuto et al., 2000; Ouyang et al., 2005; Weston et al., 1996).

Four loci (*USH2A-D*) have been associated with USH2, but the *USH2B* locus was later withdrawn by Kremer et al., (2006). The disease-causing genes in the three remaining loci have been found: USH2A is caused by mutations in *USH2A* (encodes protein usherin) (Eudy et al., 1998a; Weston et al., 2000), USH2C by mutations in *VLGR1* (very large G-protein-coupled receptor 1[VLGR1]/mass1/GPR98) (Weston et al., 2004) and USH2D by mutations in *WHRN* (whirlin) (Ebermann et al., 2007a). Mutated *USH2A* is estimated to account for 85 % of all USH2 cases (Pieke-Dahl et al., 1997; Weston et al., 2000).

USH3A was mapped to locus 3q21-25 and the *CLRN1* gene was discovered in this region (Sankila et al., 1995). Another subtype USH3B was mapped to locus 20q, but the gene in this region is still unknown (Petit, 2001). USH modifier gene *PDZD7* is located in 10q24.31. Mutated *PDZD7* can only modify USH phenotype when combined with mutated *USH2A* or *VLGR1b* (Ebermann et al., 2010).

Table 2. Known USH genes and proteins (at completion of this thesis), their chromosomal locations, structures and references. *Number in parenthesis marks identified spliced variations reported in Aceview database (Aceview [http://www.ncbi.nlm.nih.gov/IEB/Research/Acembly/], September, 2011).

USH subtype	gene	chromosome location	number of exons	cds size (nt)	known splice variants*	protein	references
Usher syndrome type 1							
USH1A		14q32 (withdrawn)					Kaplan, 1992; Gerber, 2006
USH1B	*MYO7A*	11q13.5	49 (48 coding)	6648	3 (10)	myosin VIIa	Weil, 1995
USH1C	*USH1C*	11p15.1	28	1659	2 (11)	harmonin	Verpy, 2000
USH1D	*CDH23*	10q22.1	69	10064	9 (19)	cadherin 23	Bolz, 2001
USH1E		21q21				unknown	Chaïb, 1997
USH1F	*PCDH15*	10q21.1	32	5889	12 (13)	protocadherin 15	Ahmed, 2001; Alagramam, 2001
USH1G	*SANS*	17q25.1	3	3561	1 (2)	scaffold protein containing ankyrin repeats and SAM domain	Weil, 2003
USH1H		15q22-23				unknown	Ahmed, 2009
Usher syndrome type 2							
USH2A	*USH2A*	1q41	72	15609	2 (6)	usherin	Eudy, 1998a; van Wijk, 2004
USH2B		3p23-24.2 (withdrawn)					Hmani, 1999; Kremer, 2006
USH2C	*GPR98/ VLGR1*	5q14.3-21.1	90	18921	2 (14)	G protein-coupled receptor 98/ mass1/ very large G-protein-coupled receptor	Weston, 2004
USH2D	*WHRN*	9q32-34	12	2724	3 (14)	whirlin	Ebermann, 2007a
Usher syndrome type 3							
USH3A	*CLRN1*	3q25.1	3	699	3 (5)	clarin 1	Joensuu, 2001; Adato, 2002
USH3B		20q					Chaïb, 1997
Known USH modifier gene							
	PDZD7	10q24.31	16	1554	2 (9)	PDZ domain-containing 7	Schneider, 2009; Ebermann, 2010

Several USH genes can harbor mutations that cause nonsyndromic deafness rather than USH: *MYO7A* (DFNA11 and DFNB2), *USH1C* (DFNB18), *CDH23* (DFNB12), *PCDH15* (DFNB23), *WHRN* (DFNB31) (Yan and Liu, 2010), missense and inframe changes in *USH1C*, *CDH23* and *PCDH15* cause nonsyndromic deafness and truncating mutations cause USH (Saihan et al., 2009). *USH2A* can cause nonsyndromic retinitis pigmentosa when mutated (RP39) (Yan and Liu, 2010). Recently, two mutations in *CLRN1* have been reported to cause autosomal recessive retinitis pigmentosa (arRP) (Khan et al., 2011). Studies with siblings, including twins, with USH2A point to environmental factors and genetic modifiers as the main modifiers of USH phenotype (Bernal et al., 2005; Liu et al., 1999a).

3.3 Progress from the *USH3A* locus to the *CLRN1* gene

After the *USH3* locus was localized to 3q21-q25 (Sankila et al., 1995) and the area was refined further (Joensuu et al., 1996; Joensuu et al., 2000), the *USH3A* gene was identified in 2001 (Joensuu et al., 2001). In this first study the *USH3A* gene was reported to have four exons with a coding region of 360 bp in a genomic region of ~18 kb. The original *USH3A* gene was predicted to translate a 120 aa protein with two putative transmembrane regions. An alternative splice variant for *USH3A* was discovered with five exons and a putative coding region of only 30 aa. Alternative splice variants of 4.5 kb, 1.5 kb and 1 kb in size were ubiquitously expressed in Northern blot analysis (Joensuu et al., 2001). The name of the gene was later changed to clarin 1 (*CLRN1*) when it was found that the original four exon splice variant is rare and the main variant has only three exons, the first one upstream of the original first exon. This main variant has a coding region of 696 bp encoding a 232 aa long protein with four predicted transmembrane regions (Adato et al., 2002). *CLRN1* is known to be expressed in several tissues outside retina and cochlea (Adato et al., 2002; Fields et al., 2002; Joensuu et al., 2001).

3.4 *CLRN1* sequence variants

Eighteen mutations have been discovered in the *CLRN1* gene so far (see Table 6 in Results and Discussion). The mutations discovered in Finnish USH patients are p.M120K (in combination with the Finnish founder mutation) and p.Y176X (Finnish founder mutation identified in all Finnish patients either in homozygous or heterozygous state). There is another USH3 founder mutation, p.N48K, in the Ashkenazi Jewish population responsible for similar a USH subtype distribution as

in the Finnish population (Adato et al., 2002; Fields et al., 2002; Ness et al., 2003). The other mutations have been described in sporadic cases/families throughout the world. Several sequence polymorphisms have been identified in *CLRN1* exons, introns and promoter regions. These have been categorized as benign changes (Adato et al., 2002; Fields et al., 2002).

4. Usher syndrome proteins

USH proteins function in cell adhesion, intracellular transport, scaffolding and signal transduction. Five USH proteins are transmembrane proteins and four are soluble cytoplasmic proteins (Table 3).

Table 3. Proteins coded by the USH genes, their sizes and predicted/known functions.

USH subtype	Protein	Protein symbol	size (aa)	size (approximate in kDa)	Function
USH1B	myosin VIIa	MYO7A	2215	254	soluble motor protein
USH1C	harmonin	USH1C	552	62	soluble scaffold protein
USH1D	cadherin 23	CDH23	3354	370	transmembrane cell adhesion protein
USH1F	protocadherin 15	PCDH15	1962	216	transmembrane cell adhesion protein
USH1G	scaffold protein containing ankyrin repeats and SAM domain	SANS	461	52	soluble scaffold protein
USH2A	usherin	USH2A	5202	576	transmembrane cell adhesion protein
USH2C	G-protein-coupled receptor 98/ mass1/ very large G-protein-coupled receptor 1	GPR98/ VLGR1	6306	693	transmembrane receptor protein
USH2D	whirlin	WHRN	907	97	soluble scaffold protein
USH3	clarin 1	CLRN1	232	26	transmembrane protein function unknown

4.1 USH1

The USH1 proteins have different functions. They function in transport, cell-cell adhesion or as scaffold proteins. Myosin VIIa (MYO7A) is an unconventional motor protein that moves along actin filaments. MYO7A consists of motor head domain that connects to actin and produces force for movement, five calmodulin-binding IQ motifs, two FERM domains (Protein 4.1, Ezrin, Radixin, Moesin domain) and MyTH4 domains, and one Src homomology (SH3) domain (Chen et al., 1996; Weil et al., 1996). IQ motifs are part of the rigid structure functioning as a mechanical lever in myosin, and the number of them determines the length of the step for the myosin protein along the actin filament (Bähler and Rhoads, 2002). The FERM domain is a module involved in localizing proteins to the plasma membrane, especially in several cytoskeletal associated proteins like MYO7A that interface between the plasma membrane and the cytoskeleton (Chishti et al., 1998). MYO7A is involved in intracellular lysosome transport, opsin transport through the connecting cilium in photoreceptors and melanosome transport in RPE cells as well as RPE65 correct localization. RPE65 is an enzyme that catalyzes all-*trans*-retinyl ester conversion to 11-*cis* retinol in the retinoid cycle. These are some of the processes MYO7A is involved with and problems with these could cause USH1 (Liu et al., 1998a; Liu et al., 1999a; Soni et al., 2005; Lopes et al., 2011).

Cadherin 23 (CDH23) and protocadherin 15 (PCDH15) are transmembrane cell-cell adhesion proteins. CDH23 has a single transmembrane domain, 27 extracellular Ca^{2+} -binding domains (cadherin domain), and an intracellular PDZ (post-synaptic density, disc-large, Zo-1) -domain binding motif (PBM). PCDH15 has also only one transmembrane domain, an intracellular PBM domain and either eleven (isoform A) or one (isoform B) extracellular cadherin domain (Alagramam et al., 2001; Bolz et al., 2001; Di Palma et al., 2001a, 2001b; Reiners et al., 2006; Wilson et al., 2001; Yan and Liu, 2010).

Harmonin (USH1C) and “scaffold protein containing ankyrin repeats and SAM domain” (SANS) are scaffold proteins. Harmonin has three isoforms. The shortest isoform has two PDZ domains and one coiled-coil domain, a longer isoform has three PDZ domains and one coiled-coil domain while the longest isoform has three PDZ domains as well as two coiled-coil domains and proline/serine/threonine-rich region. SANS has numerous protein-protein interaction domains: three ankyrin domains (ANK), one sterile α- motif (SAM) and one PBM (Yan and Liu, 2010).

4.2 USH2

Usherin (*USH2A*) has two alternative splice isoforms. The shorter isoform encodes an extracellular matrix protein and the longer isoform encodes a larger protein with a transmembrane region and a short cytoplasmic PBM domain. Both USH2A proteins have a signal peptide in the N-terminus and several binding domains: a laminin G domain, 10 laminin EGF domains, four fibronectin type III (FN3) domains, and a laminin VI domain. The longer isoform has two additional laminin G domains, 28 FN3 domains, as well as one transmembrane domain and an intracellular PBM domain (Bhattacharya et al., 2004; Eudy et al., 1998a, 1998b; Liu et al., 2007; van Wijk et al., 2004).

"G-protein coupled receptor 98" (GPR98) is a member of the serpentine G-protein coupled receptor superfamily. The GPR98 protein has laminin G-like binding domain, 35 Ca^{2+} -binding calcium exchanger β (Calx) domains, 7 protein-protein interaction EAR (epilepsy associated repeat)/EPTP (Epitempin repeat) repeats, 7 transmembrane regions and an intracellular PBM domain (Scheel et al., 2002; Skradski et al., 2001; Staub et al., 2002; Weston et al., 2004). GPR98 is the largest G protein -coupled receptor (GPCR) and the largest known cell surface protein (McMillan and White, 2011). Whirlin (WHRN) is a scaffold protein with three PDZ domains and one proline-rich region (Ebermann et al., 2007a).

4.3 USH3

CLRN1 is predicted to have four transmembrane domains (Adato et al., 2002). Although CLRN1 does not have any clear functional domains, CLRN1 shares homology with the tetraspanin family with four transmembrane domains (Adato et al., 2002). Tetraspanins are thought to act as scaffold proteins that bind proteins into networks in membrane microdomains (Hemler, 2005).

4.4 Usher protein network

USH proteins are thought to interact and form USH protein interactomes, where the USH proteins have different functions. In this interactome CDH23, GPR98, PCDH15 and USH2A are transmembrane proteins (Bahloul et al., 2010; Maerker et al., 2008; Reiners et al., 2005a, 2006; van Wijk et al., 2006). USH1C, SANS and WHRN are the scaffold proteins that link the USH proteins into a functional network (Bahloul et al., 2010; Maerker et al., 2008; Reiners et al., 2005a, 2006; Yan and Liu, 2010; van Wijk et al., 2006). It has been proposed that USH1C and

WHRN function as scaffold proteins in the inner ear while WHRN and SANS function as a scaffold in the retina (Maerker et al., 2008). MYO7A interacts with USH1C and SANS and through them connects the USH interactome to the actin cytoskeleton. MYO7A functions in transporting cargo along the actin filaments (Reiners et al., 2006). The scaffold proteins USH1C (Adato et al., 2005; Siemes et al., 2002), WHRN (Delprat et al., 2005), SANS (Adato et al., 2005) and transport protein MYO7A (Kremer et al., 2006) also form homodimers. The USH interactome has been suggested to function in cell polarity and cell-cell interactions (Yan and Liu, 2010). So far, CLRN1 has not been directly linked to the USH protein network. The similarity of the symptoms in patients with *CLRN1* mutations and in patients with mutations in other USH genes suggest that CLRN1 is somehow linked to this Usher protein interactome and its function.

Several other proteins have been associated with the Usher protein interactome. For example, when *PDZD7* is mutated and inherited together with mutated *USH2A* or *VLGR1* the mutated PDZD7 modifies the USH phenotype. PDZD7 is a homolog to WHRN and USH1C and linked to the USH interactome as a scaffold protein (Ebermann et al., 2010). Vezatin is a transmembrane protein that links MYO7A to membrane cadherin-catenin complexes (Küssel-Anderman et al., 2000). WHRN has been reported to function as a scaffold to "L-type calcium channel subunit $Ca_v1.3(\alpha_{1D})$" (encoded by *CACNA1D*). WHRN and $Ca_v1.3(\alpha_{1D})$ colocalize in photoreceptors connecting cilia and synapses. $Ca_v1.3(\alpha_{1D})$ subunit is assumed to have a similar function as the CACNA1F subunit, which is thought to mediate neurotransmitter release. $Ca_v1.3(\alpha_{1D})$ is associated with X-linked congenital stationary night blindness and X-linked cone-rod dystrophy (Bech-Hansen et al., 1998; Berntson et al., 2003; Jalkanen et al., 2006; Kersten et al., 2010; Strom et al., 1998). NBC3 is a sodium bicarbonate cotransporter responsible for disposal of acid H^+ accumulating in neuronal cells. This protein has been proposed to be a part of the Usher interactome since the lack of functional NBC3 causes hearing impairment and blindness in mice similar to USH (Bok et al., 2003; Reiners et al., 2006).

4.5 Usher proteins in sensory organs

USH manifests itself as retinal and cochlear cell dysfunction. Though these organs are very different, they share similar functional structures. Hair cells in the inner ear and retinal photoreceptors both have non-motile cilial structures as well as special synaptic structures, ribbon synapses. The ribbon synapses are presynaptic structures and come in various shapes and sizes. They tether hundreds of synaptic vesicles near calcium channels controlling exocytosis of

these vesicles into the synaptic cleft directly across from postsynaptic glutamate receptors. This enables rapid and continuous release of neurotransmitters. The ribbon synapses are present only in neurons that need to create continuous but graded electrical signals (rods, cones, bipolar cells and cochlear hair cells) (Fernandez-Alfonso and Ryan, 2006; LoGiudice and Matthews, 2009; Petit, 2001).

4.5.1 Retina

In photoreceptors most USH proteins localize near the connecting cilium. The connecting cilium has a central axoneme structure composed of acetylated tubulin. The tubulin core anchors protein complexes and functions as a route for tubulin associated molecular motor proteins to carry proteins up and down the cilia (Liu et al., 2010). In the connecting cilium, SANS may connect the membrane associated USH protein interactome to the tubulin cytoskeleton whereas MYO7A mediates the transport along actin filaments (Maerker et al., 2008). USH proteins form an interactome also in the periciliary scaffold, which functions in the transport of vesicular cargo between inner and outer segments of photoreceptor cells (Figure 5). This USH protein interactome located in the connecting cilium and in the periciliary region, while still hypothetical, includes the long form of USH2A, full length GPR98, CDH23, MYO7A, SANS, WHRN as well as vezatin and PDZD7 (Ebermann et al., 2010; Maerker et al., 2008; Michalski et al., 2007; Reiners et al., 2006). In this interactome the scaffold proteins SANS and WHRN bind to the intracellular segments of transmembrane proteins USH2A and GPR98. The transmembrane proteins link the photoreceptor inner segment membrane (periciliary ridge) to the connecting cilium by forming a link similar to the stereocilia ankle links across the cleft between connecting cilium and periciliary region plasma membranes (Liu et al., 2007; Maerker et al., 2008).

All USH proteins have been detected in the ribbon synapse region of photoreceptor cells and in the plexiform layers of the retina. In synaptic regions the USH proteins are thought to form an interactome similar to the interactome in the periciliary region, reaching through the synaptic cleft and participating with the synaptic vesicular traffic (Kremer et al., 2006; Reiners et al., 2003, 2005a, 2005b; 2006; Reiners and Wolfrum, 2006; van Wijk et al., 2006). This model for the USH protein interactome in synapses is widely accepted even though some studies have found contrasting results, where USH proteins could not be found in the retinal synapses (Liu et al., 2007; Williams, 2008). PDZD7 does not localize into the photoreceptor synapse. However, mutated PDZD7 has only been identified to modify the USH phenotype in USH patients when

combined with mutated *USH2A* or *VLGR1b* (Ebermann et al., 2010). PDZD7 localization in photoreceptor cilia, but not in the photoreceptor synapse, suggest that either the crucial function of the USH protein interactome is in the synapse and the absence of the USH interactome function in connecting cilia only aggravates the USH phenotype or that the PDZD7 function in the connecting cilia can be augmented if PDZD7 is mutated unless USH2A and VLGR1 are mutated as well. There is clinical evidence for synaptic function of the USH protein interactome as the *Cdh23* mutant mouse has attennuated ERG a- and b-wave amplitudes suggesting abnormal photoreceptor synaptic function (Libby et al., 2003). However, USH patients show no signs of synaptic dysfunction prior to photoreceptor degeneration (Jacobson et al., 2008).

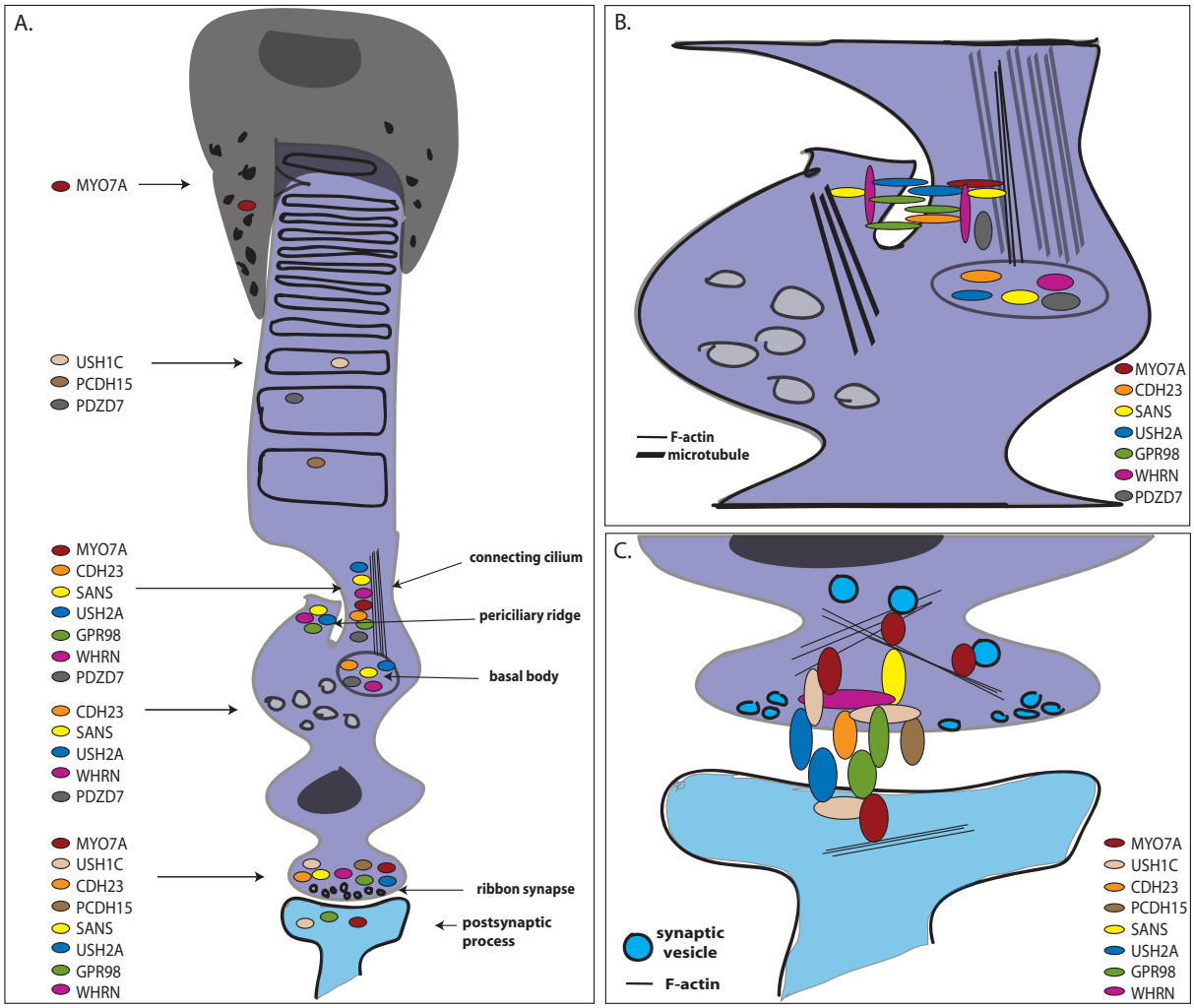

Figure 5. A) Known localizations of USH proteins in a photoreceptor cell. MYO7A localizes to the RPE cells; USH1C, PCDH15 and PDZD7 to the photoreceptor outer segment; MYO7A, CDH23, SANS, USH2A, GPR98, WHRN and PZDZ7 to the connecting cilium/periciliary ridge; CDH23, SANS, USH2A, WHRN and PDZD7 to the base of the connecting cilium; MYO7A, USH1C, CDH23, PCDH15, SANS, USH2A, GPR98 and WHRN to

the synaptic region (Liu et al., 1999a, 2007; Maerker et al., 2008; Reiners et al., 2005a, 2005b, 2006; Williams et al., 2009). B) Close up of the photoreceptor connecting cilium region. The USH interactome has been suggested to form a link between the connecting cilium and periciliary ridge (Maerker et al., 2008; Yang et al., 2010). C) Close up of the photoreceptor synapse. USH proteins localize to the synaptic region and the USH interactome has been suggested to form links crossing the synaptic cleft (Kremer et al., 2006; Reiners et al., 2003, 2005a, 2005b, 2006; Reiners and Wolfrum, 2006; van Wijk et al., 2006).

USH proteins are not exclusively localized to photoreceptor connecting cilia/periciliary ridge region and synapses. MYO7A, which is associated with F-actin traffic, functions in the transport of phagocytosized outer segment sections and melanosomes along actin filaments in RPE cells (Hasson et al., 1995; Liu et al., 1998a, 1999b; Gibbs et al., 2004). USH1C has been localized into outer segment disk membranes where it may function in organizing macromolecular complexes. PCDH15 is also localized to the outer segment plasmamembrane and disk membranes. PCDH15 as well as GPR98, SANS, USH2A and WHRN have been suggested to be part of cell-cell adhesion between photoreceptors and photoreceptor contacts with the Müller glia cells by their presence in the OLM region associated with these functions (Kremer et al., 2006; Reiners et al., 2003, 2005b). CDH23, SANS, USH2A and WHRN have been localized to the basal body near the base of the connecting cilium (Maerker et al., 2008; Reiners et al., 2005a, 2006; Williams et al., 2009). PDZD7, a modifier protein for USH, has also been identified in photoreceptor outer segments and in the base of connecting cilia (Ebermann et al., 2010).

Aside from photoreceptors and OPL, USH proteins have been reported in other layers of retina (Figure 6). PCDH15 has been localized to the IPL, OLM and GCL (Ahmed et al., 2003a; Reiners et al., 2003; 2005b), MYO7A to RPE (Hasson et al., 1995; Liu et al., 1997a), USH2A to OLM and Bruch's membrane, GPR98 to OLM and RPE precursor cells, USH1C to IPL, Müller cells and GCL (Bhattacharya et al., 2002; McMillan et al., 2002; Phillips et al., 2008/personal communication; Reiners et al., 2003; 2005a; Reiners and Wolfrum, 2006; van Wijk et al., 2006), SANS to IPL and OLM (Overlack et al., 2008), WHRN to OLM and GCL (van Wijk et al., 2006) and USH modifier PDZD7 to INL (Ebermann et al., 2010). CDH23 has only been localized to the OPL (Lagziel et al., 2009).

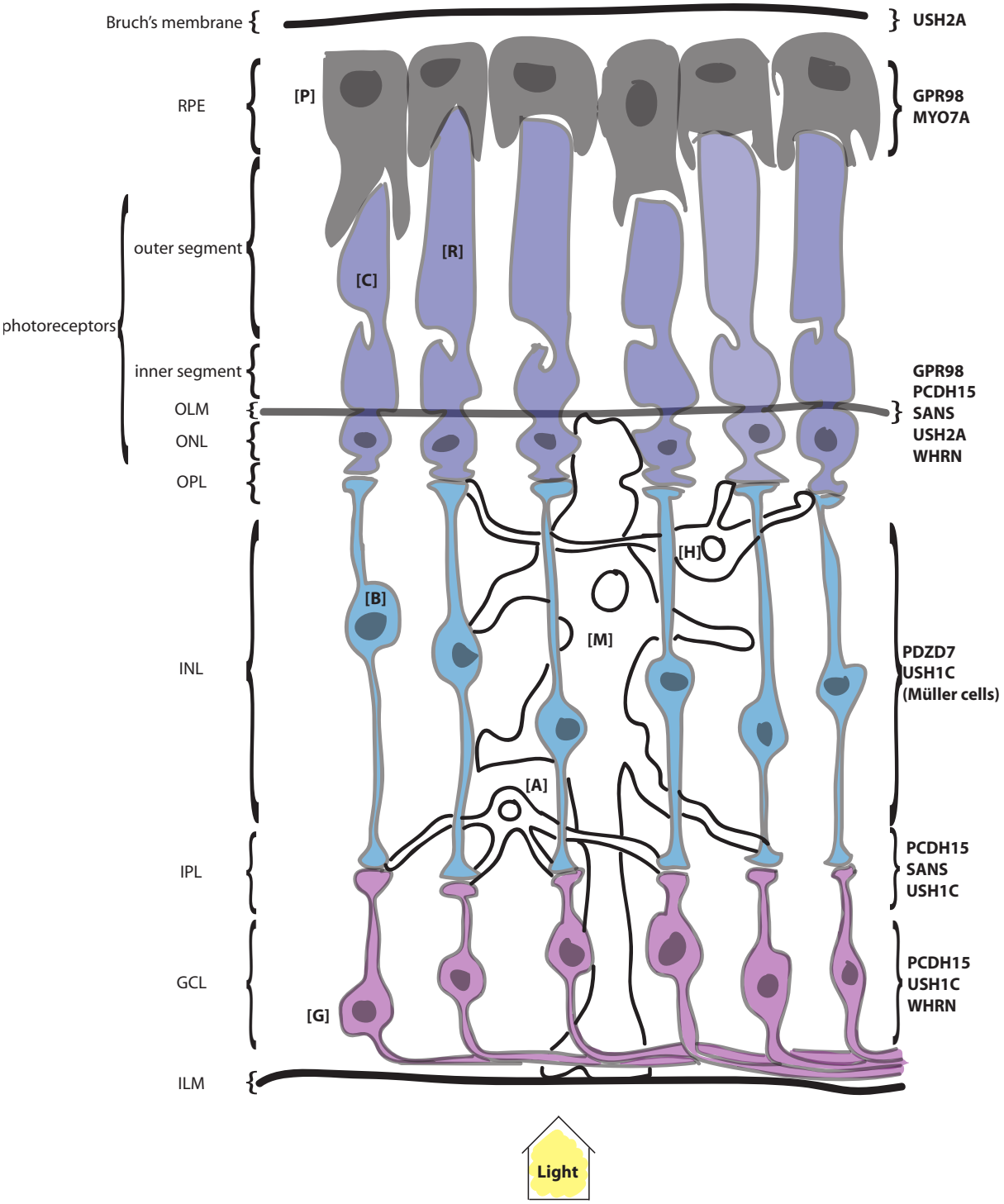

Figure 6. USH protein localization in the retina excluding photoreceptor and OPL localization depicted in Figure 5. Four of the five USH1 proteins, all the three USH2 proteins and the USH modifier protein, PDZD7, are also present in other retinal cell types.

4.5.2 Cochlea

In cochlea all the USH proteins have been localized to the inner ear hair cells (Figure 7). The reported USH protein localizations and interactions have suggested specific roles for the USH proteins in the hair cells especially in the development of stereocilia and/or kinocilia (Saihan et al., 2009). The USH proteins have been suggested to form an interactome similar to the periciliary interactome in photoreceptors especially at the ankle links of developing stereocilia (Michalski et al., 2007). Transmembrane USH2A and GPR98 proteins function in forming the transient ankle links between stereocilia (Adato et al., 2005; McGee et al., 2006). Transmembrane CDH23 and PCDH15 proteins are part of the transient lateral links and kinociliary links. In the later stage of development CDH23 and PCDH15 form heteromeric complexes in the stereocilia tip links. Scaffold protein USH1C isoform b has a similar localization pattern. It is detected along the entire stereocilia during development, but later USH1C isoform b is localized mainly to the tip of stereocilia (Böeda et al., 2002). The USH2A and GPR98 in the ankle links as well as CDH23 and PCDH15 have PDZ binding domains that can link them to USH1C and WHRN. USH1C and WHRN anchor the extracellular links. CDH23, GPR98, PCDH15 and USH2A interact through USH1C and WHRN with MYO7A and SANS connecting the extracellular links to the actin cytoskeleton (Reiners et al., 2006; Yan and Liu, 2010).

MYO7A is also connected to vezatin, a transmembrane protein that provides another link from the plasma membrane to the actin cytoskeleton. Vezatin localizes to the junctions between hair cells and supporting cells. Likewise MYO7A colocalizes to the pericuticular necklace between adherens junctions and the cuticular plate (Hasson et al., 1997; Küssel-Andermann et al., 2000). MYO7A most likely functions in transporting the other USH proteins along the stereocilia as well as vesicle traffic and membrane uptake in the pericuticular necklace region (Richardson et al., 1997; Rhodes et al., 2004). USH1C likely functions in cell polarity as well as cell-cell interactions (Johnston et al., 2004; Yan et al., 2006). The scaffold protein WHRN is linked to F-actin growth (Mburu et al., 2003). The localization of SANS in the cuticular plate region and reports that it interacts with MYO7A as well as CDH23 and USH1C suggest a role for SANS in trafficking the USH proteins towards the stereocilia (Yan and Liu, 2010; Saihan et al., 2009; Weil et al., 2003).

The fact that USH proteins associate with cilia both in the photoreceptors and in the inner ear hair cells, as well as in tissues like olfactory epithelium and spermatozoa (Adato et al., 2002; Barrong et al., 1992; Hunter et al., 1986; Reiners et al., 2006; Saihan et al., 2009; Wolfrum et al., 1998), is the reason why USH has been classified as a ciliopathy even though the USH disease

pathology lacks symptoms like primary ciliary dyskinesia, polycystic liver/kidney disease and hydrocephalus associated with other ciliopathies (Adams et al., 2007).

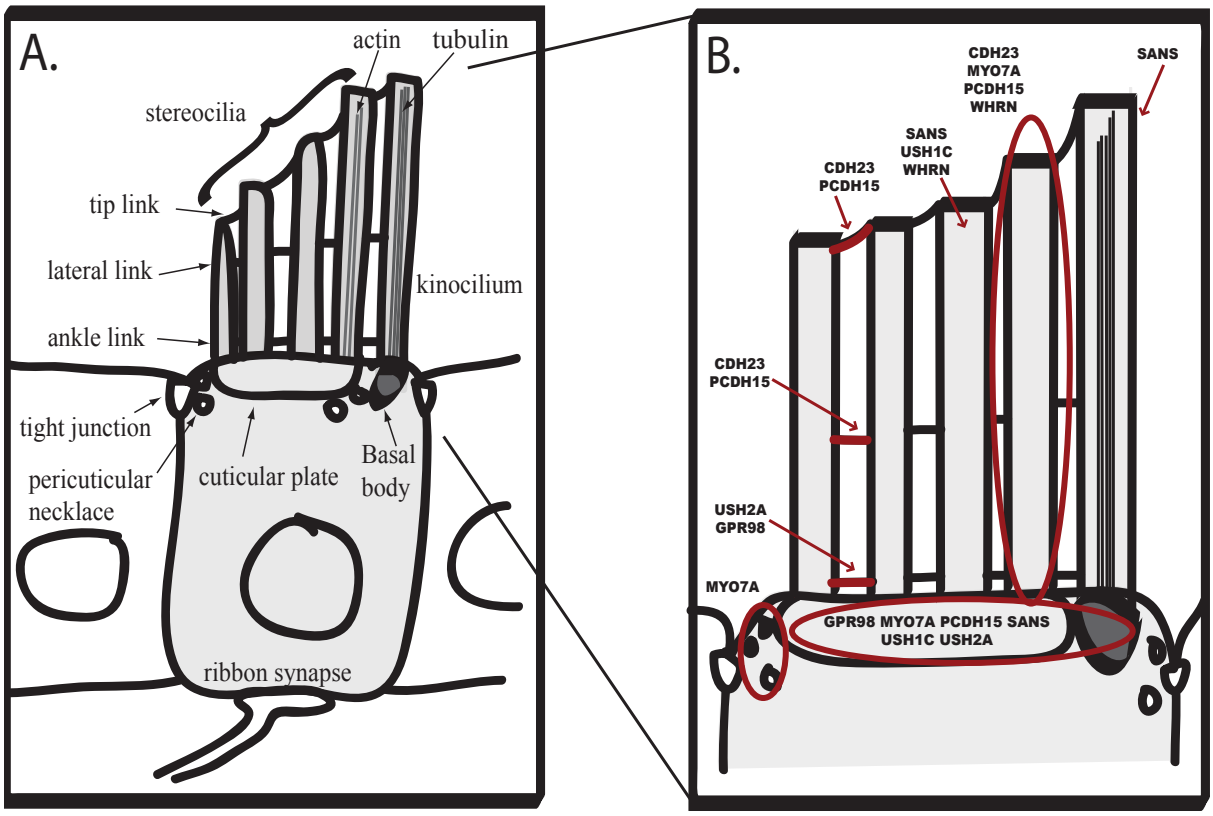

Figure 7. Structure of a hair cell (A) and localization of USH proteins in the hair cell ciliary region (B). USH2A (Adato et al., 2005) and GPR98 (McGee et al., 2006) are part of the ankle links between stereocilia, CDH23 and PCDH15 are part of the lateral links as well as tip links and kinocilial links (Lagziel et al., 2005; Michel et al., 2005; Kazmierczak et al., 2007). WHRN (Delprat et al., 2005), USH1C isoform B (Böeda et al., 2002) and SANS (Caberlotto et al., 2011) are localized to the tips of stereocilia. MYO7A is located in the pericuticular necklace (Hasson et al., 1997). GPR98 (McGee et al., 2006), MYO7A (El-Amraoui et al., 1996), PCDH15 (Yan et al., 2011), SANS (Adato et al., 2005), USH1C (Böeda et al., 2002) and USH2A (Adato et al., 2005) are located in the cuticular plate region beneath the stereocilia. CDH23 (Böeda et al., 2002) and PCDH15 (Ahmed et al., 2003a) are localized along the entire length of the stereocilia as well as MYO7A (Hasson et al., 1997; El-Amraoui et al., 1996) and WHRN (Mburu et al., 2003) that are associated with actin filaments within the stereocilia. SANS has been detected in the kinocilium (Reiners et al., 2006).

All the USH proteins also localize to the hair cell synaptic region. The hair cell synapse, like the photoreceptor synapse, has specialized synaptic structures, ribbon synapses, and a similar need for sustained synaptic activity (Kremer et al., 2006; Saihan et al.,2009; Yan and Liu, 2010). A study with mice either carrying *CDH23* with missense mutations or *CDH23* null alleles suggest

that USH is caused by the absence of CDH23. The absence of CDH23 prevents USH interactome function in stereocilia development and thus correct hair bundle organization. Nonsyndromic deafness, DFNB12, is caused by missense mutations in *CDH23*, which allow normal hair bundle organization but cause tip link loss leading to mechnotransduction defects (Schwander et al., 2009).

USH proteins in cochlea are not exclusively present in hair cells. USH proteins or USH gene expression have also been detected in spiral ganglion neurons (USH2A, PCDH15, CLRN1), Reissner's membrane (CDH23) and supporting cells (SANS, PCDH15, USH2A) (Kremer et al., 2006).

5. Usher syndrome animal models

5.1 Mouse

There are naturally occurring mouse models for six of the USH subtypes: MYO7A (*shaker-1*), CDH23 (*waltzer*), PCDH15 (*Ames waltzer*), SANS (*Jackson shaker*), WHRN (*whirler*) and USH1C (*deaf circler*) as well as genetically modified mouse models GPR98 ($VLGR1^{del7TM}$), USH1C (Ush1c216AA), $USH2A^{-/-}$ and $whirlin^{-/-}$. Only three of these models develop retinal degeneration. *Deaf circler* (*USH1C*) has mild peripheral retinal degeneration (Johnson et al., 2003b), the Ush1c216AA knock-in mouse has progressive retinal degeneration starting at the periphery (Lentz et al., 2010) and $USH2A^{-/-}$ knockout mouse has normal retina at birth, but later undergo photoreceptor degeneration (Liu et al., 2007). $Whirlin^{-/-}$ mice have shortened photoreceptor outer segments and thinner photoreceptor nuclear layers. These changes indicate that the USH mouse model develops late-onset retinal degeneration (Yang et al., 2010). *Shaker-1* (*MYO7A*), *waltzer* (*CDH23*), *Ames waltzer* (*PCDH15*) and $VLGR1^{del7TM}$ mice have reduced ERG amplitudes. *Shaker-1* (*MYO7A*) mouse also has increased opsin levels in the photoreceptor connecting cilia and aberrant melanosome and phagosome localization in the RPE. However, none of these four mouse models have a retinal degeneration phenotype (Williams, 2008), although *shaker-1* mouse was recently reported to be susceptible for light induced rod photoreceptor degeneration caused by delayed transducin translocation (Peng et al., 2011). The mouse retina consists mostly of rods whereas the human retina is cone-dominated (Chang and Harris, 1998; Harris and Messersmith, 1992). The differences in retinal composition and subsequent molecular differences could be the reason why only four mouse models develop some kind of retinal degeneration and none of the USH mice develop RP similar to human USH patients. All the USH mouse models show abnormal

inner ear hair bundle morphology that leads to hearing deficits and hair cell degeneration consistent with the human disease phenotype.

The discrepancy in the ear and eye symptoms between human and mouse has been hypothesized to be caused by species specific alternative splicing of the USH genes, functional redundancy of USH proteins in mouse or slow progression of retinal degeneration compared to the short mouse lifespan (Ahmed et al., 2003b; Liu et al., 2007). For example, *Ush1c* is expressed at lower levels in the mouse retina than in the ear, which could implicate a greater importance for *Ush1c* in the ear and explain the start of the decline in ERG amplitude at 11 months whereas the ear dysfunction is present at birth (Tian et al., 2010). There is also a mouse model for the nonsyndromic deafness DFNB12 with a missense mutation in *cdh23* (*salsa*). Curiously this mutation in the *salsa* mouse only affects mechanotransduction in the hair cells, but not the hair bundle shape, which might also explain the nonsyndromic deafness in human patients (Yan and Liu, 2010). The USH mouse models have increased the knowledge about USH protein function in the hair cells. For example, the role for MYO7A in transport is supported by the findings in the MYO7A mutant mouse (*shaker-1*). In this mouse model other USH proteins (USH1C, PCDH15, GPR98, USH2A and WHRN) are mislocalized in the stereocilia (Böeda et al., 2002; Michalski et al., 2007; Senften et al., 2006). The *shaker-1* mouse has also shed light to MYO7A function in retina. In photoreceptors, opsin concentration is increased in the connecting cilium, and in the RPE, melanosome and phagosome localization is abnormal (Gibbs et al., 2003; Gibbs et al., 2004; Liu et al., 1998a, 1999b).

5.2 Zebrafish

Since most USH mouse models do not develop retinal degeneration similar to the human USH pathology other disease models have been studied. Zebrafish has become an interesting alternative as a USH model organism.

Zebrafish development is fast compared to mouse. The chorions and embryos are transparent, with all the main organ systems formed 24 hours post fertilization (hpf). Before 48 hpf the larvae already have muscular response to stimuli and at 3 days post fertilization (dpf) the larvae are able to swim and feed. At 5 dpf over 95 % of larvae have optokinetic response (OKR) with pursuit and saccade eye movements in response to rotating stripes (Fadool and Dowling, 2006). When applied to young larvae the OKR method measures the cone response as the rods mature later in development. The rod ERG can usually be measured between 15-18 dpf (Bilotta

and Saszik, 2001). Zebrafish are diurnal and rely more on visual information for survival when compared to rodents. Zebrafish have four different types of cones with opsins sensitive to red, green, blue and UV light (Nawrocki, 1985; Vihtelic, 1999; Chinen et al., 2003). The proportion of cone photoreceptors makes the zebrafish retina more similar to human retinas than to rod-dominant rodent retinas. Therefore, it is not surprising that when *ush1c*, *ush2a*, and *gpr98* have been knocked down by gene specific morpholino (MO) injections into zebrafish embryos the larvae develop visual phenotypes unlike most of the USH mouse models (Williams, 2008).

The zebrafish ear is comparable to the inner ear of mammals, although the structures are different. Although zebrafish lack cochlea, the mechanosensory hair cells necessary for balance and hearing are concentrated in five sensory patches within the ear capsule. These hair cells are also present in neuromasts in the zebrafish lateral line. Neuromasts are hair cell structures on the surface of the fish that are specialized to sense water movement. The sensory hair cell structure as well as function and development are conserved in evolution and are comparable between human and zebrafish (Nicolson, 2005; Whitfield et al., 2002a, 2002b). There are three zebrafish USH models with mutated USH genes: *mariner* (USH1B, *myo7a*), *sputnik* (USH1D, *cdh*23) and *orbiter* (USH1F, *pcdh*15). *Myo7a* and *cdh23* mutants have balance problems, and the *myo7a* mutant has defects in melanosome localization in the RPE. Due to an ancient genome duplication event the zebrafish possesses two copies of *pcdh15*. *Pcdh15a* functions in hearing and balance and *pcdh15b* functions in photoreceptor outer segment formation. MO knockdowns have also been made for *ush1c*, *ush2a* and *gpr98*. These knockdown models for USH have balance problems and reduced visual function (Williams, 2008).

6. Development of gene therapies

The final goal for the USH research is to understand the cause for the syndrome and develop potential cures for the disease. Now that most, if not all, of the USH genes are known, gene therapy has become the ultimate goal for USH research (Williams, 2008). Gene therapy trials are already in progress for other retinal diseases. The *RPE65* gene therapy research to cure the dog model for Leber congenital amaurosis was successful and promising long-term results have been gained with Leber congenital amaurosis patient gene therapy trials (Cideciyan et al., 2008, 2009; Hauswirth et al., 2008).

USH gene therapy research is already under way. For example, *MYO7A,* the causative gene for USH1B, has been successfully transducted using a lentiviral vector to cultured RPE cells

from *Myo7a* knockout mice. The transduction was followed by *MYO7A* expression correcting melanosome motility and phagosome digestion in RPE cells. Melanosome localization and opsin transport returned to normal levels when this same transduction was done *in vivo* in these knockout mice (Hashimoto et al., 2007).

Other therapies for USH are also under investigation. One of the most recent developments is using aminoglycosides to enable translational read-through of nonsense mutations. In subtypes USH1C (underlying gene *USH1C*) and USH1F (*pcdh15*) aminoglycoside treatments have been reported to enable translation of functional proteins in cell culture studies (Goldmann et al., 2010; Rebibo-Sabbah et al., 2007). *USH1C* nonsense mutation read-through has also been studied using a compound called PTC124 in cell cultures, retinal cultures and *in vivo* in mice retinas. The results are promising with successful USH1C protein production through the nonsense mutation and good biocompatibility with the retina (Goldmann et al., 2011).

AIMS OF THE STUDY

The positional cloning and identification of the *USH3A* gene, *CLRN1,* was done prior to this study (Sankila et al., 1995; Joensuu et al., 2001; Adato et al., 2002). The first two USH3 mutations were found in Finnish patients during the identification of the gene (Joensuu et al., 2001). The two USH3 mutations were the only USH mutations known in Finland prior to this study. The molecular epidemiology of other USH types in Finland was unknown. After the discovery of the *CLRN1* gene, 11 other USH3 mutations were discovered worldwide (Adato et al., 2002; Aller et al., 2004a; Fields et al., 2002; Joensuu et al., 2001; Ness et al., 2003; Sadeghi et al., 2005). The expression of *CLRN1* in mouse cochlea was known (Adato et al., 2002) and the expression in retina and the function of CLRN1 was unknown. The aims of this study were:

1. To identify new mutations in *CLRN1* causing USH3 and to investigate the Finnish USH mutation spectrum.

2. To further study the structure of the *CLRN1* gene to provide the basis for USH3 gene therapy research.

3. To gain more information about CLRN1 function through studying the effect of different USH3 mutations on CLRN1.

4. To study the USH3 disease mechanism by developing animal models for USH3.

MATERIALS AND METHODS

1. Subjects and samples

Altogether 45 Finnish patients, 40 Canadian patients and 2 US patients were included in the mutation studies (Figure 8). All the patients gave informed consent before sample collection. The studies including patient samples were approved by the Ethics Committee of the Eye and Ear Hospital Helsinki, The Hospital for Sick Children Toronto Canada, and the University of California San Francisco (UCSF), CA, USA. Healthy controls were taken from samples provided by the Finnish Red Cross Blood Transfusion Service and Centre d'Etude du Polymorphisme Humain. The research project was approved by the Ethics Committee of the Department of Medical Genetics, University of Helsinki. Zebrafish experiments in the unpublished data (U) were approved by the Institutional Animal Care and Use Committee (IACUC) and performed in the wild-type Oregon AB background.

Stage I

***CLRN1* main exons sequenced (I-IV & U, 2005-2011)**	
45 Finnish patients:	2 USH1 -> *MYO7A* sequenced (I, 2006**)** 7 USH2 22 USH3 14 USH subtype unknown --- 45 Finnish USH patients
40 CANADIAN PATIENTS:	USH1: 2 USH2: 9 USH3: 3 26 USH subtype unknown --- 40 Canadian USH patients
2 US PATIENTS:	USH3: 2

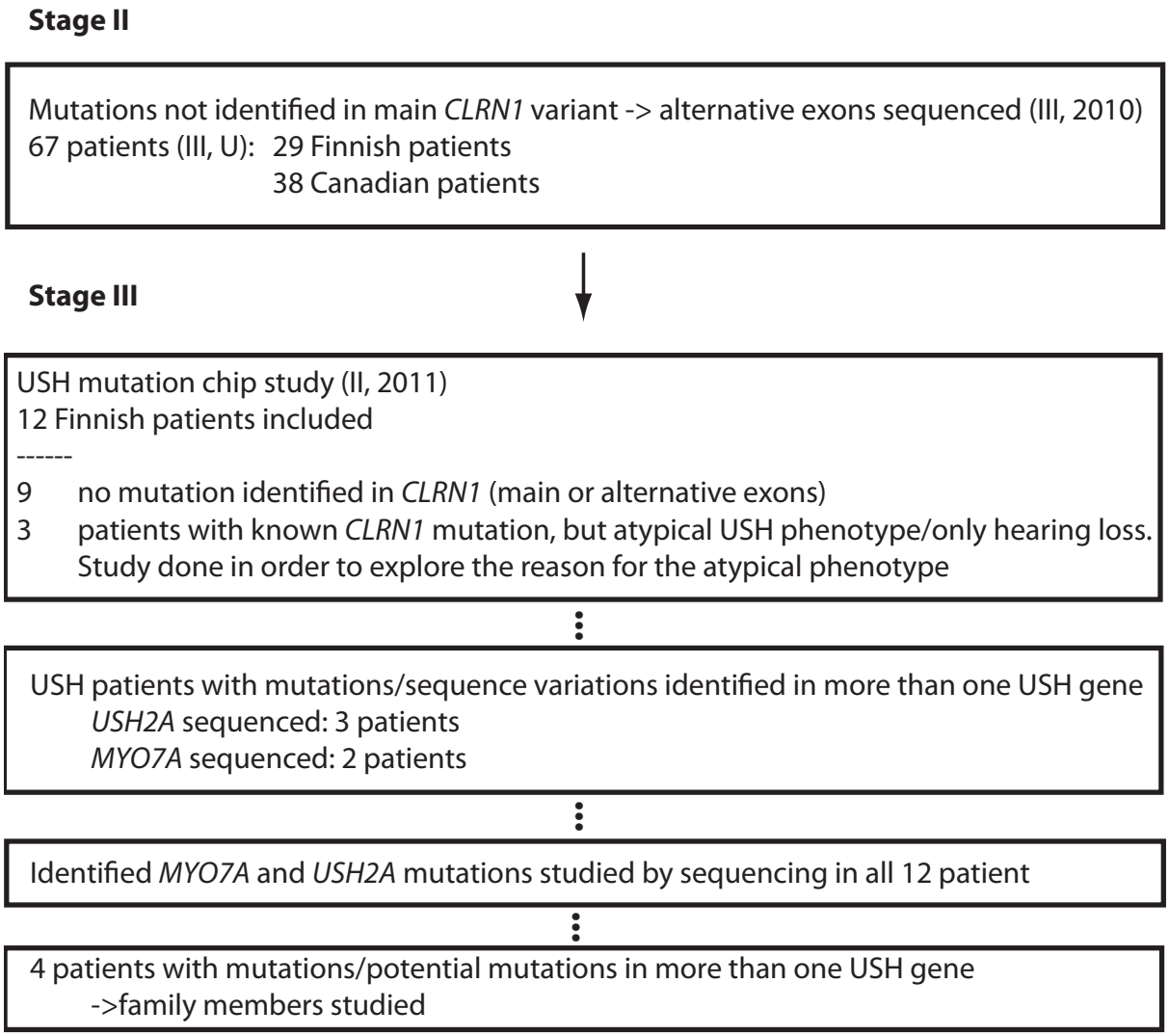

Figure 8. Patient samples included in this thesis study (Patients not clinically diagnosed as USH3 were included in the *CLRN1* sequencing study for their uncertain USH subtype diagnosis), the articles they were included in (I-IV and U) and the methods the samples were studied with.

2.Methods

2.1 Common methods (I-IV)

DNA was extracted and purified either with Oragene™ saliva kits (DNA Genotek Inc., Ottawa, Canada) or DNA Purification Kits (Gentra Systems, MN, USA). RNA was extracted with the RNeasy® mini kit (Qiagen, Germany), RNAqueous® -4PCR Kit (Ambion Inc., TX, USA) or using TRIzol® reagent (Invitrogen, ON, USA) and cDNA synthesized with the M-MLV enzyme (Promega,

WI, USA). Polymerase chain reactions (PCR) were performed with Advantage® -GC 2 (Clontech, CA, USA), Amplitaq Gold™ (Applied Biosystems, CA, USA), Biotools DNA Polymerase (Biotools B&M Labs, Spain), Dynazyme™ II DNA polymerase (Finnzymes, Finland), FastStart Taq DNA polymerase (Roche, Germany) or Titanium® Taq (Clontech). The amplification conditions are described in the articles. When required the amplified samples were run through an agarose gel and the size separated DNA samples were extracted with the QIAquick® Gel Extraction Kit (Qiagen). The PCR products were purified using Exo-SAP (USB, OH, USA) and sequenced using the ABI PRISM BigDye® Terminator v3.1 Cycle Sequencing Kit (Applied Biosystems) and ABI3730 Automatic DNA sequencer (Applied Biosystems).

2.2 Sequence and mutation analysis (I-IV)

Sequences were analyzed using Sequencher 4.1 (Gene Codes corporation, MI, USA) and compared to the control sequences obtained either from healthy individuals or from databases (Aceview: [http://www.ncbi.nlm.nih.gov/IEB/Research/Acembly/], EMBL-EBI [European Molecular Biology Laboratory's European Bioinformatics Institute]: http://www.ebi.ac.uk/, NCBI [National Center for Biotechnology Information]: http://www.ncbi.nlm.nih.gov/, UCSC Genome Browser [University of California Santa Cruz]: http://genome.ucsc.edu/). Some of the patient's DNA samples were also analyzed by a USH mutation chip constructed by the arrayed primer extension (APEX) method (Asper Biotech, Estonia). Restriction enzyme digestion was used in mutation detection by running the restriction products through an agarose gel to detect the change in PCR product size. The restriction enzymes and conditions are reported in the original articles.

2.3 Bioinformatics (I-IV)

Primers were designed by Primer3 (http://frodo.wi.mit.edu/cgi-bin/primer3/primer3_www.cgi) when possible. Sequence comparisons and searches were performed with NCBI-BLAST (http://blast.ncbi.nlm.nih.gov/Blast.cgi) and UCSC Genome Browser Blat (http://genome.ucsc.edu/cgi-bin/hgBlat). ClustalW (http://www.ebi.ac.uk/Tools/clustalw2/index.html) and LALIGN (http://www.ch.embnet.org/software/LALIGN_form.html) programs were used to compare protein and DNA sequences. Protein weights were predicted using the Protein Molecular Weight Program (http://www.bioinformatics.org/sms/prot_mw.html), transmembrane regions using TMHMM2.0

(http://www.cbs.dtu.dk/services/TMHMM/) and TMpred (http://www.ch.embnet.org/software/TMPRED_form.html). CpG islands were identified with EMBOSS CpG island prediction software (http://emboss.ch.embnet.org/wEMBOSS/) and transcription factor binding sites with TESS (http://www.cbil.upenn.edu/tess). The pathogenicity of sequence variations were studied with ASSP (http://es.embnet.org/~mwang/assp.html), MutationTaster (http://www.mutationtaster.org/), NNsplice (http://www.fruitfly.org/seq_tools/splice.html), PolyPhen-2 (http://genetics.bwh.harvard.edu/pph/) and Spliceview (http://zeus2.itb.cnr.it/~webgene/wwwspliceview_ex.html). Sequence evolutionary conservation was studied using the UCSC Genome Browser (UCSC: Human, Rhesus, Mouse, Dog, Chicken [http://genome.ucsc.edu/]).

2.4 Recombinant DNA techniques (III, IV)

Amplified promoter DNA segments were inserted into pGluc-Basic vector (New England BioLabs, MA, USA). *CLRN1* coding region and alternative splice variants, amplified by designing primers to the known or predicted exon sequences within the *CLRN1* region and nearby ESTs, were cloned into TOPO TA cloning vectors (Invitrogen, CA, USA). The *CLRN1* coding region was also inserted into hemagglutinin (HA)-tag containing phCMV3 Xi cloning vector (Gene Therapy Systems Inc., CA, USA). The QuickChange site-directed *in vitro* mutagenesis kit (Stratagene, CA, USA) was used to mutate the wt *CLRN1* vector and create the USH3 mutant vector constructs.

2.5 Cell culture studies (II-IV, U: unpublished work)

Patient and healthy control lymphoblastoids cell lines were cultured and used as a source of RNA. Mouse retinal primary neurons were cultured by homogenizing dissected fetal mouse retinas, E14-E16, in PBS. After DNase I (Roche) and Trypsin-EDTA (HUSLAB, Biomedicum Helsinki, Finland) treatment, the cells were mixed in Neurobasal® medium (Gibco, CA, USA) with Gibco® B-27 supplement (Gibco) and Penicillin-Streptomycin antibody (HUSLAB) and plated on Matrigel™ Basement Membrane Matrix (Becton Dickinson Labware, NJ, USA) coated cell culture dishes. The cells were incubated at +37˚C and transfected three days after plating with CLRN1-HA (phCMV3 Xi) plasmid.

Baby hamster kidney (BHK-21, CCL-10, the American Type Culture Collection [ATCC]), African green monkey kidney (COS-1, CRL-1650, ATCC), human embryonic kidney

(HEK-293, CRL-1573, ATCC), human cervical cancer (HELA, CCL-2, ATCC), human retinoblastoma (WERI-Rb-1, HTB-169, ATCC) cell cultures and mouse retinal neuron cultures were transfected with plasmid constructs (see 2.4) using either Fugene®6 or Fugene®HD transfection reagents (Roche Diagnostics, Switzerland). When protein degradation speed was studied, the protein production was stopped by adding 50 µg/ml cycloheximide (Sigma-Aldrich) into the cell culture media for 4 hours before fixing the cells. The transfected cells were fixed after 24 or 48 hours of transfection with 4 % paraformaldehyde (PFA) and permeabilized by treatment with ice cold methanol or 0.2 % saponin (Sigma-Aldrich, Germany).

For the immunofluorescent staining, the cells were treated with 5 % bovine serum albumin (BSA) (Jackson ImmunoResearch, PA, USA). Then the cells were incubated with antibodies against HA (HA.11 [MMS-101R]; Covance, CA, USA), endoplasmic reticulum protein disulfide isomerase (PDI [spa-891]; Stressgen, Victoria, Canada) and plasmamembrane sodium potassium ATPase (ab7671; Abcam, UK) that were diluted in BSA. The cells were then incubated with secondary antibodies conjugated either with Cy2 or Cy3 (Jackson ImmunoResearch). Cells were mounted with Gel/Mount (Biomeda, CA, USA). The cells were analysed with Zeiss Axioplan 2 and Leica CMR confocal microscopes.

The promoter activity studies were performed using cell culture media collected after 48 hours of transfection. The transfections were performed with pGluc Basic vector inserted with *CLRN1* alternative promoter regions that were considered interesting according to the *in silico* studies (1-1550 nt upstream of exon 0, exon 1, exon 2 and exon 3 as well as 1-500 nt and 1-1000 nt upstream of *CLRN1* exon 0) and pCMV-Gluc control vector (New England Biolabs). The media samples were analysed with the Gaussian Luciferase Assay kit (New England Biolabs) using a Victor 2 Wallac 1420 multilabel counter (Perkin Elmer, MA, USA).

2.6 cDNA panels and RACE (III, U)

Splice variant expression profiles were studied with cDNA from human retinal cDNA library (Clontech), human retinal pigment epithelial cell line (ARPE-19), human cochlear cDNA and Human Multiple Tissue cDNA panels I and II (Clontech). Rapid amplification of cDNA ends (RACE) was performed to find the alternative 5’ and 3’ ends of *CLRN1* splice variants using the RACE system Version 2.0 (Invitrogen).

2.7 CLRN1 protein studies (IV, U)

Cells transfected with protein expression vectors were collected by centrifugation. Samples were separated by running them through-polyacrylamide (PAGE) gels (National Diagnostics, GA, USA) and transferred to Trans-Blot® nitrocellulose membranes (Bio-Rad, CA, USA). The membranes were immunostained and visualized by SuperSignal® West Pico Chemiluminescent staining (Pierce, IL, USA) and captured on X-ray film (Sigma-Alrich). When glycosylation was studied the samples were pre-treated with N-glycosidase F enzyme PNGase F (New England Biolabs).

For the CLRN1 antibody production studies, GST-tagged CLRN1 peptides were designed by inserting *CLRN1* coding sequences into pGEX-4T-1 vector (GE Healthcare, UK). The TNT® T7 Quick Coupled Transcription/Translation System (Promega) was used for protein production and proteins were collected using the MagneGST™ Pull-Down System (Promega).

2.8 Phage display antibody search (U)

Antibodies against CLRN1 epitopes were searched with the GST-tagged CLRN1 constructs using phage display technology (Hoogenboom and Chames, 2000). The antibody library used in the screening was made from 50 Finnish Red Cross Blood Transfusion Service lymphocyte samples. The human library was called naïve because the light- chain and heavy-chain IgM-V-gene pools obtained from B cells were from nonimmunized humans. The antibody library displayed by phagemid vectors was screened by attaching the CLRN1 antigens on to wells of 96 well plates and washing with the phagemids displaying the antibody library. The antibodies binding to the CLRN1-GST antigen were selected for further screenings. The research procedure is further explained in (Turunen et al., 2009).

2.9 Morpholino design and injections (U)

Morpholino oligonucleotides (MO) were designed to bind either to the zebrafish *clrn1* first exon donor splice site (Clrn1MOsplice) or the translation start site (Clrn1MOatg) (Gene Tools LLC, OR, USA). The MOs were injected into one-cell stage zebrafish embryos using different

concentrations and volumes, with the quantity of MO ranging from 17 ng to 51 ng per injection.

2.10 *In situ* hybridization (U)

Clrn1 gene expression was studied using *in situ* hybridization. The zebrafish were fixed in 4 % PFA in PBS-T (PBS with 0,01 % Tween-20) overnight at 4°C, washed with PBS-T and dehydrated with methanol at -20°C overnight. The zebrafish were then rehydrated in descending concentration of methanol in PBS-T and washed with PBS-T containing first 10 % sucrose and then 30 % sucrose in PBS overnight at 4°C. The zebrafish were then embedded into 1.5 % agar and 5 % sucrose and sunk in 30 % sucrose overnight. The embedded fish were then cut with a cryostat into 16 µm sections. *In situ* hybridization was performed with a *Clrn1* specific probe using NBT (Nitro blue tetrazolium chloride) and BCIP (5-Bromo-4-chloro-3-indolyl phosphate) staining to visualize the binding (Ebermann et al., 2010; Jensen et al., 2001).

2.11 Immunohistochemistry (U)

Cryosectioned fish samples were blocked using 10 % normal goat serum (NGS) and 2 % BSA in PBS, then treated with primary antibodies (anti-acetylated tubulin, Sigma-Aldrich; anti-Clrn1, Strategic Diagnostics Inc, DE, USA; anti-glutamine synthetase, Millipore, MA, USA; synaptic marker (synaptic vesicle protein 2 [SV2], provided by Buckley KM, Harvard Medical School, MA, USA) diluted in blocking solution. After incubation with the primary antibody and further washes in PBS, the sections were treated with secondary antibodies (AlexaFluor 488 or Alexa Fluor 568, Molecular Probes, OR, USA) diluted in blocking solution. The slides were then washed with PBS and mounted with Vectashield (Vector Laboratories Inc, CA, USA). Zeiss LSM5 or Bio-Rad Radiance 2100 confocal microscopes were used in antibody binding detection.

2.12 Zebrafish behavioral analysis (U)

The fish were maintained as described in Westerfield, 2007. Zebrafish balance/hearing analysis was done either by twirling the dish and observing the zebrafish larvae recovery after twirling the media or tapping the petri dish and observing the fish response to the tap. Zebrafish vision was analyzed by measuring OKR (optokinetic response) while the larvae were suspended in an upright position in a petri dish containing 3 % methyl cellulose. The petri dish was mounted on a platform surrounded by a rotating drum. OKR was done by recording larvae eye movements following moving stripes within one minute, changing once the direction of stripe movement from clockwise to counter clockwise.

2.13 Statistical analysis (U)

Unpaired *t* tests were used to calculate statistical significance between control and MO injected zebrafish larvae groups. P values equal to or less than 0.01 were considered significant (http://www.graphpad.com/quickcalcs/ttest1.cfm?Format=SD).

RESULTS AND DISCUSSION

1. Usher syndrome mutations

The Finnish USH mutation spectrum was studied to help clinical diagnostics. The unique Finnish population history marked by isolation defines the Finnish mutation spectrum (Norio, 2003a,b,c). Since only two mutations specific to Finnish patients were identified in Finnish USH3 patients (Joensuu et al., 2001), USH1 and USH2 were expected to be caused by a small number of specific mutations as well. The USH1 and USH2 mutations could either be unique to the Finnish population or the mutations could predate the migration and isolation of the original Finnish settlers and thus could also be present in other populations.

1.1 USH1 and USH2 in Finland (I, II)

The search for Finnish USH1 mutations started by sequencing the *MYO7A* gene, mutated in USH1B, from two Finnish USH1 patient DNA samples. The first Finnish USH1 mutations were identified in these patients. The three *MYO7A* mutations identified were all novel (p.K923AfsX8, p.Q1896X and p.E1349K) (Table 4). After the discovery of these three mutations, we also studied 12 patients with a mutation chip containing known USH mutations (Cremers et al., 2007). The Finnish patients were selected for further studies based on two reasons: 9 USH patients did not have any known USH mutations, and 3 patients in 2 families with USH3 were studied because they had only hearing loss or atypical USH3. Subsequently the exons of the *MYO7A* and *USH2A* genes were sequenced from 2 (*MYO7A*) and 3 (*USH2A*) patients studied with the USH mutation chip. Two novel mutations, a *MYO7A* mutation p.R873W and a *USH2A* mutation c.14343+2T>C, were identified by sequencing. Also two known mutations were identified either by sequencing (*MYO7A* p.K923AfsX8) or by USH mutation chip analysis (*USH2A* p.N346H). The two identified *USH2A* mutations are the first USH2 mutations reported in Finnish USH patients (Table 4). In one patient, the heterozygous *MYO7A* p.K923fsX8 mutation was identified by sequencing even though the mutation was not detected by the Asper mutation chip. This shows that the mutation chip is not as reliable as direct sequencing. As stated by the provider, the results should always be verified by sequencing when the chip is used in diagnostics.

Two of the identified USH1B mutations, p.K923AfsX8 and p.Q1896X, result in premature termination codons which truncate the MYO7A protein. The mutation p.E1349K changes a

conserved glutamic acid located in the FERM domain mediating MYO7A attachment to the plasma membrane (Chishti et al., 1998). The mutation p.R876W is located in the coiled-coil domain that mediates formation of MYO7A homodimers (Weil et al., 1997). The *USH2A* mutation p.N346H is located in the N-terminal Laminin domain and the mutation c.14343+2T>C influences splicing and thus protein structure upstream of the last Fibronectin type 3 domain before the transmembrane domain anchoring USH2A to the plasma membrane (Dreyer et al., 2000; van Wijk et al., 2004).

The other *MYO7A* and *USH2A* sequence variations identified from Finnish USH patients (either by sequencing or chip analysis) have either been reported as benign polymorphisms or changes that can have an effect on USH severity and pathogenesis, but do not cause USH by themselves (Table 5). The intronic variation *MYO7A* c.4568+12C>G was studied further as it was identified in two of the studied families. Several splice variants were identified in this *MYO7A* region including exons 33 to 37. Most of the splice variants were created by splicing machinery even without the *MYO7A* c.4568+12C>G variation, but four out of ten splice variants were identified exclusively in heterozygous *MYO7A* c.4568+12C>G carriers. The number of splice variants complicates the analysis of this region, but it is possible that this intronic variation causes changes to the MYO7A splicing. It is known that all mutations in *MYO7A* do not necessarily cause typical USH1 with RP and congenital hearing loss. Mutations can cause recessive atypical USH (Liu et al., 1998b; Zina et al., 2001), recessive non-syndromic deafness (DFNB2) (Liu et al., 1997b; Liu, 2002) and dominant non-syndromic deafness (DFNA11) (Liu et al., 1997c; Luijendijk et al., 2004; Tamagawa et al., 1996). Mutations in *USH2A* have also been reported to have variable pathogenicity. Mutation p.C759F is associated with nonsyndromic retinitis pigmentosa (RP39) (Aller et al., 2004b), but this mutation has been also identified in homozygous form in asymptomatic siblings (Bernal et al., 2005). Thus the effect the USH2A mutations have on USH phenotype may be changed by genetic modifiers perhaps in other USH genes.

The novel MYO7A p.R873W mutation was discovered in heterozygous form in a patient from family 75 (II) with no USH3 mutations. We were also able to identify the *MYO7A* sequence variation that may cause splicing changes (*MYO7A* c.4568+12C>G) in this family. Additionally, four *USH2A* sequence variations with unknown pathology were identified in family 75 (c. 1328+35delTGAT, p.I1665T, p.R2875Q and p.N3099S). The affected patient in family 75 had the combination of *MYO7A* p.R873W*,* c.4568+12C>G and *USH2A* c.1328+35delTGAT, p.I1665T, p.R2875Q, p.N3099S sequence variations, and no unaffected member of the family had the same combination of changes. Therefore it is possible that the patient in family 75 represents a case of

digenic USH. The novel USH2A c.14343+2T>C splice site mutation was discovered in heterozygous form in a family (II: Family 7) with no other known mutations, but the patients also carried *MYO7A* (*MYO7A* c.4568+12T>C) and *USH2A* (*USH2A* c.849-25A>G and p.E478D) sequence variations. This family represents another possible case for digenic inheritance of *MYO7A* and *USH2A*. Two Finnish USH families with the USH3 founder mutation, *CLRN1* p.Y176X, and atypical USH3 phenotype were discovered to have possibly modifying changes in *USH2A*. In family 15 (II) the patients were homozygous for *CLRN1* p.Y176X and heterozygous for *USH2A* p.R2875Q and p.L2886F. In family 12 (II) the USH patients were homozygous for *CLRN1* p.Y176X, but the sister with more severe USH3 was also heterozygous for *USH2A* p.V2562A. Additionally the father, who had non-syndromic sensorineural deafness, was heterozygous for both *CLRN1* p.Y176X and *USH2A* p.V2562A. The CLRN1, MYO7A and USH2A proteins are assumed to be part of the USH protein network and alterations in this interactome in two different proteins could cause or modify the symptoms of USH by impairing the function of the interactome. Digenic inheritance has earlier been published in RP. Mutations in the *ROM1* gene alone are not pathogenic but together with heterozygous mutations in the peripherin/*RDS* gene the normal photoreceptor function is disrupted (Kajiwara et al., 1994). Digenic inheritance has been reported for deafness with heterozygous mutations in CDH23 and PCDH15 (Zheng et al., 2005). Potential digenic inheritance for USH with *MYO7A* and *USH2A* has been suggested previously (Cremers et al., 2007; Jaijo et al., 2010) and potential digenic and trigenic inheritance with USH genes have been reported in 8 of 54 USH patients studied by Bonnet et al., 2011. In addition a heterozygous mutation in *MYO7A* has been suggested to enhance the USH phenotype in a patient homozygous for *CLRN1* mutations (Adato et al., 1999).

All four Finnish USH1 mutations were identified in *MYO7A* and all were novel. As with USH1, we identified USH2 mutations only from one USH2 gene, *USH2A*. *MYO7A* and *USH2A* were the only genes sequenced and this is an obvious reason for finding novel mutations only in these two genes. However, twelve patients were studied with the USH mutation chip that contained known mutations from all the USH genes. Only the mutation USH2A p.N346H was previously reported and identified by the USH mutation chip (Dreyer et al., 2000; Dreyer et al., 2008) whereas we identified five novel mutations by sequencing that could either be specific to the Finnish population or yet to be reported elsewhere. So far all the *MYO7A* and *USH2A* mutations have been compound heterozygous and none of the Finnish USH1 and USH2 patients have been homozygous as most of the Finnish USH3 patients are for p.Y176X, the *CLRN1* Finnish founder mutation. Two USH1 mutations, MYO7A p.K923AfsX8 and p.R873W, were identified in more than

one patient. The intronic change, *MYO7A* c.4568+12T>C, was identified in two patients as well as in 4.5 % of the control chromosomes. This sequence variation could be pathogenic when combined with other mutations as suggested by the findings in Families 7 and 75 (II). All in all, the mutation spectrums for USH1 and USH2 are much more variable than that of USH3.

Screening for USH3 mutations in Finnish patients has been relatively simple since one founder mutation could be identified in homozygous form in most USH3 patients. The situation is not that simple for USH1 and USH2. We were able to find six USH1 and USH2 mutations in seven Finnish USH patients and none of them were found in homozygous form. There are still unknown Finnish USH mutations since we weren't able to identify the mutations causing USH in four of the studied USH patients or identify a definite disease-causing mutation in the second allele in five USH patients. Worldwide, nine genes are known to cause USH when mutated, 340 *MYO7A* and 376 *USH2A* sequence variants are listed in USH mutation database (The Universal Mutation Database [UMD]-USHbases; http://www.umd.be/usher.html). The Finnish USH mutation spectrum is unique, four of the six USH1 and USH2 mutations are not included in the USH mutation chip and had to be identified by sequencing all the *MYO7A* and *USH2A* exons. For example, the most prevalent *USH2A* mutation in Scandinavia as well as in patients with a European caucasian background, c.2299delG, was not identified in Finnish USH patients (Dreyer et al., 2008; Yan et al., 2009). Knowing the specific USH mutations to screen in Finnish USH patients would help in designing simpler and faster tests for patient diagnostics.

Table 4. USH1 and USH2 mutations identified in Finnish USH patients (I, II).

USH subtype	Gene	Exon	Nucleotide change	Amino acid change
USH mutations:				
USH1	*MYO7A*	22	c.2617C>T	p.R873W
	MYO7A	23	c.2766-2779del14nt	p.K923AfsX8
	MYO7A	31	c.4045G>A	p.E1349K
	MYO7A	41	c.5686C>T	p.Q1896X
USH2	*USH2A*	6	c.1036A>C	p.N346H
	USH2A	65	c.14343+2T>C	intronic change

Table 5. Possibly pathogenic or modifying USH1 and USH2 sequence variations identified in Finnish USH patients and studied with *in silico* prediction programs. The sequence variations were classified either as potential mutations or polymorphisms by their inheritance in the USH families. Table has been modified from II.

USH type	Gene	Amino acid change/ Intronic change	Prev in Finnish controls	Polyphen-2 prediction	Mutation Taster	NNsplice	ASSP	Spliceview	Conservation
Potential USH mutations or modifying variations									
USH1	*MYO7A*	c.3503+12_+33del23	59,7 %	Likely non-pathogenic	ND	Benign	no change	no change	no
	MYO7A	c.4568+12C>G	4,5 %	polymorphism	polymorphism	Benign	no change	no change	no
	MYO7A	p.T1566M	0,0 %	possibly damaging	polymorphism	ND	ND	ND	no
USH2	*USH2A*	c.849-25A>G	0,0 %	Likely non-pathogenic	polymorphism	Benign	no change	no change	yes
	USH2A	c.1328+35delTGAT	1,6 %	Likely non-pathogenic	polymorphism	Benign	change	no change	no
	USH2A	p.E478D	0,5 %	possibly damaging	disease causing	ND	ND	ND	yes
	USH2A	p.I1665T	11,1 %	benign	disease causing	ND	ND	ND	yes
	USH2A	c.5573-34delC	67,2 %	Likely non-pathogenic	polymorphism	Benign	no change	no change	no
	USH2A	p.V2562A	0,6 %	benign	polymorphism	ND	ND	ND	no
	USH2A	p.R2875Q	5,7 %	benign	polymorphism	ND	ND	ND	no
	USH2A	p.N3099S	4,5 %	possibly damaging	polymorphism	ND	ND	ND	yes
Likely Polymorphisms									
USH1	*MYO7A*	p.L16S	ND	benign	polymorphism	ND	ND	ND	no
	MYO7A	c.3924+12C>T	ND	Likely non-pathogenic	polymorphism	Benign	no change	no change	ND
	MYO7A	p.S1666C	ND	benign	polymorphism	ND	ND	ND	no
	MYO7A	p.L1954I	ND	benign	polymorphism	ND	ND	ND	no
USH2	*USH2A*	p.A125T	ND	benign	polymorphism	ND	ND	ND	no
	USH2A	p.D644V	ND	benign	disease causing	ND	ND	ND	no
	USH2A	p.R1486K	ND	benign	polymorphism	ND	ND	ND	no
	USH2A	p.Y1992C	ND	probably damaging	disease causing	ND	ND	ND	yes
	USH2A	p.I2106T	ND	benign	polymorphism	ND	ND	ND	no
	USH2A	p.I2169T	ND	benign	polymorphism	ND	ND	ND	no
	USH2A	p.R2292H	ND	benign	polymorphism	ND	ND	ND	no
	USH2A	p.L2886F	ND	benign	polymorphism	ND	ND	ND	no
	USH2A	p.D3144N	ND	benign	polymorphism	ND	ND	ND	no
	USH2A	p.E3411A	ND	benign	polymorphism	ND	ND	ND	no
	USH2A	p.M3868V	ND	benign	polymorphism	ND	ND	ND	no
	USH2A	p.V4422L	ND	benign	polymorphism	ND	ND	ND	yes

1.2 USH3 in Finland (II, IV, U)

Prior to this study, two USH3 mutations had been discovered in Finnish USH patients. The *CLRN1* Finmajor (p.Y176X) mutation is the main cause for USH3 in Finland and had been identified as homozygous or compound heterozygous in all Finnish USH3 patients. Finminor (p.M120K) has been identified as a compound heterozygous mutation with Finmajor (Adato et al., 2002; Joensuu et al., 2001). The *CLRN1* gene was sequenced for 45 Finnish patients during this thesis project. The Finmajor mutation was identified either in homozygous or heterozygous state in all studied Finnish USH3 patients. A third mutation in the *CLRN1* gene, the Ashkenazi Jewish founder mutation p.N48K, was discovered in a Finnish USH3 patient in heterozygous state with Finmajor (Figure 9). In Finland the prevalence of the Finmajor mutation explains the high prevalence of the USH3 subtype whereas in the Ashkenazi Jewish population the mutation p.N48K explains a similar prevalence of USH3. Our patient was the first reported case with both founder mutations.

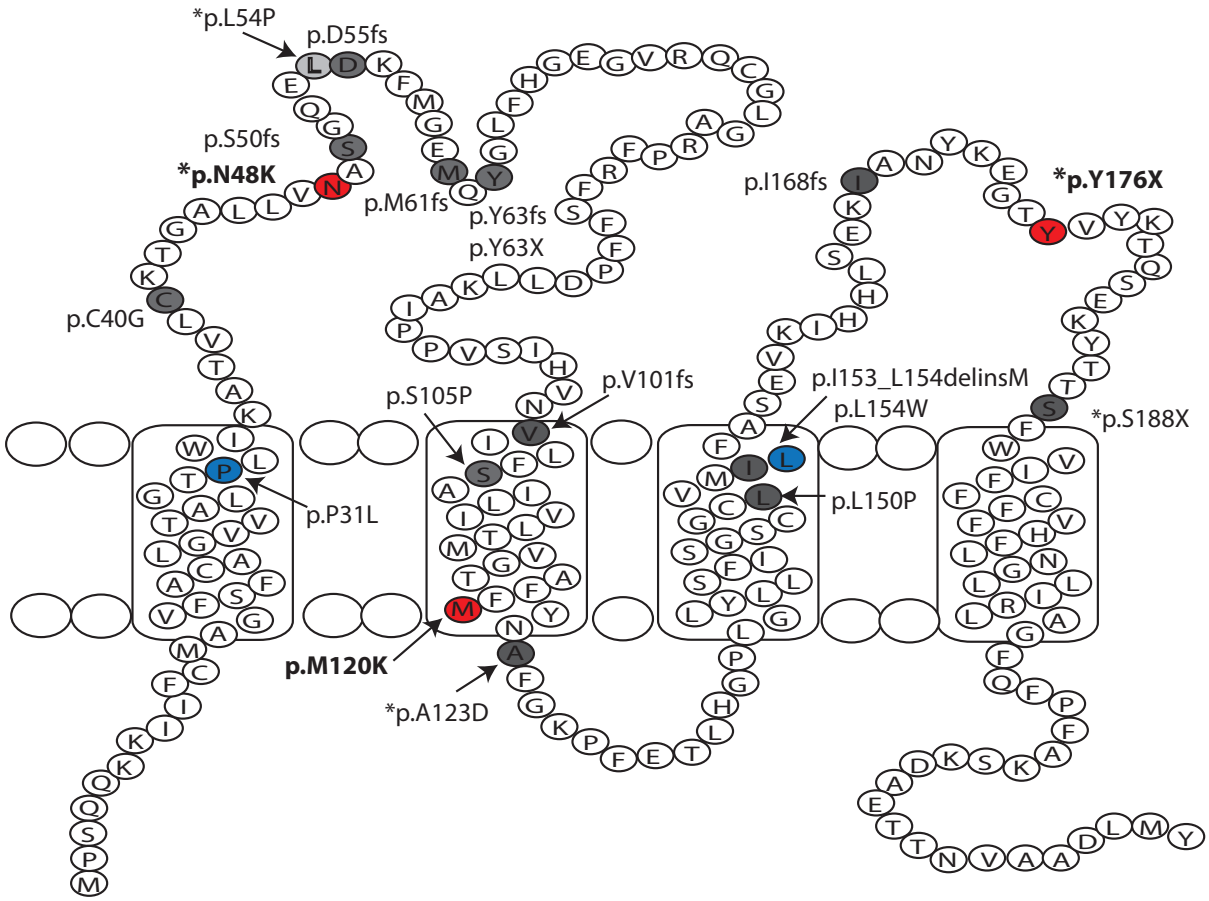

Figure 9. Predicted CLRN1 protein topology and transmembrane domains (Modified from III). Pathogenic USH mutations are indicated on the CLRN1 protein amino acid sequence. The two

mutations, p.P31L and p.L154W, reported to cause arRP are marked with blue. The sequence variation p.L54P is also indicated on the sequence with lighter grey. USH3 mutations discovered in Finnish USH3 patients are indicated with red and bold, mutations (either novel or known) identified in USH patients during this thesis project are indicated with an asterisk. The Ashkenazi Jewish founder mutation p.N48K was also identified in a Finnish patient.

1.3 USH3 mutations worldwide (IV, U)

During this thesis project 42 non-Finnish USH patients were sequenced for mutations in *CLRN1*. We discovered a novel p.S188X mutation in a US patient (Ratnam et al., 2011) and a p.A123D mutation in a patient from Dominica (Figure 9, Table 6). A new sequence variation p.L54P was also identified in heterozygous state in a Canadian patient. The p.54 leucine change is conserved and the variation was not identified in healthy controls. Even though this p.L54P change does not cause similar localization and stability changes to the CLRN1 protein as the known mutations (studied with cell culture expression described in sections 3.1 and 3.2), it is possible that this change causes a functional change in CLRN1 and is pathogenic. The PolyPhen (Polymorphism Phenotyping: http://genetics.bwh.harvard.edu/pph/) program predicted the p.L54P change to be probably damaging to CLRN1. A similar p.L76P change is predicted to be located either in the transmembrane region or in the first extracellular loop of a structurally similar small transmembrane protein with four transmembrane regions, connexin 26. This p.L76P change is reported to be a mutation and cause nonsyndromic recessive deafness (Batissoco et al., 2009).

Nine of the sixteen known USH3 mutations cause either frameshifts or premature termination codons (p.S50fs, p.D55fs, p.M61fs, p.Y63fs, p.Y63X, p.V101fs, p.I168fs, p.Y176X, p.S188X) that can either lead to nonfunctional proteins or mRNA degradation through nonsense-mediated decay (NMD) (Khajavi et al., 2006). The other seven USH3 mutations alter CLRN1 protein structure by changing one amino acid for another (p.C40G, p.N48K, p.S105P, p.M120K, p.A123D, p.L150P) or by replacing two amino acids with one methionine (p.I153_L154delinsM). Mutant CLRN1 proteins with p.N48K, p.A123D and p.L150P were shown to be unstable while CLRN1 proteins with p.M120K and p.I153_L154delinsM were stable, however, all of these mutated CLRN1 proteins were mislocalized in cell culture studies (described in sections 3.1 and 3.2).

Table 6. Known USH3 mutations in the *CLRN1* gene. All mutations cause USH3 except p.P31L and p.L154W that have been reported to cause arRP (Khan et al., 2011). This table has been modified from IV.

USH3 mutation	**Origin of patients**	**Note**	**Number of novel patients/ families reported**	**Reference**
p.P31L c.92C>T	Pakistani	Compound heterozygote with p.L154W	11/2	Khan et al., 2011
p.C40G c.118T>G	Spanish	Homozygote	1/1	Aller et al. 2004a
p.N48K c.144T>G	Eastern European Jewish	5/6 pts homozygotes, 1/6 heterozygote, other allele not found	6/4	Adato et al. 2002
	Ashkenazi Jewish	Homozygote	16/11	Ness et al. 2003
	Ashkenazi Jewish	Homozygote Heterozygote with p.L150P	5/5 1/1	Fields et al. 2002
	Jewish (USA)	Homozygote	5/5	Sadeghi et al. 2005
	Ashkenazi Jewish	Homozygote Heterozygote, other allele not found	7/6 2/2	Herrera et al. 2008
	Canadian	Homozygote	1/1	(IV)
	Finnish	Compound heterozygote with p.Y176X	1/1	(IV)
p.S50fs c.149_152delins TGTCCAAT	Scottish-Irish (USA)	Homozygote Compound heterozygote with p.Y176X	1/1 1/1	Fields et al.2002
	UK (USA)	Homozygote	1/1	Sadeghi et al.2005
	German	Compound heterozygote with c. 502_503insA	3/1	Ebermann et al. 2007b
p.D55fs c.165delC	Dutch (USA)	Heterozygote, other allele not found	1/1	Fields et al. 2002
	Dutch (USA)	Heterozygote, other allele not found	4/1	Sadeghi et al.2005
p.M61fs c.181delA	Turkish	Homozygote	1/1	Dreyer et al., 2008
p.Y63fs c.187_209del	Yemenite Jewish	Homozygote	2/1	Adato et al. 2002
p.Y63X c.189C>A	Spanish	Homozygote	3/1	Adato et al. 2002
p.V101fs c.301_305del GTCAT	Lebanese	Homozygote	2/1	Akoury et al., 2011
p.S105P c.313T>C	Turkish	Homozygote	2/1	Sadeghi et al. 2005
p.M120K c.359T>A	Finnish	Compound heterozygote with p.Y176X	4/2	Joensuu et al. 2001

p.A123D c.368C>A	French Canadian Dominican (Canadian)	Homozygote Homozygote	1/1 1/1	Ebermann et al. 2007c (IV)
p.L150P c.449T>C	Ashkenazi Jewish	Compound heterozygote with p.N48K	1/1	Fields et al. 2002
p.I153_L154delinsM c.459_461del	Italian	Homozygote	4/1	Joensuu et al.2001
p.L154W c.461T>G	Pakistani	Compound heterozygote with p.P31L	11/2	Khan et al., 2011
p.I168fs c.502_503insA	German	Compound heterozygote with c.149_152delinsTGTCCAAT	3/1	Ebermann et al. 2007b
p.Y176X c.528T>G	Finnish Northern European, one family Scottish-Irish (USA) Finnish-Swedish Scottish-Irish (USA)	Homozygote Homozygote Homozygote Compound heterozygote with c.149_152delinsTGTCCAAT	52/21 11/6 13/5 3/1	Joensuu et al. 2001 Fields et al.2002 Sadeghi et al. 2005 Sadeghi et al. 2005
p.S188X c.563C>A	Chinese (USA)	Compound heterozygote with p.N48K	1/1	(U)

2. *CLRN1* gene structure

Upon the start of this thesis project, the *CLRN1* gene was described to contain a major splice variant transcribed from exons 0, 2 and 3 and two rare splice variants (exons 1, 2, 3 and 4) and (exons 1, 1b, 2 and 3) (Adato et al., 2002; Joensuu et al., 2001). Northern blot results showed that *CLRN1* was expressed in numerous tissues and there were three transcripts. The 1.0 kb and 4.5 kb transcripts were present in all studied tissues and a third 1.5 kb transcript was identified only in spleen. RNA *in situ* hybridization detected *Clrn1* expression in the mouse cochlear spiral ganglion cells and hair cells. The three *CLRN1* splice variants were amplified from human retina cDNA (Adato et al., 2002; Fields et al., 2002; Joensuu et al., 2001).

2.1 Splice variants (III)

CLRN1 splice variants either include new exons in addition to those found in the main variant (Figure 10: 1), exclude *CLRN1* exons or use alternative 5' or 3' splice sites. The three alternative splice forms of *CLRN1* that were known prior to this study are depicted in Figure 10 (variants: 1,4,5). Three additional

alternative splice variants were later reported in databases (UCSC [http://genome.ucsc.edu/], Aceview [http://www.ncbi.nlm.nih.gov/IEB/Research/Acembly/], NCBI [http://www.ncbi.nlm.nih.gov]) (Figure 10: 6,10,11). Five new alternative splice variants were identified from human retinal cDNA in this thesis project (Figure 10: 2,3,7,8,9). In all, 11 *CLRN1* splice variants are known at this point. Most of the novel splice variants identified in this study contain premature termination codons. The translation interrupting stop codons are located in exons 0b, 1b, and in exon 2 of the 0-1-2-3 splice variant (Figure 10: marked with a star). If these splice variants are processed further, they are most likely destroyed in NMD. Even though these splice variants are unlikely to encode proteins, they might have a regulatory function by influencing expression levels of the main *CLRN1* splice variant. One of the alternative splice variants changes the protein structure by adding 13 aa into the primary structure (Figure 10: 2). This splice variant is a potentially translated and functional form of CLRN1. Splice variants with extended exon 0 (Figure 10: 10) and exon 0 spliced into extended exon 2 (Figure 10: 11) potentially also escape NMD and might be translated into functional proteins.

CLRN1 has splice variants that start from *CLRN1* exon 2 and continue splicing to ESTs further downstream from *CLRN1* (BE673203, DV080481 and DV080691) (Figure 10: 15,16,17). These variants have unknown 5' ends, but to our knowledge share only exon 2 with the *CLRN1* gene (Figure 10: 12,13,14). These extended variants could be produced by faulty splicing during the complex splicing process. The extended variants have potential ORF regions and since the 5' ends remain unknown, it is unclear whether these variants are translated or not. Thus we can not rule out potential functional roles for these extended splice variants either in *CLRN1* transcription or other cellular function at the RNA or protein level.

The mouse has three known *Clrn1* splice variants and four known exons. The two splice variants that have been isolated from retinal and cochlear RNA would correspond to human 0-2-3 (Figure 10: 18) and 0-3 variants (Figure 10: 20)(Adato et al., 2002; Zallocchi et al., 2009). Zebrafish, on the other hand, have a main *clrn1* splice variant (0-2-3) (Figure 10: 22) as well as an alternative EST sharing only part of exon 2 with the main variant (Figure 10: 23). We did an extensive search designing primers within the known zebrafish *clrn1* exons and using the human and mouse splice variant alternative exons for reference as well as nearby zebrafish ESTs. However, we were unable to find more zebrafish *clrn1* alternative splice variants (unpublished).

The main *CLRN1* three-exon splice variant identified in human, mouse and zebrafish seems to be the main functional form and all mutations associated with USH3 pathology have been reported within these three exons (section 1.3: Table 6). However, most of the mutations are in exons 0 and 2. Exon 0 is included in eight alternative splice variants (Figure 10: 2,3,6-11) and

exon 2 is included in six alternative splice variants (Figure 10: 2-6,11). The complex splicing pattern of human *CLRN1* is not surprising in light of our new knowledge about the structure of a gene and the complexity of the human genome. It has been reported that almost all genes have complex splicing patterns (Gerstein et al., 2007; Johnson et al., 2003a; Matlin et al., 2005; Pan et al., 2008; Wang et al., 2008). Nevertheless, the presence of several splice variants makes it harder to design a gene therapy for USH3 patients. The main *CLRN1* splice variant with exons 0, 2 and 3 should be enough to replace the mutated *CLRN1* in patient retinal and cochlear tissue. However, more research is needed to determine that the alternative splice variants are not needed in some crucial CLRN1 function either together with the main splice variant or in alternative subcellular localizations or cell types to the main splice variant.

Human *CLRN1* splice variants

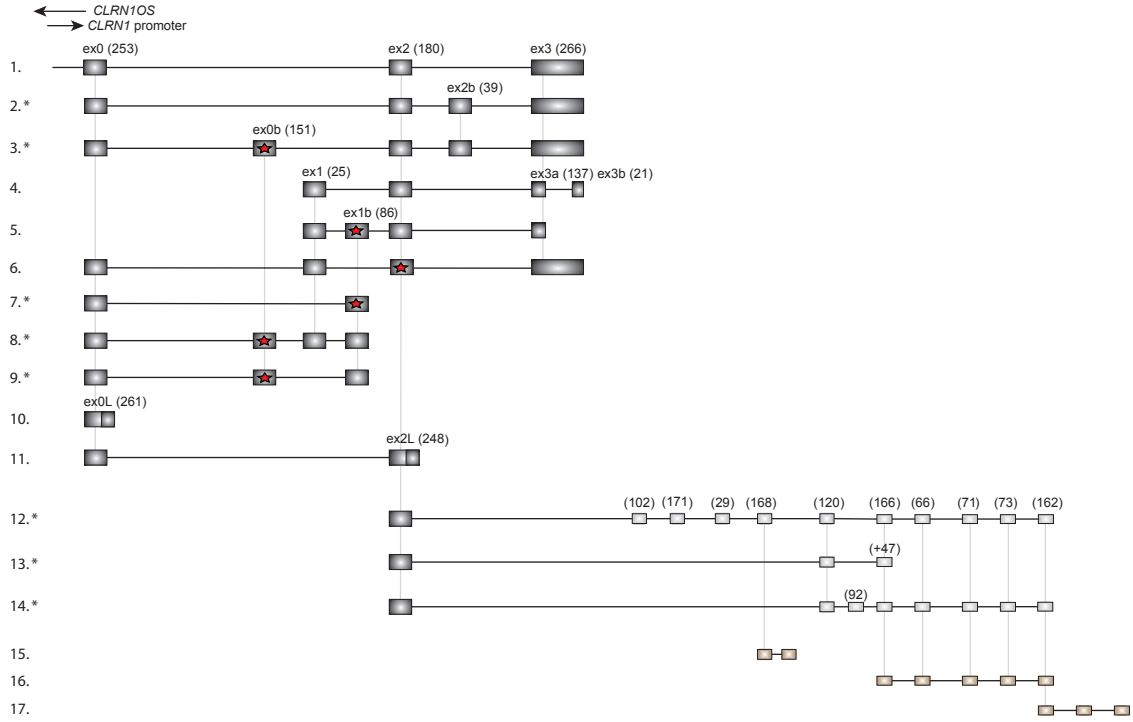

Mouse *Clrn1* splice variants

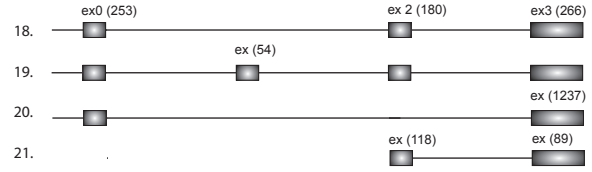

Zebrafish *clrn1* splice variants

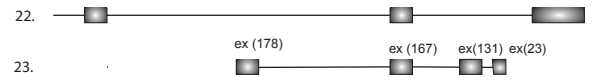

Figure 10. Known *CLRN1* alternative splicing in human, mouse and zebrafish (Modified from III). Five new splice variants were identified by us during this thesis (2,3,7-9), other splice variants were reported before this thesis (1,4,5) and additional splice variants were discovered in parallel to this thesis (6,10,11). There are three splice variants that have only one exon in common with *CLRN1* (12-14) and extend to ESTs further downstream from *CLRN1* (15-17). The mouse *Clrn1* has four known splice variants (18-21) and zebrafish only two (22,23). The main variant with exons 0, 2 and 3 have been described in human, mouse and zebrafish (1,18,22).

2.2 Promoter region (III)

In silico studies were done using the *CLRN1* genomic region to determine the size of the *CLRN1* proximal promoter region and possible alternative promoters, enhancers and silencers of the main and alternative *CLRN1* splice variants. Genomic sequence near the *CLRN1* gene was studied for evolutionary conservation by comparing sequences between mouse and human. *In silico* programs were used to identify known control sequence motifs near *CLRN1*. There was only one potential CpG island in the *CLRN1* region, located in the longest intron between exons 0 and 1. Potential TBP (TATA binding protein) binding sites were found upstream of exons 0 and 2. Even though TATA boxes usually correlate with tissue specificity, the identified Sp1 and YY1 binding sites in these promoter regions are associated with more ubiquitous expression (Schug et al., 2005). The ubiquitous expression profile is more in line with our *CLRN1* expression results (described in section 2.3).

The *in silico* genomic regions near *CLRN1* exons that were most promising for transcriptional control were inserted into an expression vector. In the expression vector the promoter regions controlled expression of a marker gene when transfected into cultured cell lines. The main promoter region (upstream translation start site in exon 0) was the most conserved between mouse and human sequences and was also the most active in the luciferase reporter assays (Figure 11). The sequence conservation of the *CLRN1* promoter region upstream of exon 0 between human and mouse diminishes with distance from the translation start site, which correlates with the observation that important promoter region information is likely more proximal to the transcription initiation site. The functional studies showed that the most active region of the proximal promoter is around 1000 nt in length and the region between 1000 and 1550 nt upstream of exon 0 contains one or more silencer domains. For example, CA_{23} repeat 1107-1152 nt upstream of the 5' translational start site has a possible binding site for WT1-KTS. This protein functions in transcriptional repression (Hewitt et al., 1996). Interestingly, variations in the length of the CA repeat region in the *PAX6* gene P1 promoter region have been associated with high myopia (Ng et al., 2009). *CLRN1* expression may also be influenced by antisense transcriptional control. *CLRN1OS* (Figure 10) is a pseudogene running in the opposite direction to *CLRN1. CLRN1* and *CLRN1OS* share the same promoter region and the 5' untranslated regions (UTR) are partly overlapping. The *CLRN1OS* pseudogene may control *CLRN1* expression by interfering with *CLRN1* transcription/translation or *CLRN1* mRNA stability (Katayama et al., 2005).

It is unlikely that the proximal promoter contains all the required signals for the proper function of *CLRN1* in all cell types and developmental stages. Even in cell culture conditions, the activity varied between cell culture age, stage and cell type. The activity of the potential promoter region upstream of exon 2 varied the most between cell culture types suggesting a potential promoter in alternative developmental stages and cell types (unpublished results). The potential promoter region upstream of exon 1, which was the original promoter for the first published *CLRN1* splice variant (Figure 10:4), was the least conserved as well as the least active. Unless the exon 1 promoter region is specific to conditions in certain cell types or specific developmental stages, the region upstream of exon 1 is not a promoter region. The presence of TATA binding sites upstream of exons 0 and 2, but not proximal to exons 1 and 3, correlates well with our promoter activity studies; the data show that regions upstream of exons 0 and 2 have higher activity levels than regions upstream of exons 1 and 3. Additionally, the observed promoter region conservation is in concordance with the observed higher activity levels of the more conserved 5' regions upstream of exons 0 and 2, when compared to the weaker regions upstream of exon 1 and exon 3.

We could only predict the combination of regulatory (positive and negative) elements present in the cochlea and retina with *in silico* studies. There was an H1 core sequence in the main promoter region (upstream of exon 0) and the H1 sequence was also identified within the exon 1 and exon 2 promoter regions studied. The photoreceptor-specific transcription factor Crx has been reported to bind to this H1 core sequence (Young et al., 2003). Exon 2b was associated with intronic downstream control sequences: splicing repressor CUCUCU is repeated once at 79 nt downstream of exon 2b, whereas a possible neuron-specific Nova family splicing factor signal, YCAY, is repeated three times within 140 nt downstream of exon 2b, and splicing enhancer GGGGG is repeated three times approximately 890-1 080 nt downstream of exon 2b. Both CUCUCU and GGGGG repeat elements have previously been shown to affect the splicing of a small neuron-specific exon in the mouse *c-src* gene (Black, 2003; Modafferi and Black, 1999; Wang and Burge, 2008).

The *CLRN1* proximal promoter region and the possible alternative promoter regions may not encompass all the information required for proper *CLRN1* expression in all developmental stages and cell types. Additional elements such as enhancers and/or silencers may be located more distantly downstream or upstream, and could provide additional information that is required for the proper expression level of the *CLRN1* main variant as well as the alternative variants. Moreover, expression can be modulated by regulatory sequences in intronic regions.

However, according to this study, the 1000 nt region upstream the translation start site in exon 0 is the main promoter region and likely to regulate the ubiquitous expression in most tissue types.

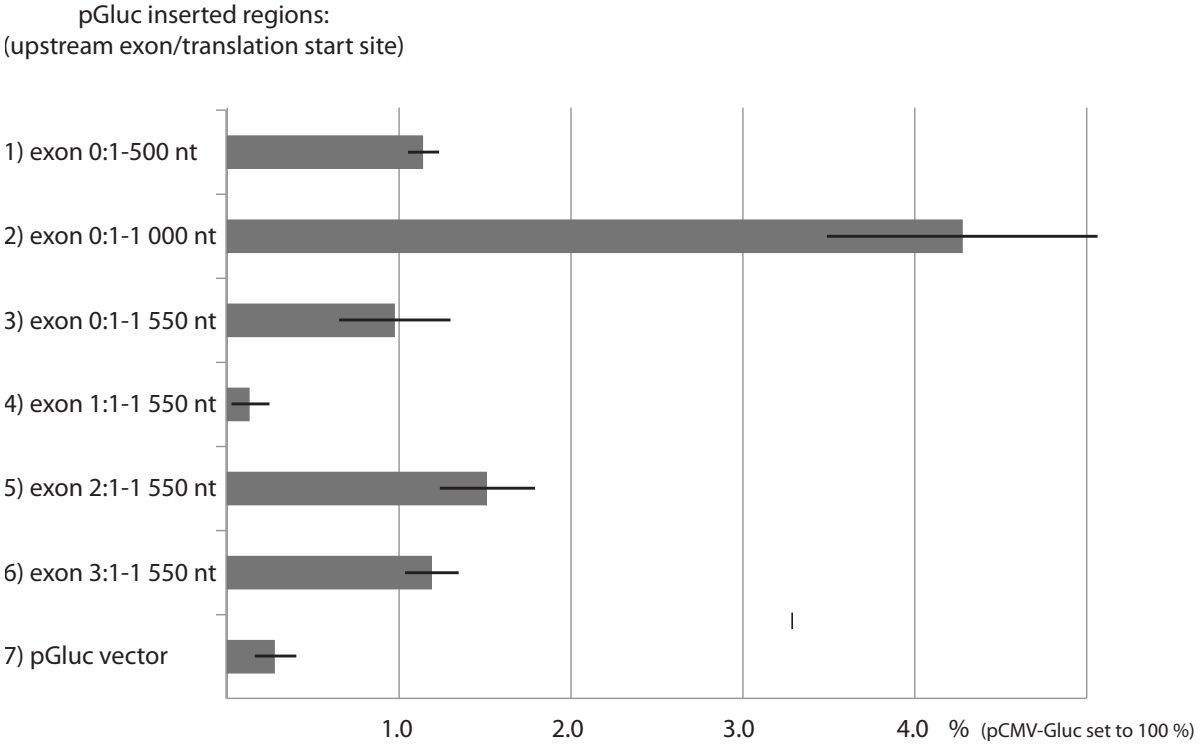

Figure 11. Alternative promoter region activity levels in luciferase activity assays (modified from III).

2.3 Expression (III)

All the *CLRN1* splice variants were initially identified from human retinal cDNA. Amplification with exon specific primers showed that the *CLRN1* main splice variant (0-2-3) was transcribed in several human tissues: retina, cochlea, RPE (ARPE-19 cell line) as well as brain, placenta, liver, kidney, pancreas, prostate, testis, ovary, small intestine and colon. The *CLRN1* splice variant with exon 2b (0-2-2b) was expressed in several tissues, most importantly in human retina and cochlea but also in heart, brain, placenta, lung, skeletal muscle, pancreas and ovary. The splice variant (0-1b-2-3) was also found in testis and (0-0b-2-2b) in heart, brain, placenta and pancreas.

The main splice variant (0-2-3) encoding a 232 aa protein and the most likely functional alternative splice variant (0-2-2b-3) encoding a 245 aa protein were expressed in numerous tissues. The expression profile of these splice variants would suggest a ubiquitous function for these proteins, but the presence of USH3 symptoms only in retina and inner ear would suggest

otherwise. The other splice variants are not as widely transcribed, but present in retinal cDNA. The function for these splice variants could be retina-specific or developmental since the alternative splice variant expression was not studied in all developmental stages.

3. CLRN1 protein

During this thesis several attempts were made to raise an antibody against either human or mouse CLRN1 protein. GST-fusion proteins were created linking the predicted human and mouse extra cellular loops and C-terminal regions to a GST-tag. The CLRN1 antigens were used to raise antibodies in rabbit, chicken and by using the phage display technique (Hoogenbloom et al., 1998; Kretzschmar and von Rüden, 2002). Only one antibody raised against mouse CLRN1 in chicken showed limited specificity to CLRN1 (Geller et al., 2009). One antibody was reported to recognize CLRN1 in mouse retina and cochlea sections (Zallocchi et al., 2009) but the specificity of this antibody has been questioned later (John Flannery, personal communication). The lack of a specific CLRN1 antibody is not surprising as the predicted CLRN1 structure resembles that of a tetraspanin protein and tetraspanins are known to be small membrane proteins protruding only around 4-5 nm above the membrane (Hemler, 2005). Prior to this thesis, the predicted transmembrane regions and similarity to tetraspanins were hypothesized to mean that CLRN1 is a small protein embedded in the cellular membranes (Joensuu et al., 2001; Adato et al., 2002).

3.1 CLRN1 localization (IV)

At the beginning of the thesis research the lack of a functional antibody against CLRN1 was compensated by incorporating a HA-tag to the CLRN1 protein C-terminus. The HA-tag, and the CLRN1 protein linked to it, could then be detected using an antibody against the HA-peptide. In cultured BHK cells the wt CLRN1 construct was transported through the ER to the plasma membrane. Our results are in line with the results of parallel study, which suggests that CLRN1 is localized into microdomains enriched with cholesterol within the plasma membrane (Tian et al., 2009). When CLRN1-HA protein was transiently expressed in mouse retinal primary neurons CLRN1 colocalized with synaptophysin (green) suggesting that CLRN1 is localized in retinal and cochlear synapses (Figure 12, unpublished results).

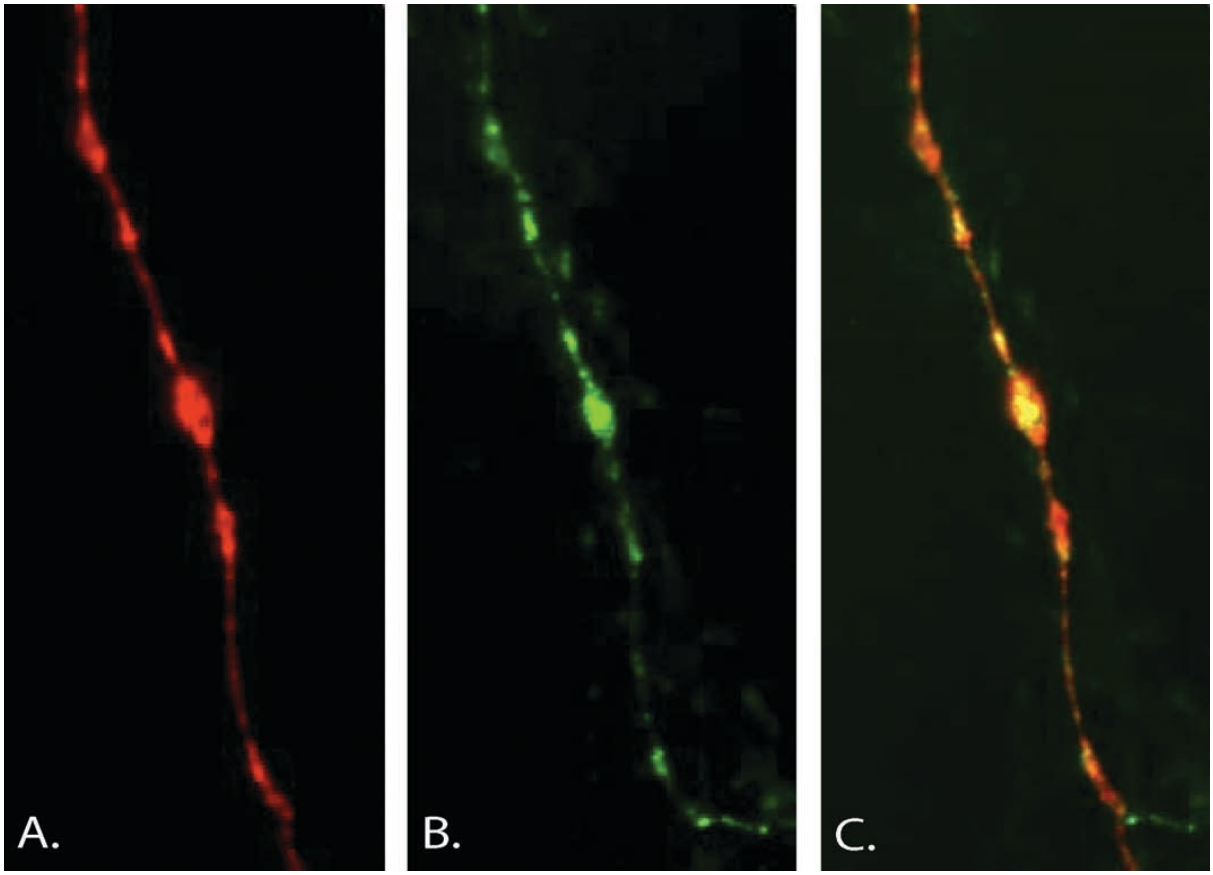

Figure 12. CLRN1 localization in mouse retinal primary neuron culture transiently transfected with HA-tagged CLRN1 protein expression plasmid. HA-CLRN1 (red, A) and synaptophysin (green, B) are colocalized in a neuron (yellow, C).

Alternative splicing has been described to be important in USH1C localization. The alternative USH1C isoforms exhibit alternative tissue specificities as well as localize to alternative compartments in photoreceptors (Reiners et al., 2003). The 0-2-2b-3 CLRN1 isoform, with the additional 13 aa, might have a similar alternative function as it has been shown that small tissue-specific exon modifications are important in nervous system-specific isoforms (Stetefeld and Ruegg, 2005). The lack of antibodies specific to the alternative CLRN1 protein variants made it impossible to study the subcellular localization of these proteins in different cell types in retina and cochlea.

We studied how the known USH3 mutations affect CLRN1 localization. When the wt CLRN1 was mutated (p.A123D, p.I153_L154delinsM, p.L150P, p.M120K and p.N48K) the proteins were not transported to the plasma membrane but were retained in the ER. This mislocalization of mutated CLRN1 proteins prevents the correct function of CLRN1. The results suggest that the absence of correctly localized CLRN1 leads to gradual cell death in retina and cochlea in USH3

patients. The accumulation of mutated CLRN1 in the ER may be another contributor to cell death in USH3, as the accumulation of mutated proteins in the ER has been shown to cause ER stress that may lead to cell death if the condition is not corrected (Lin et al., 2008; Rasheva and Domingos, 2009).

3.2 CLRN1 stability (IV)

The stability of wt CLRN1 protein, and the impact of USH3 mutations on stability, was studied using the HA-tagged CLRN1 protein expression plasmid transfected into cell cultures. CLRN1 protein production was interrupted with cyclohexamide introduced to the cell culture. After four hours wt CLRN1 was still present and stable as were the p.I153_L154delinsM and p.M120K mutant proteins. Unlike the wild type protein p.N48K, p.A123D and p.L150P mutant proteins were unstable and almost absent four hours after protein production was arrested by the drug treatment. The instability of these mutant CLRN1 proteins, therefore, leads to absence of functional CLRN1 in USH3 patient retinal and cochlear cells.

CLRN1 protein stability and localization to the plasma membrane were used to ascertain the pathogenicity of two newly identified USH3 mutations in Canadian patients. Mutation p.A123D was found to alter protein localization and stability similar to known mutations, while the sequence variation p.L54P was found not to change CLRN1 stability or localization. Thus p.A123D was deemed to be a mutation and p.L54P as a potentially benign polymorphism, although the possible changes p.L54P causes to CLRN1 function beyond those assayed could not be determined. This same approach was later also used by Khan et al. (2011) to ascertain the pathogenicity of two *CLRN1* mutations p.P31L and p.L154W causing arRP, the mutated proteins were reported to remain in ER and not to be correctly trafficked to the plasma membrane.

3.3 CLRN1 polymerization and interactions (IV, U)

Wt HA-tagged CLRN1 protein and p.N48K mutated HA-tagged CLRN1 proteins were analyzed by western blot analysis after deglycosylation treatment with PNGase F. The shift in protein mobility was consistent with oligosaccharide side chain attachment to p.N48 in wt protein. The p.N48 glycosylation was also reported by Tian et al., 2009. The analysis revealed the wt CLRN1 protein is glycosylated at the p.N48 position.

The western blot studies also revealed that the wt CLRN1 protein forms dimers and multimers. The discovered homomeric interaction between CLRN1 proteins is consistent with the results that CLRN1 proteins form multimers with hydrophobic interactions and cholesterol rich microdomains in the plasma membrane (Geller et al., 2009; Tian et al., 2009). It is possible that if the alternative CLRN1 isoforms (especially the 0-2-2b-3) are translated they could form multimers with the main CLRN1 isoform, but the alternative splice variants could also have different functions and localize to different regions than the main CLRN1 isoform as do alternative USH1C isoforms (Reiners et al., 2003) or alternative PCDH15 isoforms that have different functions in cochlear hair cells (Webb et al., 2011).

During this thesis we also conducted yeast two-hybrid (Y2H) screens against CLRN1 outer loops and C-terminal region (unpublished results). We discovered several interaction partners but most of them were considered false positives. The most interesting potential interacting proteins that we discovered were thioredoxin 2 and ELMO1 (Engulfment and Cell Motility protein 1) (unpublished results). Thioredoxins have a role in protecting retinal cells from oxidative stress by activating several transcription factors and functioning as neuroprotective factors (Kong et al., 2010). Over expression of thioredoxin was recently reported to delay inherited photoreceptor degeneration caused by light-induced or oxidative stress in a mouse model for sensorineural deafness and retinal dystrophy (Kong et al., 2010). ELMO1 is part of the Rho GTPase signaling pathway leading to Rac1 activation that affects cytoskeletal rearrangements and engulfment of apoptotic cells (Gurnienny et al. 2001). Further research is needed to determine whether thioredoxin 2 and ELMO1 interact with CLRN1 in retinal and cochlear cells. Therefore, their connection to USH3 progression when CLRN1 is mutated remains undetermined.

4. USH3 animal models

RT-PCR results show that mouse *Clrn1* is expressed from E12 onwards. In the developing retina *Clrn1* expression could be clearly detected with RNA *in situ* hybridization only in P7 mice. In developing cochlea *Clrn1* could be detected with RNA *in situ* hybridization from E16.5 onwards (Geller et al., 2009; Geng et al., 2009). In adult mice the *Clrn1* gene is expressed in cochlear hair cells and ganglion cells as well as retinal Müller cells (Adato et al., 2002; Geller et al., 2009).

During this thesis project our collaborators created a USH3 mouse model by knocking out *Clrn1* (Geller et al., 2009). The USH3 mice showed clear structural deterioration in cochlear hair cells that led to hearing loss. However, no visual function defects or retinal degeneration were detected during the lifetime of these animals (Geller et al., 2009). Several mouse models with mutations or deletions of other USH genes have also exhibited clear defects in mechanosensory hair cells, but attenuated or absent visual symptoms. In contrast, visual function defects or retinal cell degeneration have been noted in zebrafish models of *myo7a*, *pcdh15*, *ush1c*, *ush2a* and *gpr98* (Ebermann et al., 2010; Williams, 2008), prompting the study of USH3 zebrafish. The zebrafish USH3 study results are represented in the following sections describing *clrn1* expression, Clrn1 protein localization and Clrn1 knockdown studies. The zebrafish USH3 study was performed in collaboration with Jennifer Phillips and Professor Monte Westerfield.

4.1 *clrn1* expression in zebrafish (U)

The expression of wt *clrn1* was studied using RNA *in situ* hybridization. The *in situ* experiments found *clrn1* to be expressed in zebrafish larvae inner ear hair cells as well as larvae and adult retina INL, photoreceptors and RPE. RT-PCR showed that *clrn1* transcript was first detectable at 24 hpf and from then on *clrn1* can be visualized by *in situ* hybridization in the developing ear and eye (Figure 13). The prolonged expression of *clrn1* in the retina is in contrast to the transient expression pattern of mouse *Clrn1* that peaks at P7 (Geller et al., 2009). Zebrafish *clrn1* expression in retina was detectable with RT-PCR on adult retina extracts and *in situ* hybridization in all developmental stages and ages studied. The differences in the duration of *Clrn1* expression between zebrafish and mouse could indicate alternative developmental needs for CLRN1 in each species. Mouse retinal cells express *Clrn1* only in a certain stage of development and its absence does not result in retinal pathology. The zebrafish retina, however, has constant *clrn1* expression and lack of Clrn1 causes abnormal visual function (described in section 4.3.2).

4.2 Clrn1 localization (U)

An antibody was commissioned from the company SDIX (Strategic Diagnostics Inc., DE, USA) against the first outer loop of zebrafish Clrn1 by our collaborators in Oregon, USA. The antibody recognizing zebrafish Clrn1 (Dr-Clrn1-ab) was shown to be specific using transiently transfected cells with expression vector coding HA-tagged zebrafish-Clrn1 protein and observing the colocalization between HA-tag (Clrn1 protein) and Dr-Clrn1-ab (Figure 14). The Dr-Clrn1-ab was used to study Clrn1 localization in zebrafish retina and mechanosensory hair cells. Clrn1 was found to be localized in the retinal INL and photoreceptors as well as RPE in concordance with our zebrafish RNA *in situ* hybridization results (Figure 13).

In zebrafish Clrn1 can be detected with the antibody from 2 dpf onward, through all larval and adult stages examined. In the retina Clrn1 can be seen first in the developing INL and later when photoreceptors mature also in the photoreceptor layer. In the adult retina Clrn1 localizes to Müller cells, to the region of the connecting cilia and at synapses (Figure 15 and 16). Clrn1 protein and mRNA transcript can also be found in the RPE after PTU (1-phenyl-2-thiourea) treatment of the larvae, which suppresses melanocyte formation so that molecules within RPE cells can be visualized.

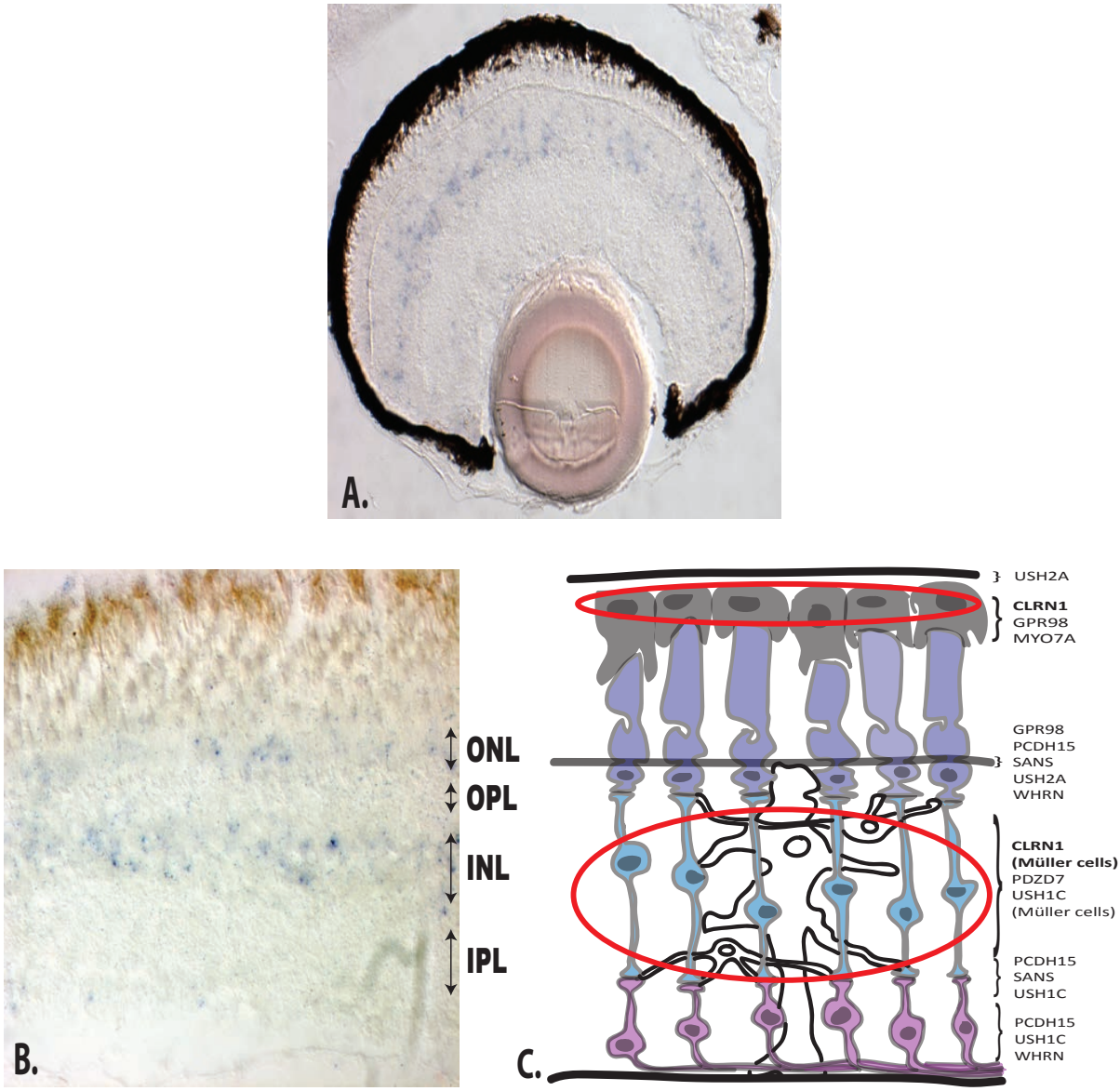

Figure 13. *In situ* detection of zebrafish *clrn1*. The blue staining (*clrn1* probe binding) can be seen in INL layer of 5 dpf larvae eye (A) and in the INL and ONL layers of adult retina (B).Zebrafish *clrn1* expression (*in situ* hybridization results) and Clrn1 localization (described in section 4.2) in retina (marked with red circles) compared to the reported localizations of other USH proteins in the mouse retina excluding the photoreceptors and OPL (described in Review of the literature, section 4.5.1) (C).

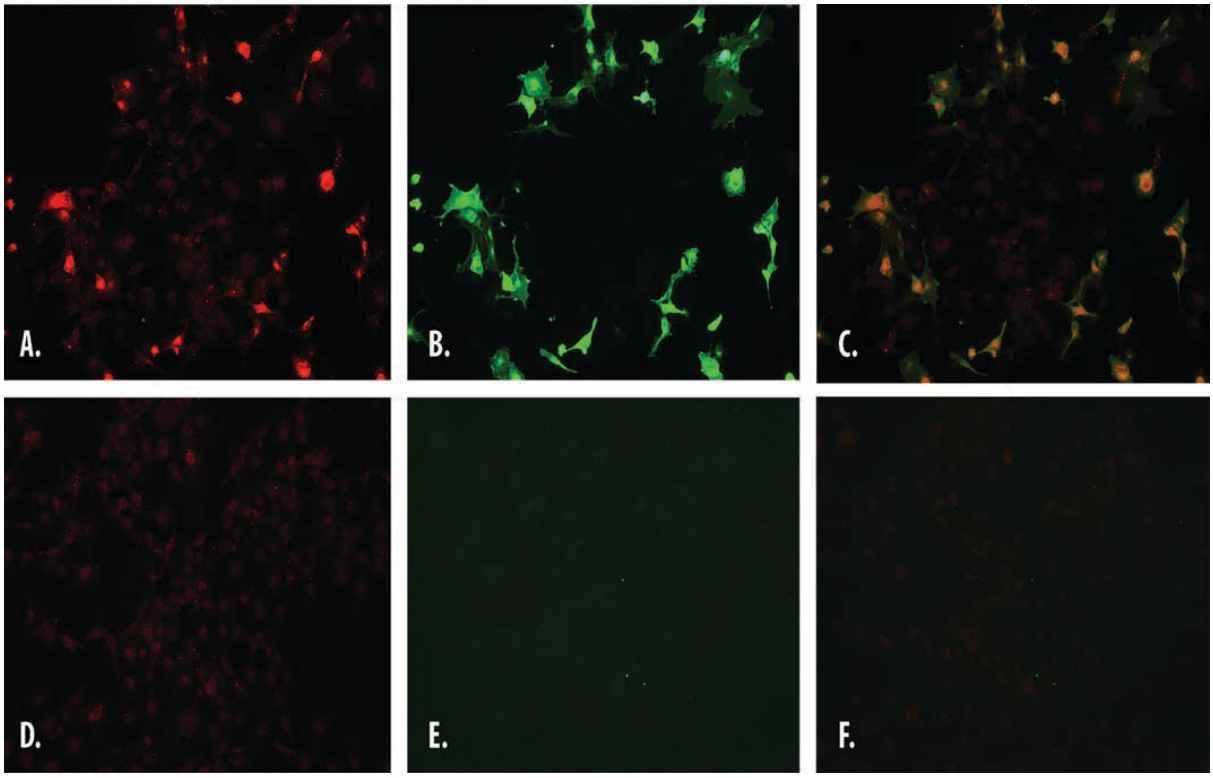

Figure 14. Testing the antibody recognizing zebrafish Clrn1 in transiently transfected BHK cell culture. HA-tagged zebrafish Clrn1 transfected cell culture treated with Clrn1-antibody (red) (A), antibody against HA tag in Clrn1-HA (green) (B), untransfected cells treated with Clrn1-antibody (red) (D), untransfected cells treated with HA tag -antibody (green) (E). Co-localization (yellow, C and F) between the Clrn1 antibody (red) and HA-tag antibody (green).

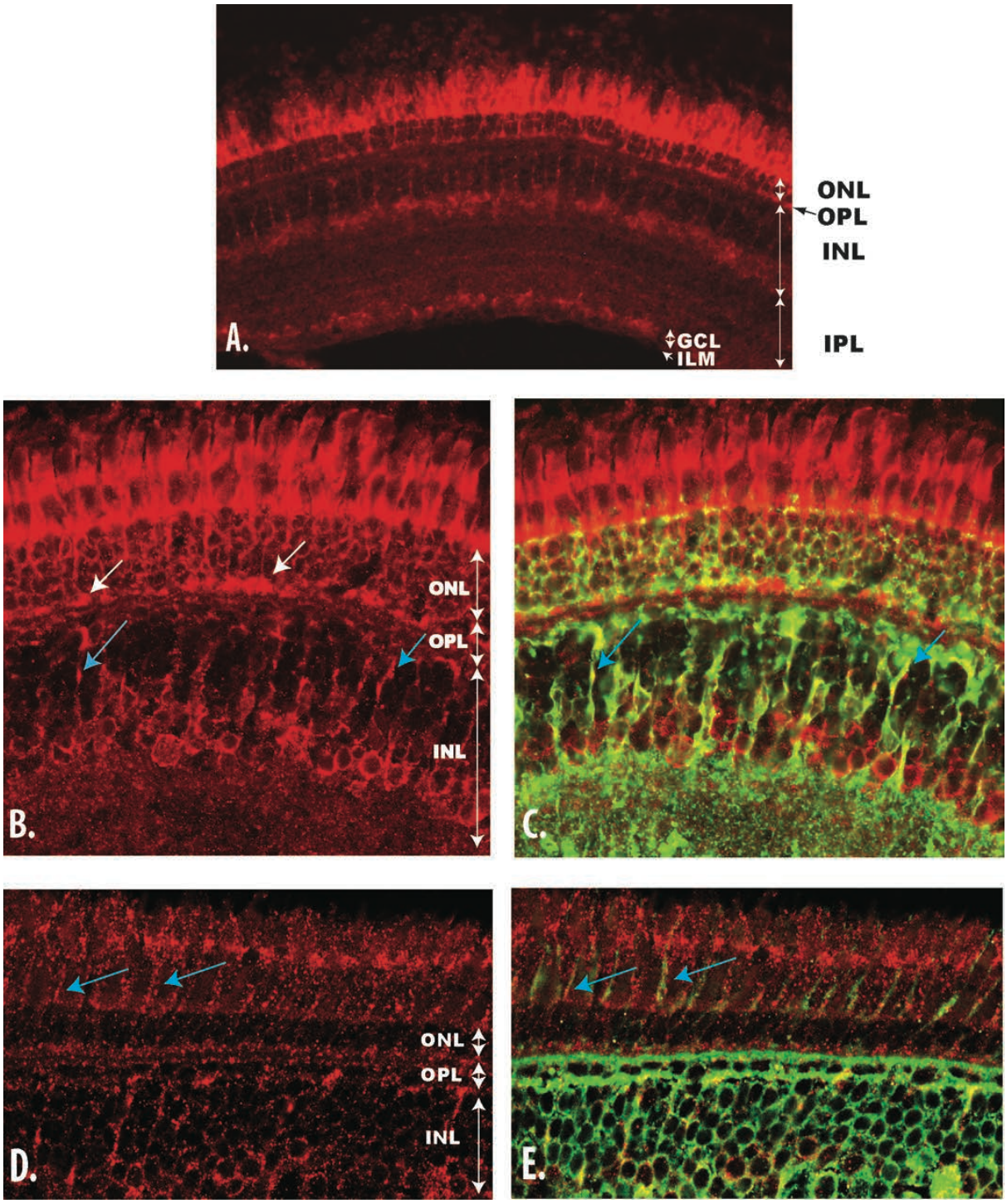

Figure 15. Clrn1 localization (red) in zebrafish retina. Dr-Clrn1-ab (red) treated zebrafish retina sections: Dr-Clrn1-ab staining of zebrafish adult retina (A), Dr-Clrn1-ab colocalization (yellow [blue arrows]) with Müller glial cell processes (glutamine synthetase, green) in 6 dpf zebrafish retina (B and C), Dr-Clrn1-ab colocalization (yellow [blue arrows]) with photoreceptor connecting cilia (tubulin marker, green) in 5 dpf zebrafish retina (D and E). White arrows indicate Clrn1 synaptic localization in cone photoreceptor pedicles (B).

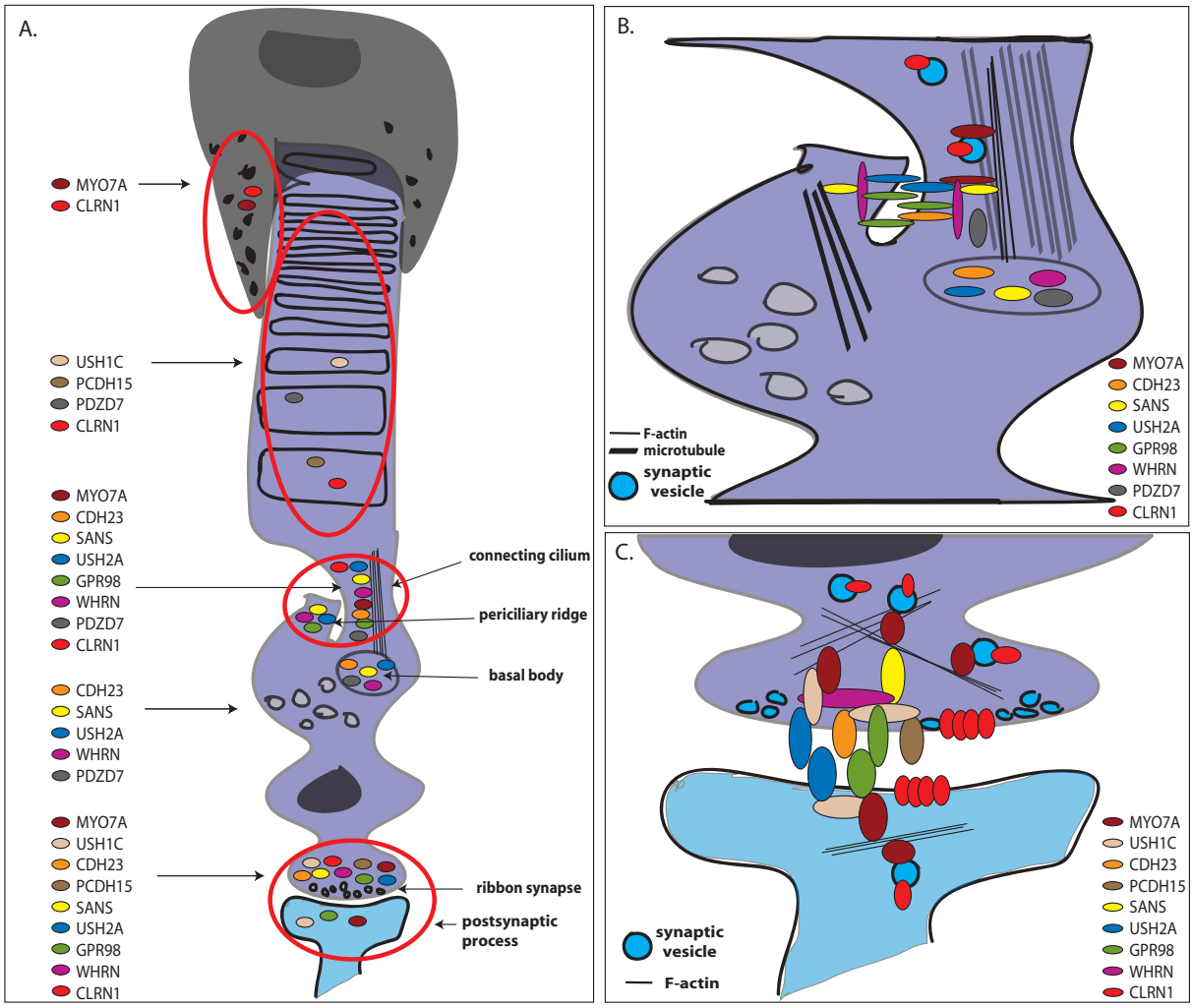

Figure 16. Detected and inferred CLRN1 localizations (marked with red circles and schematic red CLRN1 proteins) in a photoreceptor cell (A), connecting cilium region (B) and photoreceptor synapse (C) compared to the reported localizations of other USH proteins (described in Review of the literature, section 4.5.1).

The absence of functional CLRN1 leads to progressive death of retinal cells in RP in humans. It remains unclear whether the gradual retinal cell death begins with the malfunction of the photoreceptors themselves or of the cells supporting photoreceptor function (Müller and RPE cells). For example, RPE cells function in phagocytosis of shedded membranous disks from photoreceptor OS and delivering nutrients to photoreceptors as well as secreting growth factors (Schraermayer and Heimann, 1999; Strauss, 2005). Such functions are crucial for photoreceptor maintenance. One of the functions of Müller cells in retina is to recycle the released glutamate from neuronal synapses back to neurons as glutamine as well as produce factors influencing photoreceptor survival (Zachs and Esguerra, 2006). In photoreceptors CLRN1 could be part of the

synaptic vesicle traffic to the synaptic region or transport vesicle traffic through connecting cilium into or out of the outer segment of the photoreceptor cell. For example, the gradual cell death seen in USH3 patients could be explained by impaired function of the connecting cilium. Ten billion opsins are trafficked every second in a single human retina from the inner segment to outer segment through the connecting cilium (Liu et al., 1999b). If this transport is affected opsins or other proteins may accumulate in inappropriate subcellular locations, leading to a decline in photoreceptor cell integrity and ultimately to RP.

The zebrafish protein localization and *in situ* mRNA hybridization results are in contrast to the mouse *in situ* mRNA hybridization results in which detection of *Clrn1* in the retina peaks at P7, and diminishes afterwards (Geller et al., 2009). Zallocchi et al. (2009) have published controversial results using an antibody and localizing CLRN1 in mouse adult retina photoreceptors to the connecting cilia, inner segment and ribbon synapses which correlates with our zebrafish results. The discrepancy between mouse *in situ* hybridization and antibody detection results could be explained by *Clrn1* transcription levels that are too low for RNA *in situ* hybridization. On the other hand, the specificity of the antibody used by Zallocchi et al. (2009) has been questioned (John Flannery, personal communication).

In mouse, CLRN1 is present from E18 to P10 in mouse cochlear hair cells. CLRN1 is localized to the basal and apical parts of the hair cell. The CLRN1 localization in the hair cells could implicate a function in hair cell synaptic maturation (Zallocchi et al., 2009). In mouse hair cells the absence of CLRN1 causes disorganized stereocilia, which indicates that CLRN1 also has a similar function as other USH proteins affecting the organization of the stereocilia in cochlear hair cells (Yan and Liu, 2010). In zebrafish the timing and localization of Clrn1 is consistent with a role in stereocilia organization. Zebrafish Clrn1 is present in ear and neuromast hair cells throughout the studied developmental stages, from 2 dpf to 7 dpf. Clrn1 was found to localize to the hair cell kinocilium and apical periciliary region as well as to the basal synaptic region (Figure 17).

Figure 17. Localization of Clrn1 in hair cells of a zebrafish otic sensory patch (the perimeter of a single cell is marked with a circle) (A-D). Dr-Clrn1-ab (red) colocalizes (yellow) with tubulin (green) at 2 dpf (A and B) and at 4 dpf (C and D). Clrn1 localization is noted in the apical region of the hair cells and basal position consistent with involvement at hair cell synapses (A-D). The red circles in bold indicate regions where zebrafish Clrn1 can be detected with immunohistochemical studies compared to the reported localizations of other USH proteins (E and F, described in Review of the literature, section 4.5.2).

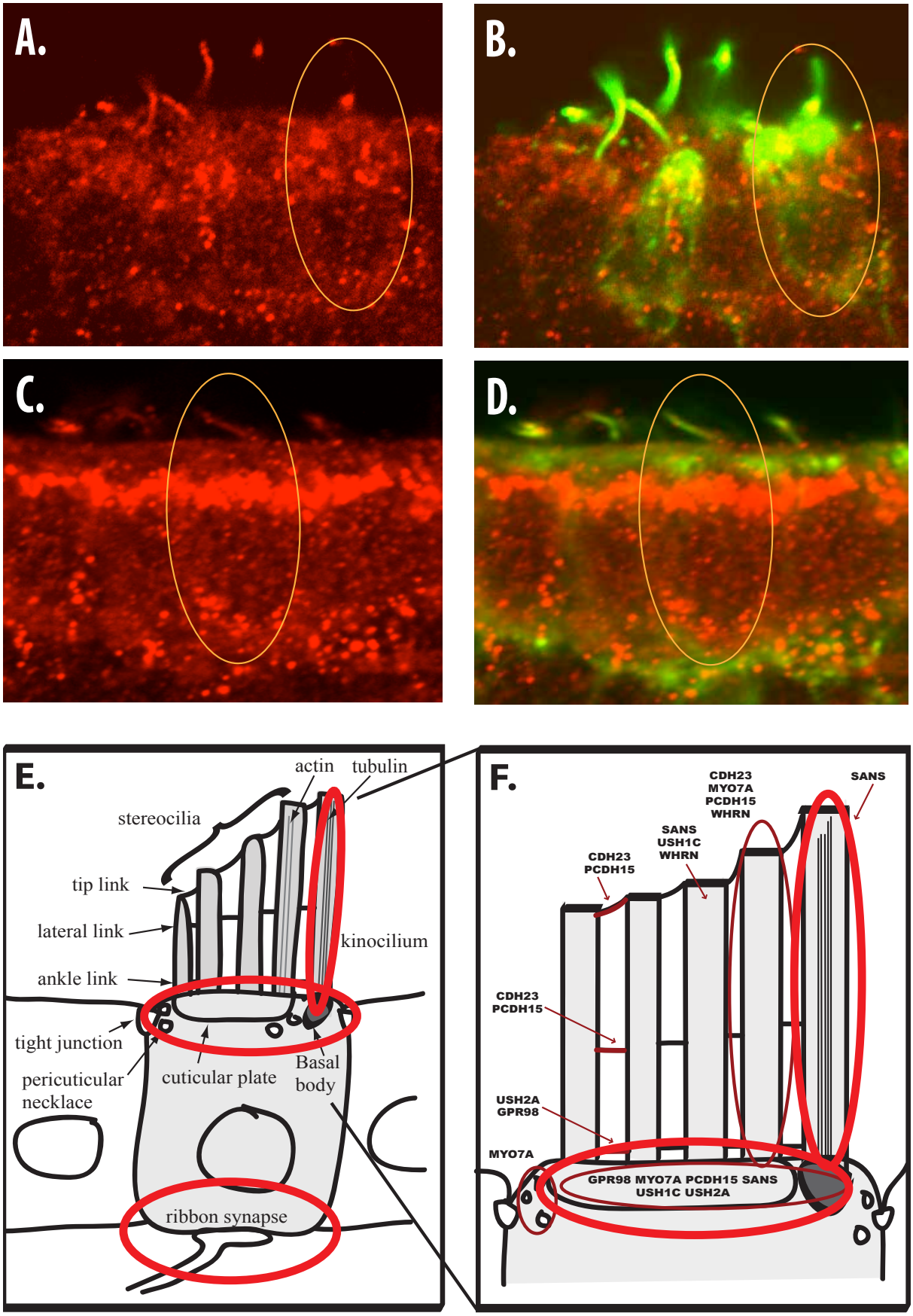
A.
B.
C.
D.
E.
actin
tubulin
stereocilia
tip link
lateral link
kinocilium
ankle link
tight junction
pericuticular necklace
cuticular plate
Basal body
ribbon synapse
F.
CDH23 MYO7A PCDH15 WHRN
SANS
SANS USH1C WHRN
CDH23 PCDH15
CDH23 PCDH15
USH2A GPR98
MYO7A
GPR98 MYO7A PCDH15 SANS USH1C USH2A

4.3 Clrn1 knockdown (U)

The production of Clrn1 was knocked down by injecting either a translation blocking morpholino (Clrn1MOatg) against the *clrn1* translation start site or a splice site blocking morpholino (Clrn1MOsplice) against the zebrafish *clrn1* exon 0 3' splice site into 1-cell stage zebrafish embryos. Immunohistochemistry studies with Dr-Clrn1-ab showed that both morphant larvae had lower levels of Clrn1 protein in the retina (Figure 18). The transient knockdown of Clrn1 levels in zebrafish allowed us to observe the effect on zebrafish development. As the absence of functional CLRN1 causes USH3 in human patients, our main interest was to observe the consequences of Clrn1 knockdown in zebrafish larvae vision and hearing/balance. MO efficacy periods are variable, and dependent upon degradation of the oligonucleotide and turnover rates of the endogenous proteins. The MO ability to suppress protein production also diminishes, because the MO amount injected into the single cell stage stays the same during cell proliferation and organ development. With both Clrn1MOs we found that Clrn1 levels began rising after 4 dpf. This transient knockdown of Clrn1 allowed us to observe the consequences of depleting Clrn1 during sensory organ development and assay for possible recovery of behavioral phenotypes when functional levels of Clrn1 were restored.

4.3.1 Hearing and balance (U)

The Clrn1 morphant zebrafish had obvious balance problems compared to the control 4 dpf larvae. Zebrafish balance was studied by observing the response to swirling the media. While the uninjected larvae were able to correct themselves after swirling, some of the MO injected fish had clear problems with balance with no ability to sense which direction was up or down. These fish had also a tendency to float on the surface of the water. In the tapping test, the startle response to the tap on the petri dish was measured for MO and control animals. Only 5 % of 4 dpf uninjected control larvae (N=327) failed to respond to tapping on the petri dish. In contrast, 20 % of Clrn1MOsplice larvae (N=161) and 38 % of Clrn1MOatg larvae (N=58) had no startle response at 4 dpf (Figure 19).

Our studies with the Clrn1 morphant zebrafish show unequivocally that the larvae develop balance/hearing problems similar to the deafness and balance problems reported in USH3 mouse model. The fact that USH3 mouse and zebrafish models develop similar symptoms

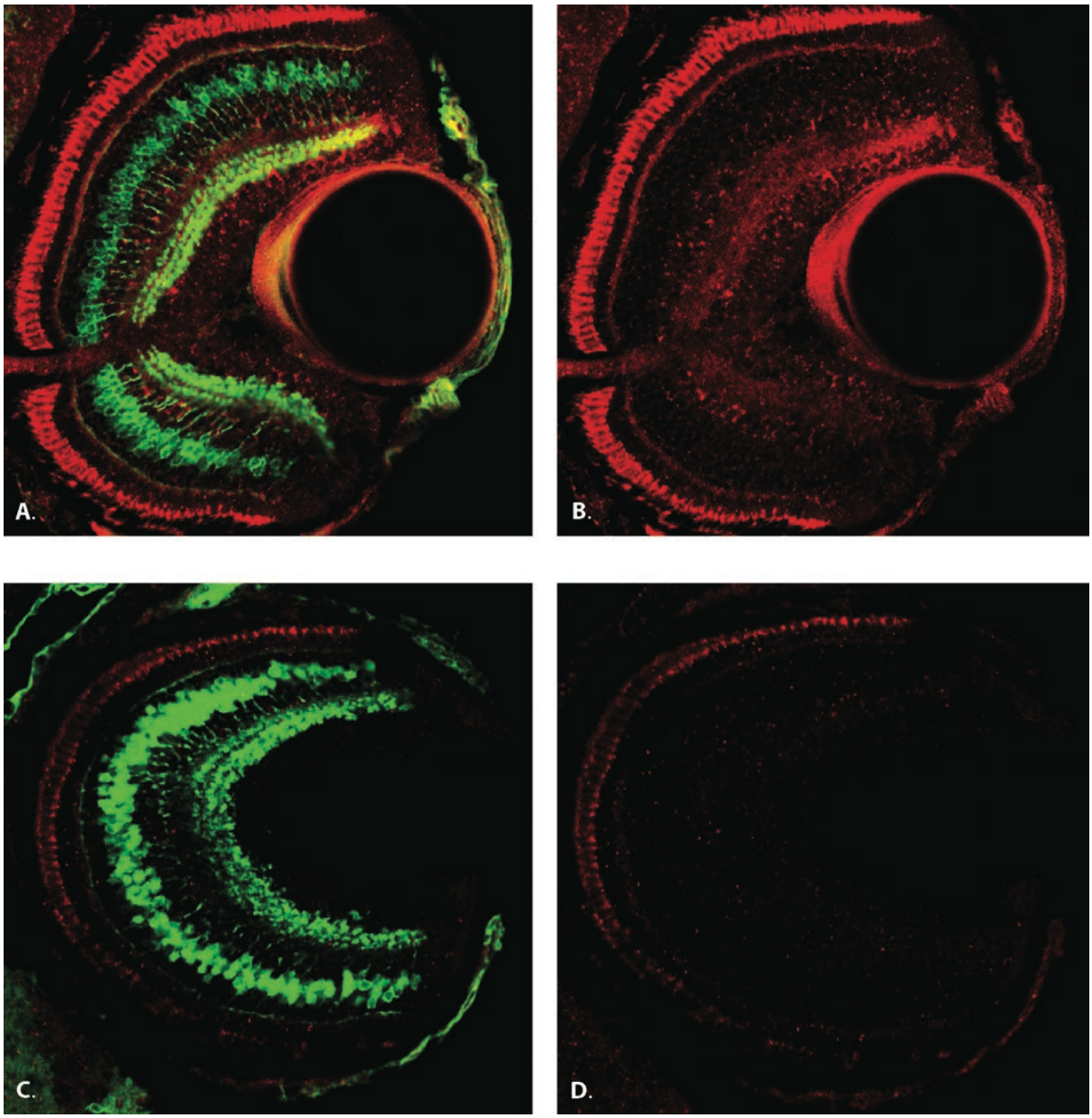

Figure 18. Effect of translation blocking Clrn1MOatg on Clrn1 presence in zebrafish larval retina. Uninjected control (A,B) and MO injected (C,D) 5 dpf larval retina sections stained with Dr-Clrn1-ab. Antibody stainings; Clrn1 (red) in all panels and PKCa bipolar cell marker (green) in panels A and C.

in hearing and balance suggests that the CLRN1 function in ear hair cells is similar and equally important. In mouse the absence of functional CLRN1 causes disruption of stereocilia organization (Geller et al., 2009) and it remains to be seen whether the deafness and balance problems in our USH3 zebrafish model is caused by similar stereocilia disorganization.

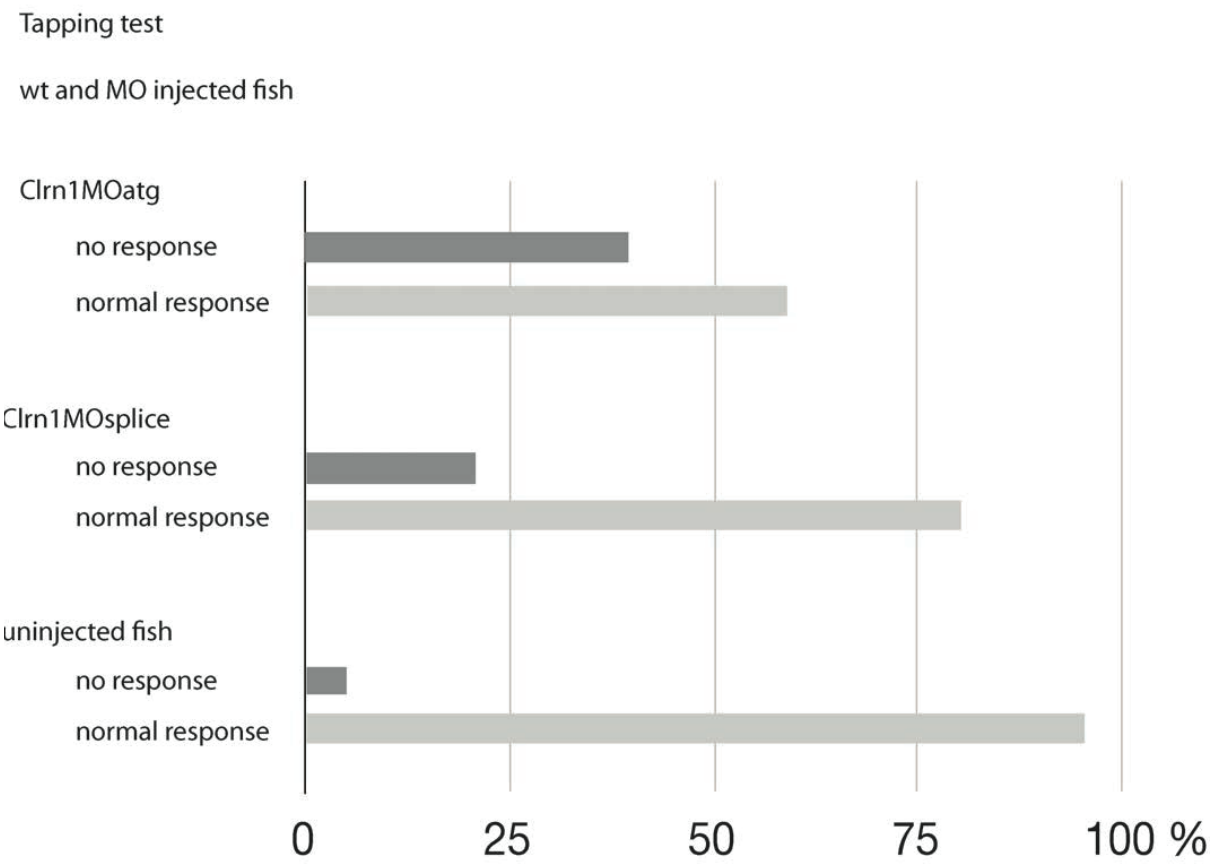

Figure 19. Startle response is significantly impaired in Clrn1MO treated zebrafish larvae. The results of the tapping tests performed on the uninjected control fish (N=327) and MO injected zebrafish larvae (Clrn1MOatg N=58 and Clrn1MOsplice N=161). The results are presented as percentages of the studied larvae.

4.3.2 Vision (U)

The Clrn1 morphant larvae had significantly slower optokinetic responses (OKR) compared to wild type larvae. Reduction in visual function was highly significant (P value < 0,001, ***) at 4 dpf with both the Clrn1MOatg and Clrn1MOsplice. Significant statistical (P value ≤ 0.01, **) differences between morphants and controls lasted past 4 dpf only when Clrn1MOatg was used (Figure 20).

Unlike the USH3 mouse that was shown not to develop visual problems, the zebrafish retina seems to require functional Clrn1 from early developmental time points for proper function. The results suggest that either *Clrn1* function is unnecessary in mouse retina or there is another protein that can functionally replace the absent CLRN1. Short life span has been suggested as a reason for lack of progressive RP in USH3 mice. However, in Clrn1 knockdown

zebrafish the symptoms appear during retinal development. There seems to be crucial differences in the molecular landscape between the mouse, zebrafish and human retina. Differences in the arrangement and abundance of different photoreceptor types could be one of the key elements. The mouse retina is rod dominant, suitable for function in low-light conditions whereas zebrafish and human retinas contain cones necessary for rich color vision for diurnal life. The differences in environments in which the retinas have evolved to function have produced alternative retinal cell subtypes (i.e. ganglion cells subtypes and cone types) in the mouse, human and zebrafish retinas (Gouras, 2009). Perhaps Clrn1 is required in proper cone function or cone connections and interactions with other retinal cell types (i.e. other cones, rods, horizontal cells, RPE cells, Müller cells). In humans and zebrafish the absence of this CLRN1 specific function leads to RP. The importance of cones is supported by the results that the symptoms of retinal degeneration in USH3 patients doesn't necessarily start with night blindness like in USH1 and USH2 (Pakarinen, 1995b, 1996, 1997). This supports the theory that cones have an important role in the development of USH3.

The USH3 mouse model hearing loss is not progressive, but congenital (Geller et al., 2009). The hearing loss/balance deficit and vision loss in zebrafish is not progressive, but present already during development. A theory for this discrepancy is that USH3 in human patients is progressive because the human *CLRN1* alternative splicing is more complex and mutated CLRN1 can retain some functionality forming multimers with alternative splice variants when the main CLRN1 variant is either absent or deformed. However, our research shows that zebrafish Clrn1 morphants represent good USH3 animal models for studying the USH3 disease mechanism.

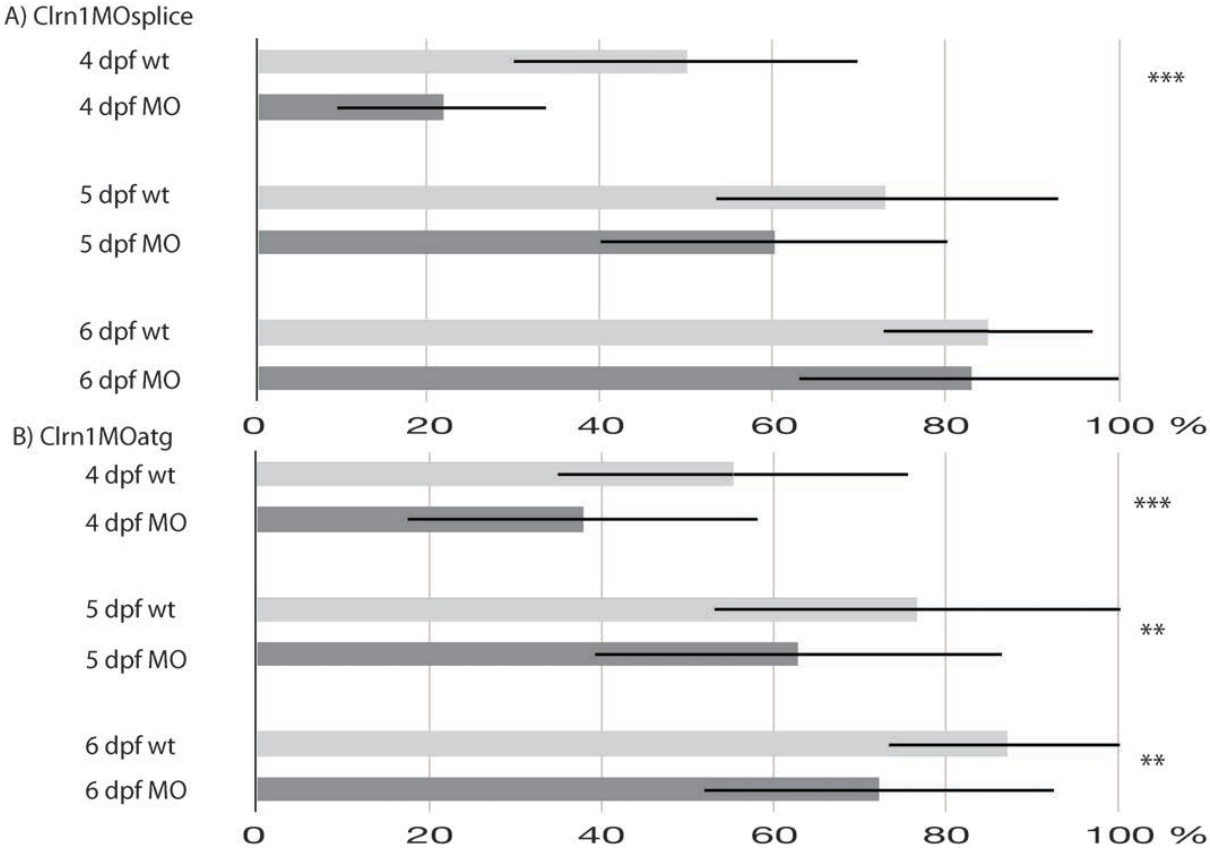

Figure 20. Results of visual function analysis in zebrafish larvae. Visual function was studied using OKR in which the number of moving stripes the larvae detected within one minute was measured. The results are presented as percentage of moving stripes larvae detected. The significance was depicted with an asterisk: highly significant (P value < 0,001, ***) or significant (P value ≤ 0.01, **).

CONCLUDING REMARKS

Mutations in nine genes are known to cause Usher syndrome. The severity of the syndrome in each patient is dictated by the USH genes mutated, and the mutations. The molecularly identified USH genes encode proteins that function in a USH protein network. All the USH proteins, except for CLRN1, have been shown to interact within this USH protein interactome. However, the similarity of clinical symptoms between all USH subtypes suggest that all the USH proteins, including CLRN1, are part of the same functional network in retina and cochlea.

The spectrum of USH mutations present in Finland is unique to the Finnish population. In this study we identified four novel USH1B mutations and one novel USH2A mutation as well as one known USH2A mutation from Finnish USH patients. The USH mutation spectrum is still anything but clear. Our USH families with possible digenic USH inheritance show that sequence variations are sometimes difficult to ascertain as either pathogenic or benign. Additionally, the fact that USH can be caused by at least nine genes and at least one modifier gene, PDZD7, complicates the mutation search. Everyone carries several USH sequence variations in their genome. Only extensive research can determine whether these USH variations are just polymorphisms or potential mutations and whether these variations can affect the USH phenotype when combined with mutations.

Before this thesis, the *CLRN1* main splice variant was known to be composed of three exons. During this study several new splice variants were found. Most of them have translation termination signals in them and thus are not translated into functional proteins. The simple three exon *CLRN1* gene seems to be the main functional form and all the known USH3 causing mutations are within these three exons. Why genes produce these alternative splice variants is as yet unknown. Is the *CLRN1* main variant the only functional one and the rest of the splice variants only mistakes by the splicing machinery? Another option would be that the other splice variants have some function perhaps important in certain cell types or developmental stages or that they function in controlling the transcription and translation of the main variant. All the splice variants have been discovered in human retinal cDNA and their function might be limited to the retinal function of otherwise ubiquitously expressed *CLRN1.*

During this thesis study we discovered that wt CLRN1 is transported to the plasma membrane in cultured cells. Mutated CLRN1 proteins can be unstable, but all the studied CLRN1 mutant proteins remain in the ER and are not transported to the plasma membrane. The reason behind progressive hearing loss and RP development in the inner ear and retina, respectively,

could be the incorrectly localized CLRN1 and the ER stress the mutated CLRN1 proteins cause over time.

The ultimate goal in studying *CLRN1* has been the development of a gene therapy for USH3 patients. Perhaps the most crucial question for the success of gene therapy is not the function of CLRN1, but when CLRN1 functions. If functional CLRN1 is not present during retinal and cochlear development can the effect of CLRN1 absence be augmented later? Or is CLRN1 needed too early in development with too drastic structural importance to be augmented after the symptoms become present in USH3 patients? The USH3 knockout mice have no visual symptoms even without functioning CLRN1. The results of the gene therapy trials to cure the deafness present in these USH3 mice are thus far inconclusive. However, while the human hearing loss and retinal degeneration are progressive, the hearing defects in the mouse are early onset and there is no notable retinal degeneration. Thus, the USH3 knockout mouse presents a useful but limited model in which to test treatments for human USH3. The Clrn1MO injected zebrafish larvae completed early developmental stages with depleted Clrn1 function, but began producing Clrn1 as the morpholino effect wore off. Some Clrn1 morphants recovered auditory or visual function by 10 dpf, whereas other morphants showed no signs of recovery. Thus the question remains: Can the development of USH3 be stopped by adding functional CLRN1 or has the damage been done when the cells/contacts between the cells/the sensory organs develop?

ACKNOWLEDGEMENTS

Tämä väitöskirja on tehty Folkhälsanin tutkimuskeskuksessa perinnöllisyystutkimuksen laitoksella ja Helsingin yliopiston lääketieteellisen tiedekunnan lääketieteellisen genetiikan osastolla vuosien 2005-2011 aikana. Olen kiitollinen tutkimuslaitosten nykyisille sekä entisille professoreille Anna-Elina Lehesjoelle, Per-Henrik Groopille, Leena Palotielle, Kristiina Aittomäelle, Päivi Peltomäelle sekä Irma Järvelälle upeiden työskentelymahdollisuuksien luomisesta, niin tutkimukseen tarvittavien materiaalien, kuin kannustavan ja tutkimuksesta innostuneen työympäristön suhteen.

This thesis study received funding from the Biomedicum Helsinki Foundation, De Blindas Vänner - Sokeain Ystävät Foundation, European Molecular Biology Organization (EMBO), Finnish Eye and Tissue Bank Foundation, Foundation Fighting Blindness, Helsinki University Chancellor's travel grants, Helsinki University Medicine Fund, Hope for Vision, Maud Kuistila Memorial Foundation, Oskar Öflunds Foundation, Otto A Malm Foundation, Paulo Foundation, Research Foundation of the University of Helsinki, Retina Finland, Understödsförening Liv och Hälsa and the Folkhälsan Research Foundation. I am truly grateful for their support, without them this thesis project would not have been possible.

Syvimmät kiitokset tutkimukseen osallistuneille ja sen siten mahdollistaneille potilaille ja heidän sukulaisilleen/ My deepest gratitude to the patients and their family members who participated in this thesis study and thereby made it possible.

Kiitos Helena Kääriäiselle ja Katarina Pelinille tämän väitöskirjan kriittisestä lukemisesta ja käsikirjoituksen kommentoinnista. Lisäksi haluan kiittää Irma Järvelää suostumisestaan tämän väitöksen kustokseksi sekä hänen mielenkiinnostaan tutkimusaihetta kohtaan.

Haluan kiittää Aila Riikosta, Jaana Welin-Haapamäkeä, Madeleine Avellania, Marjatta Valkamaa, Stephan Keskistä, Solveig Halosta sekä Nina Forssia aina avuliaista neuvoista tutkimustyön toimistopuolella ja käytännön asioiden järjestämisestä tutkimuksen mahdollistamiseksi. Lisäksi kiitosta kaipaavat kaikki ne tutkimuskeskuksen ulkopuolella järjestetyt tapahtumat, joilla meitä yritettiin houkutella ulos laboratoriosta.

Haluan kiittää kanssakirjoittajiani Leenamaija Kleemolaa ja Liisa Jauholaa. Lisäksi kiitokset tutkimuksessa ja artikkeleiden kirjoituksessa auttaneille: Sirpa Kivirikko, Reijo Norio, Eva Roomets ja Tiina Tyni. Kiitos teille kaikille avusta ja innostuksesta Usher-tutkimuksen edistämiseksi.

Kiitos Sinikka Lindhille avusta potilasnäytteiden kanssa ja Jinmin Miaolle avusta solulinjojen kanssa. Haluan myös kiittää Carina Wallgren-Petterssonia avuliaista kommenteista. Lisäksi syvä

kiitos Katarina Pelinille sekä Pekka Heinolle kannustuksesta ja neuvoista opintojeni viimeistelyssä. Ilman teitä tätä väitöskirjaa ei olisi.

Ohjaajalleni Eeva-Marja 'Eevis' Sankilalle kiitokset näistä vuosista. Tie, joka alkoi palohälytyksestä on ollut mutkainen ja täynnä kuoppia. Uskosi projektiin on kantanut kuitenkin kaikki nämä vuodet. Vuosien varrella ryhmä on muuttunut ympärillämme, tutkimussuunnitelmat tarkentuneet ja artikkelit valmistuneet. Samalla on kuitenkin ollut aikaa matkustella, juhlia, oppia elämää ja väitellä asioista aina Harry Potterista virusvektoreihin. Sydämelliset kiitokset toiselle ohjaajalleni Anna-Elinalle, jonka neuvot ja kannustus auttoivat tämän kirjan valmistumisessa. Kiitos vuosien aikana saadusta tuesta ja varsinkin laboratorion hienon yhteishengen luomisesta. Lisäksi ekstra-kiitos kaikista luvista ylimääräisiin ja yleensä öisiin labra-aktiviteetteihin.

Kiitokset niin yhteistyöstä, ystävyydestä kuin kannustuksesta Usher-ryhmän entisille jäsenille Sari Tuupaselle ja Anne Aittakorvelle. Reetta Vainionpäälle, jonka kanssa on selvitty niin konferenssimatkojen luennoista, ostosmaratooneista, karmaisevista öistä Bates-hotelleissa jossain puhelimen tuolla puolen, ajosta kaistoja arpoen sateisessa Atlantassa kuin hivuttautumisesta läpi poliisiratsian... En olisi varmasti jaksanut ilman maalaisjärkeäsi ja vakaata tukeasi läpi tämän väitösprosessin. Laura Pietola, kanssasi olen jakanut viimeisten askeleiden painon, turhautumiset, jäähyväiset ja horisontin näkemisen ilon. Juhalle kiitos tutustuttamisesta väitöskirjanteon arkeen ja sen taidon opettamisesta, jolla tunnistaa mitkä kulmat kannatti suoristaa ja koska seurata sääntöjä. Vuodet ovat olleet kaikkea muuta kuin tylsiä. Olkoon Voima Kanssasi :) Jussi 'JJ' Jerolle ja Antti 'AAA' Aarnisalolle kiitokset järkähtämättömästä uskosta ja kiinnostuksesta tutkimukseen kaikkien karikoidenkin aikana. Yhteistyö kanssanne on ollut niin mielenkiintoista kuin opettavaakin.

I'm grateful to all the international collaborators for their help and interest towards my work: Carsten Bergmann, Hanno J Bolz, Frans Cremers, Astra Dinculescu, Jacque Duncan, Elise Heon, Christine Neuhaus, William W Hauswirth. I'm especially grateful to Scott F Geller and John G Flannery for their advice and support as well as making the reach for our study truly international. I'm grateful to the shoulders of giants: Professor Monte Westerfield, Jennifer Phillips, Berde Blanco, Jeremy Wegner, Sabrina Toro, Judy Peirce. When I came to Oregon I knew next to nothing about zebrafish, but you helped me through tanks, rigs and neurobunkers and into the Eugene way of life. Congratulations Jeremy and Sabrina! I'll be thinking of you during the evening party 'Karonkka' on 11.11.11!

I want to thank Jodie Painter for her comments on this manuscript and friendship during her years in FIG as well as advice on the movie screenplays.

Folkhälsanin tutkimuskeskuksen - nykyinen ja muualle karannut - sekalainen sakki kaipaa vain ylistystä. Teidän seassanne on ollut hieno olla, oppia ja kasvaa “aikuiseksi”. Moni jakaa kanssani mielipiteen, että Folkenstainin poppoolla ja Hotelli Kalifornialla on yksi yhteinen tekijä: “You can check out any time you like, but you can never leave.”. Tänne tullaan, mutta lähteminen on vaikeaa. Olette mukavia, avuliaita, ymmärtäväisiä, ystävällisiä ja kaikkea muuta kuin tylsiä. Harvemmin sitä on saanut luvan kanssa listiä työkavereitaan :P

Tarja Joensuulle ja Riikka Hämäläiselle kiitos tutkijan urani aloituksesta. Kesätyöstä vuonna 0, jolloin opettelin ajamaan PCR:ää ja valamaan geelejä. Avusta vuosien saatossa astuessani Usher-tutkimuksen kaaokseen. Kiitos aina iloisesta avusta ja neuvoista, joita sain kysymättäkin.

Kiitokset FIGin muille “väitösvangeille”. Saara Tegelbergille kiitos kumppanuudesta FIGin viidakossa (ja vähän muissakin ryteiköissä). Hengenheimolaisuudesta jaetuissa kampanjoissamme: ‘DRDs to the rescue, Let’s get the Terminator healthcare plan, Safe the preteen royalty, Beware of the religious androids…’ Aina löytyy uusi syy nousta barrikadeille. Mervi Kuroselle kiitokset seurasta ja järkkymättömästä kiinnostuksesta tutkimukseen. Saara ja Mervi, tiedän kenelle soittaa jos joskus joudun pulaan! Vilma-Lotta Lehtokari, the viisas, kiitos kun olet raahannut ‘Nuuskamuikkusen’ seikkailuihin tietokoneen näytöltä. Olet h@*#&^%n uskomaton! Jaakko Sarparanta, olet täydellinen tiedemies ja kultaa kalliimpi. Otto ‘kesä-Jeesus’ Manninen, Anni Laari, Inken Körber, Maria Kousi, Minttu Marttila Koittakaa kestää - Väitöspäivä lähenee!/ Hang in there - the Defense date will come! Nykyiset Tohtorit: Kirsi Alakurtti, Anna-Kaisa ‘AK’ Anttonen, Kati Donner, Vilma-Lotta Lehtokari, Anna Naukkarinen, Liina Nevalaita, Milja Kaare, Jukka Kallijärvi, Juha Kolehmainen, Anne Saarinen, Maria Sandbacka ja Eija Siintola, teidän jalanjälkiänne on ollut helppo seurata. Kiitos niin ystävyydestä kuin upeasta esimerkistä näinä vuosina. Hanne Ahola, Mira Aronen, Nina Aula, Nina Ekman, Paula Hakala, Mubashir Hanif, Hanna Hellgren, Jeanette Holmlund-Hampf, Per Harald Jonson, Kaisa Kettunen, Outi Kopra, Mairi Kuris, Ulla Lahtinen, Sara Lehtinen, Maria Lunkka-Hytönen, Helena Luque, Laura Mustaniemi, Elina Nuutinen, Olesya Okuneva, Anne Polvi, Mark Screen, Merja Soininen, Minnamari Talvitie, Teija Toivonen, Marilotta Turunen, Jouni Vesa, Pauliina Vornanen, Maija Wessman ja Albert Ferrés i Coy ynnä muut - kiitokset kaikille mielenkiintoisesta seurasta, keskusteluista, kannustuksesta ja avusta näinä vuosina. Erityiskiitos leffaryhmälle: “ruumiille/pahiksille/uhreille/aktivisteille/kameran toisella puolella raataneille” heidän *lähes* rajattomasta “innostuksesta/heittäytymisestä leikkiin/ huumorista/kaikkensa antamisesta/kyvystä jäädä työpaikalle auringonnousuun asti”. Peter Hackmanille kyvystä innostua jokaisesta ideasta, jonka olen ehdottanut. Siitä, että on jaksanut kantaa “pää -roolinsa” urhoollisena ja ihailtavasta kyvystä nauttia muurinpohjaletuista kiisseliin valeltuna rantapusikossa. Anja Koskela, Adile Samaletdin ja Tuula Soppela, kiitokset ruokapyödän keskusteluista ja viisaista katsantokannoista, joita ei itse aina ymmärrä ajatella. Kiitos Ann-Liz Träskelinille, laboratorion “äidille” upeasta seurasta, avusta ja iloisesta asenteesta. Anna

Naukkariselle, Anne Juvoselle ja Vilma-Lotta Lehtokarille erikoiskiitokset kaikesta avusta väitöskirjan loppumetreillä. Siitä, että olen voinut soitella milloin vain ja saada viisailta Tohtoreilta vastauksia Maisterin yksinkertaisiin kysymyksiin, vaikkakin etanolilla lahjomalla.

'Tarkkis-huoneelle', sen alkuperäisille jäsenille: AK, Anna, Saara ja Juha: koripallon pelaaminen, mesettely metrin päähän, roskapostien jakaminen, yleinen sekasorto sekä mitä mielenkiintoisimmat keskustelun aiheet, jotka lähtevät aina tangentilla käsistä. Ansaitsimme kaikki valitukset niin hyvässä kuin pahassa. Kumarran ja kiitän siitä, että vuosiin huonetta ei kukaan voinut kutsua vakavalla naamalla TYÖpaikaksi. Nykyisille uusille tulokkaille, Kaisalle ja Marialle, kiitokset ymmärryksestä viimeisten aikojen katoamisten ja vuoristoratojen kanssa, sekä soluttautumisesta outoon porukkaamme. Special thanks to Maria for sharing my fondness for night shifts and sharing the thesis panic.

Kiitokset ystäville, jotka ovat seuranneet vierestä pitkää matkaa. Marita, Marko ja Minna, siitä on pitkä matka kun lähdin Etelä-Pohjanmaalta Helsinkiin. Matka on ollut pitkä, mutta vasta alussa meillä kaikilla. Sami, olet ehkä maailman positiivisin mies ja kiitos että jaksat innostua aina uusista ideoista, joita heittelen ilmaan. Satu ja Adrian, Lontoon vuodesta on jäänyt vain hyviä muistoja. Taistelimme läpi homeen, sienien, outojen sytkärien... Satulle olen kiitollinen siitä, että hän raahasi minut Intiaan juuri kun tarvitsin sitä kaikkein eniten. Minne seuraavaksi päädytään, ei (onneksi) kukaan tiedä. Tanssivintin omistautuneet tanssijat. Wilma: kiitos siitä, että jaksat valloittaa maailman joka aamu yhä uudestaan ja jaat kanssani maailman, jossa ei ole rajoituksia. Heidi, jääkaapin vainukoira: olet sisareni kyvyttömyydessä tuntea häpeää ja kykysi raahata minut jos minnekkin mitä lyhyimmillä varoitusajoilla on traumatisoiva. Meeri, joka onneksi ei antanut periksi: koita jaksaa kohta ei tarvitse hajota enää koulun kanssa. Niinalle kiitos, että olen saanut keskittyä muihinkin mielenkiintoisiin projekteihin tämän kirjan kirjoituksen aikana. Olet kurinalaisuudessa kunnioitusta herättävä, älä menetä uskoasi. Tähän pitäisi liittää tunteitani kuvastava tanssi - sanat kun vain eivät riitä kuvaamaan kiitollisuutta seurastanne näiden vuosien aikana. Kiitos kaikesta! Fatimalle kiitosta uskosta ja viisaudesta. Telinevoimistelijoille varsinkin kesän omatoimi-ryhmälle ja Iinalle treenien jälkeisistä palautus/motivaatio "kahveista". Kiitos siitä, että jaksatte niin inspiroida kuin kannustaa takomaan päätä kanveesiin ja tekemään asioita, joihin ei usko pystyvänsä. Marylou, I love our conversations and the occasions we manage to be in the same space-time co-ordinates.

Aunelle ja Bertalle, kahdelle täysin erilaiselle isoäidille. Tiedän kuinka paljon tämä olisi merkinnyt teille. Leenalle, Veikolle, Jussille, Nikolle, Airille, Jarille, Ullalle, Roosalle, Sinikalle mitä rakkaimmat kiitokset. Suku on pieni, mutta sitä rakkaampi. Kiitos jokaisesta hetkestä ja kaikesta ymmärryksestä ja tuesta vuosien varrelta! Leenalle pahoittelut siitä, että lääkärin sijasta tuli

hajamielinen tohtori, tosin lääketieteen laitokselle. Oli kannustavaa seurata kuinka innostuneena jaksoit opiskella uuden ammatin tämän väitösprojektin aikana.

Marketalle, en ole elämässäni tavannut toista ihmistä, joka olisi päässyt yhtä pitkälle pelkällä sisulla ja uskolla tulevaan. Vaihtaessasi nyt uusien haasteiden kimppuun, murehtien yhä minunkin omiani, muistathan kaikkien harmaiden hiuksien keskellä mitä Kanadassa käskivät kääntää sinulle :) Erkki, ilman sinua jalkani eivät edes viistäisi maata. Olet elämäni vaikein vastaväittäjä. Yliopistolla olisi paljon opittavaa metodeistasi. Jaksat aina kuitenkin vastustuksesta huolimatta kannustaa ja yllättää loihtimalla mitä älyttömimpiä tarvikkeita jos mihinkin projekteihin.

Elina. Kiitos. Tiedekonferenssin alter-egoni, jonka todennäköisyys uhmaa tieteellistä maailmankuvaani. Kilistelkäämme aina shampanjaa katsoessamme kuolemaa silmiin. Ja sitten se muistutus, jonka olen sanonut jo kerran aikaisemmin: Do not get lost in the Limbo! Todistetusti sieltä pääsee pois. P.S. Love Love jne...

Tämä väitöskirja on omistettu Pentti Tanniselle

Helsinki, Syyskuu 2011

"YOU'VE BEEN IN MY LIFE SO LONG, I CAN'T REMEMBER ANYTHING ELSE"
-ELLEN RIPLEY, ALIEN[3]

REFERENCES

Adams NA, Awadein A, Toma HS. The retinal ciliopathies. Ophthalmic Genet 2007; 28:113-25.

Adato A, Kalinski H, Weil D, Chaib H, Korostishevsky M, Bonne-Tamir B. Possible interactions between USH1B and USH3 gene products as implied by apparent digenic deafness inheritance. Am J Hum Genet 1999; 65:261-5.

Adato A, Vreugde S, Joensuu T, Avidan N, Hämäläinen R, Belenkly O, Olender T, Bonne-Tamir B, Ben-Asher E, Espinos C, Millán JM, Flannery JG, Avraham KB, Pietrokovski S, Sankila EM, Beckmann JS, Lancet D. USH3A transcripts encode clarin-1, a four-transmembrane- domain protein with a possible role in sensory synapses. Eur J Hum Genet 2002; 10:339-50.

Adato A, Michel V, Kikkawa Y, Reiners J, Alagramam KN, Weil D, Yonekawa H, Wolfrum U, El-Amraoui A, Petit C. Interactions in the network of Usher syndrome type 1 proteins. Hum Mol Genet 2005; 14:347-56.

Ahmed ZM, Riazuddin S, Bernstein SL, Ahmed Z, Khan S, Griffth AJ, Morell RJ, Friedman TB, Wilcox ER. Mutations of the protocadherin gene PCDH15 cause Usher syndrome type 1F. Am J Hum Genet 2001; 69:25-34.

Ahmed ZM, Riazuddin S, Ahmad J, Bernstein SL, Guo Y, Sabar MF, Sieving P, Riazudding S, Griffith AJ, Friedman TB, Belyantseva IA, Wilcox ER. PCDH15 is expressed in the neurosensory epithelium of the eye and ear and mutant alleles are responsible for both USH1F and DFNB23. Hum Mol Genet 2003a; 12:507-19.

Ahmed ZM, Riazuddin S, Wilcox ER. The molecular genetics of Usher syndrome. Clin Genet 2003b; 63:431-44.

Ahmed Z, Riazuddin S, Khan SN, Friedman PL, Riazuddin S, Friedman TB. USH1H, a novel locus for type 1 Usher syndrome, maps to chromosome 15q22-23. Clin Genet 2009; 75:86-91.

Akoury E, El Zir E, Mansour A, Mégarbané A, Majewski J, Slim R. A novel 5-bp deletion in clarin 1 in a family with Usher syndrome. Ophthalmic Genet 2011 (epub ahead print).

Alagramam KN, Yuan H, Kuehn MH, Murcia CL, Wayne S, Srisailpathy CR, Lowry RB, Knaus R, Van Laer L, Bernier FP, Schwartz S, Lee C, Morton CC, Mullins RF, Ramesh A, Van Camp G, Hageman GS, Woychik RP, SMith RJ. Mutations in the novel protocadherin PCDH15 cause Usher syndrome type 1F. Hum Mol Genet 2001; 10:1709-1718.

Aller E, Jaijo T, Oltra S, Alió J, Galán F, Nájera C, Beneyto M, Millán JM. Mutation screening of USH3 gene (clarin-1) in Spanish patients with Usher syndrome: low prevalence and phenotypic variability. Clin Genet 2004a; 66:525-9.

Aller E, Nájera C, Millán JM, Oltra JS, Pérez-Garrigues H, Vilela C, Navea A, Beneyto M. Genetic analysis of 2299delG and C759F mutations (USH2A) in patients with visual and/or auditory impairments. Eur J Hum Genet 2004b; 12:407-10.

Alsina B, Giraldez F, Pujades C. Patterning and cell fate in ear development. Int J Dev Biol 2009; 53:1503-13.

Ashmore J, Gale J. The cochlea. Curr Biol 2000; 10:R325-7.

Astuto LM, Weston MD, Carney CA, Hoover DM, Cremers CW, Wagenaar M, Möller C, Smith RJ, Pieke-Dahl S, Greenberg J, Ramesar R, Jacobson SG, Ayuso C, Heckenlively JR, Tamayo M, Gorin MB, Reardon W, Kimberling WJ. Genetic heterogeneity of Usher syndrome: analysis of 151 families with Usher type 1. Am J Hum Genet 2000; 67:1569-74.

Bahloul A, Michel V, Hardelin J-P, Nouaille S, Hoos S, Houdusse A, England P, Petit C. Cadherin-23, myosin VIIa and harmonin, encoded by Usher syndrome type I genes, form a ternary complex and interact with membrane phospholipids. Hum Mol Genet 2010; 19:3557-65.

Barrong SD, Chaitin MH, Fliesler SJ, Possin DE, Jacobson SG, Milam AH. Ultrastructure of connecting cilia in different forms of retinitis pigmentosa. Arch Ophthalmol 1992; 110:706-10.

Batissoco AC, Auricchio MTBM, Kimura L, Tabith-Junior A, Mingroni-Netto RC. A novel missense mutation p.L76P in the GJB2 gene causing nonsyndromic recessive deafness in a Brazilian family. Braz J Med Biol Res 2009; 42:168-71.

Beatty CW, McDonald TJ, Colvard DM. Usher's syndrome with unusual otologic manifestations. Mayo Clin Proc 1979; 54:543-6.

Bech-Hansen NT, Naulor MJ, Maybaum TA, Pearce WG, Koop B, Fishman GA, Mets M, Musarella MA, Boycott KM. Loss-of-function mutations in a calcium-channel alpha1- subunit gene in Xp11.23 cause incomplete X-linked congenital stationary night blindness. Nat Genet 1998; 19:264-7.

Becker W, Naumann HH, Pfaltz CR, Herberhold C, Kastenbauer E. Ear. In: Buckingham RA (ed) Ear, Nose, and Throat Diseases, 2nd ed. Thieme Medical Publishers Inc, New York, 1988, pp 1-30.

Bernal S, Meda C, Solans T, Ayuso C, Garcia-Sandoval B, Valverde D, Del Rio E, Baiget M. Clinical and genetic studies in Spanish patients with Usher syndrome type II: description of new mutations and evidence for a lack of genotype -phenotype correlation. Clin Genet 2005; 68:204-14.

Berntson A, Taylor WR, Morgans CW. Molecular identity, synaptic localization, and physiology of calcium channels in retinal bipolar cells. J Neurosci Res 2003; 71:146-51.

Bhattacharya G, Miller C, Kimberling WJ, Jablonski MM, Cosgrove D. Localization and expression of usherin: a novel basement membrane protein defective in people with Usher's syndrome type IIa. Hear Res 2002; 163:1-11.

Bhattacharya G, Kalluri R, Orten DJ, Kimberling WJ, Cosgrove D. A domain -specific usherin/ collagen IV interaction may be required for stable integration into the basement membrane superstructure. J Cell Sci 2004; 117:233-42.

Bilotta J, Saszik S. The zebrafish as a model visual system. Int J Dev Neurosci 2001; 19:621-9.

Bitner-Glindzicz M, Lindley KJ, Rutland P, Blaydon D, Smith VV, Milla PJ, Hussain K, Furth-Lavi J, Cosgrove KE, Shepherd RM, Barnes PD, O'Brien RE, Farndon PA, Sowden J, Liu XZ, Scanlan MJ, Malcom S, Dunne MJ, Aynsley-Green A, Glaser B. A recessive contiguous gene deletion causing infantile hyperinsulinism enteropathy and deafness identifies the Usher type 1C gene. Nat Genet 2000; 26:56-60.

Black DL. Mechanisms of alternative pre-messenger RNA splicing. Annu Rev Biochem 2003; 72:291-336.

Bok D, Galbraith G, Lopez I, Woodruff M, Nusinowitz S, BeltrandelRio H, Huang W, Zaho S, Geske R, Montgomery C, Van Sligtenhorst I, Friddle C, Platt K, Sparks MJ, Pushkin A, Abuladze N, Ishiyama A, Dukkipati R, Liu W, Kurtz I. Blindness and auditory impairment caused by loss of the sodium bicarbonate cotransporter NBC3. Nat Genet 2003; 34:313-9.

Bolz H, von Brederlow B, Ramirez A, Bryda EC, Kutsche K, Nothwang HG, Seeliger M, de C-Salcedó Cabrera M, Vila MC, Molina OP, Gal A, Kubisch C. Mutations of CDH23, encoding a new member of the cadherin gene family, causes Usher syndrome type 1D. Nat Genet 2001; 27:108-12.

Bonnet C, Grati M, Marlin S, Levilliers J, Hardelin JP, Parodi M, Naisme-Grare M, Zelenika D, Delepine M, Feldmann D, Jonard L, El-Amraoui A, Weil D, Delobel B, Vincent C, Dollfus H, Eliot MM, David A, Calais C, Vigneron J, Montaut-Verient B, Bonneau D, Dubin J, Thauvin C, Duvillard A, Francannet C, Mom T, Lacombe D, Duriez F, Drouin -Garraud V, Thuillier-Obstoy MF, Sigaudy S, Frances AM, Collignon P, Challe G, Couderc R, Lathrop M, Sahel JA, Weissenbach J, Petit C, Denoyelle F. Complete exon sequencing of all known Usher syndrome genes greatly improves molecular diagnosis. Orphanet J Rare Dis 2011; 6:21.

Bork JM, Peters LM, Riazuddin S, Bernstein SL, Ahmed ZM, Ness SL, Polomeno R, Ramesh A, Schloss M, Srisailpathy CR, Wayne S, Bellman S, Desmukh D, Ahmed Z, Khan SN, Kaloustian VM, Li XC, Lalwani A, Bitner-Glindzicz M, Nance WE, Liu XZ, Wistow F, Smith RJ, Griffith AJ, Wilcox ER, Friedman TB, Morell RJ. Usher syndrome 1D and nonsyndromic autosomal recessive deafness DFNB12 are caused by allelic mutations of the novel cadherin-like gene CDH23. Am J Hum Genet 2001; 68:26-37.

Bähler M, Rhoads A. Calmodulin signaling via the IQ motif. FEBS Lett 2002; 513:107-13.

Böeda B, El-Amraoui A, Bahloul A, Goodyear R, Daviet L, Blanchard S, Perfettini I, Fath KR, Shorte S, Reiners J, Houdussse A, Legrain P, Wolfrum U, Richardson G, Petit C. Myosin VIIa, harmonin and cadherin 23, three Usher I gene products that cooperate to shape the sensory hair cell bundle. EMBO J 2002; 21:6689-99.

Caberlotto E, Michel V, foucher I, Bahloul A, Goodyear RJ, Pepermans E, Michalski N, Perfettini I, Alegria-Prévot O, Chardenoux S, Do Cruzeiro M, Hardelin JP, Richardson GP, Avan P, Weil D, Petit C. Usher type 1G protein sans is a critical component of the tip-link complex, a structure controlling actin polymerization in stereocilia. PNAS 2011; 108:5825-30.

Chaïb H, Kaplan J, Gerber S, Vincent C, Ayadi H, Slim R, Munnich A, Weissenbach J, Petit C. A newly identified locus for Usher syndrome type I, USH1E, maps to chromosome 21q21. Hum Mol Genet 1997; 6:27-31.

Chang WS, Harris WA. Sequential genesis and determination of cone and rod photoreceptors in Xenopus. J Neurobiol 1998; 35:227-44.

Chen ZY, Hasson T, Kelley PM, Schwender BJ, Schwartz MF, Ramakrishnan M, Kimberling WJ, Mooseker MS, Corey DP. Molecular cloning and domain structure of human myosin- VIIa, the gene product defective in Usher syndrome 1B. Genomics 1996; 36:440-8.

Chinen A, Hamaoka T, Yamada Y, Kawamura S. Gene duplication and spectral diversification of cone visual pigments of zebrafish. Genetics 2003; 163:663-75.

Chishti AH, Kim AC, Marfatia SM, Lutchman M, Hanspal M, Jindal H, Liu SC, Low PS, Rouleau GA, Mohandas N, Chasis JA, Conboy JG, Gascard P, Takakuwa Y, Huang SC, Benz EJ Jr, Bretscher A, Fehon RG, Gusella JF, Ramesh V, Solomon F, Marchesi VT, Tsukita S, Tsukita S, Hoover KB. The FERM domain: a unique module involved in the linkage of cytoplasmic proteins to the membrane. Trends Biochem Sci 1998; 23:281-2.

Cideciyan AV, Aleman TS, Boye SL, Schwartz SB, Kaushal S, Roman AJ, Pang JJ, Sumaroka A, Windsor EA, Wilson JM, Flotte TR, Fishman GA, Heon E, Stone EM, Byrne BJ, Jacobson SG, Hauswirth WW. Human gene therapy for RPE65 isomerase deficiency activates the retinoid cycle of vision but with slow rod kinetics. Proc Natl Acad USA 2008; 105:1511-7.

Cideciyan AV, Hauswirth WW, Aleman TS, Kaushal S, Schwartz SB, Boye SL, Windsor EAM, Conlon TJ, Sumaroka A, Pang J, Roman AJ, Byrne JB, Jacobson SG. Human RPE65 gene therapy for Leber congenital amaurosis:persistence of early visual improvements and safety at 1 year. Hum Gene Ther 2009; 20:999-1004.

Cremers FP, Kimberling WJ, Külm M, de Brouwer AP, van Wijk E, te Brinke H, Cremers CW, Hoefsloot LH,

Banfi S, Simonelli F, Fleischhauer JC, Berger W, Kelley PM, Haralambous E, Bitner-Glindzicz M, Webster AR, Saihan Z, De Baere E, Leroy BP, Silvestri G, McKay GJ, Koenekoop RK, Millan JM, Rosenberg T, Joensuu T, Sankila EM, Weil D, Weston MD, Wissinger B, Kremer H. Development of a genotyping microarray for Usher syndrome. J Med Genet 2007; 44: 153-160.

Davenport SLH, Omenn GS. The heterogeneity of Usher syndrome, publication 426. Amsterdam, Excerpta Medica Foundation, International Congress Series, abstract 215, 1977, pp 87-8.

Delprat B, Micehl V, Goodyear R, Yamasaki Y, Michalski N, El-Amraoui A, Perfettini I, Legrain P, Richardson G, Hardelin JP, Petit C. Myosin XVa and whirlin, two deafness gene products required for hair bundle growth, are located at the stereocilia tips and interact directly. Hum Mol Genet 2005; 14:401-10.

Di Palma F, Holme RH, Bryda EC, Belyantseva IA, Pellegrino R, Kachar B, Steel KP. Noben-Trauth K. Mutations in Cdh23, encoding a new type of cadherin, cause stereocilia disorganization in waltzer, the mouse model for Usher syndrome type 1D. Nat Genet 2001a; 27: 103-7.

Di Palma F, Pellegrino R, Noben-Trauth K. Genomic structure, alternative splice forms and normal and mutant alleles of cadherin 23 (Cdh23). Gene 2001b; 281: 31-41.

Dreyer B, Tranebjaerg L, Rosenberg T, Weston MD, Kimberling WJ, Nilssen Ø. Identification of novel USH2A mutations: implications for the structure of USH2A protein. Eur J Hum Genet 2000; 8:500-6.

Dreyer B, Brox V, Tranebjaerg L, Rosenberg T, Sadeghi AM, Möller C, Nilssen Ø. Spectrum of USH2A mutations in Scandinavian patients with Usher syndrome type II. Hum Mutat 2008; 29:451.

Ebermann I, Scholl HP, Charbel Issa P, Becirovic E, Lamprecht J, Jurklies B, Millan JM, Aller E, Mitter D, Bolz H. A novel gene for Usher syndrome type 2: mutations in the long isoform of whirlin are associated with retinitis pigmentose and sensorineural hearing loss. Hum Genet 2007a; 121:203-11.

Ebermann I, Wilke R, Lauhoff T, Lübben D, Zrenner E, Bolz HJ. Two truncating USH3A mutations, including one novel, in a German family with Usher syndrome. Mol Vis 2007b; 13:1539-47.

Ebermann I, Lopez I, Bitner-Glindzicz M, Brown C, Koenekoop RK, Bolz HJ. Deafblindness in French Canadians from Quebec: a predominant founder mutation in the USH1C gene provides the first genetic link with the Acadian population. Genome Biol 2007c; 8:R47.

Ebermann I, Phillips JB, Liebau MC, Koenekoop RK, Schermer B, Lopez I, Schäfer E, Roux A-F, Dafinger C, Bernd A, Zrenner E, Claustres M, Blanco B, Nürnberg G, Nürnberg P, Ruland R, Westerfield M, Benzing T, Bolz HJ. PDZD7 is a modifier of retinal disease and a contributor to digenic Usher syndrome. J Clin Inv 2010; 120:1812-23.

El-Amraoui A, Sahly I, Picaud S, Sahel J, Abithol M, Petit C. Human Usher 1B/mouse shaker-1: the retinal phenotype discrepancy explained by the presence/absence of myosin VIIA in the photoreceptor cells. Hum Mol Genet 1996; 5:1171-8.

Espinos C, Millan JM, Beneyto M, Najera C. Epidemiology of Usher syndrome in Valencia and Spain. Community Genet 1998; 1:223-8.

Eudy JD, Yao S, Weston MD, Ma-Edmonds M, Talmadge CV, Cheng JJ, Kimberling WJ, Sumegi J. Isolation of a gene encoding a novel member of the nuclear receptor superfamily from the critical region of Usher syndrome type IIa et 1q41. Genomics 1998a; 50:382-4.

Eudy JD, Weston MD, Yao S, Hoover DM, Rehm HL, Ma-Edmonds M, Yan D, Ahmad I, Cheng JJ, Ayuso C, Cremers C, Davenport S, Moller C, Talmadge CB, Beisel KW, Tamayo M, Morton CC,

Swaroop A, Kimberling WJ, Sumegi J. Mutation of a gene encoding a protein with extracellular matrix motifs in usher syndrome type 2a. Science 1998b; 280:1753-7.

Fadool JM, Dowling JE. Zebrafish models of retinal development and disease. In: Sernagor E, Eglen S, Harris B and Wong R (eds) Retinal development. Cambridge University Press, New York, 2006, pp 342-70.

Fernandez-Alfonso T, Ryan TA. The efficiency of the synaptic vesicle cycle et central nervous system synapses. Trends Cell Biol 2006; 16:413-20.

Fields RR, Zhou G, Huang D, Davis JR, Möller C, Jacobson SG, Kimberling WJ, Sumegi J. Usher syndrome type III: revised genomic structure of the USH3 gene and identification of novel mutations. Am J Hum Genet 2002; 71:607-17.

Fishman GA, Kumar A, Joseph ME, Torok N, Anderson RJ. Usher's Syndrome. Ophthalmic and Neuro-otologic Findings Suggesting Genetic Heterogeneity. Arch Ophthalmol 1983; 101:1367-74.

Geller SF, Guerin KI, Visel M, Pham A, Lee ES, Dror AA, Avraham KB, Hayashi T, Ray CA, Reh TA, Bermingham-McDonogh O, Triffo WJ, Bao S, Isosomppi J, Västinsalo H, Sankila EM, Flannery JG. CLRN1 is nonessential in the mouse retina but is required for cochlear hair cell development. PLoS Genet 2009; 5:e1000607.

Geng R, Geller SF, Hayashi T, Ray CA, Reh TA, Bermingham-McDonogh O, Jones SM, Wright CG, Melki S, Yoshikazu I, Palczewski K, Alagramam KN, Flannery JG. Usher syndrome IIIA gene clarin-1 is essential for hair cell function and associated neural activation. Hum Mol Genet 2009; 18:2748-60.

Gerber S, Bonneau D, Gilbert B, Munnich A, Dufier JL, Rozet JM Kaplan J. USH1A:chronicle of a slow death. Am J Hum Genet 2006; 78:357-9.

Gerstein MB, Bruce C, Rozowsky JS, Zheng D, Du J, Korbel JO, Emanuelsson O, Zhang ZD, Weissman S, Snyder M. What is a gene, post-ENCODE? History and updated definition. Genome Res 2007; 17:669-81.

Gibbs D, Kitamoto J, Williams DS. Abnormal phagocytosis by retinal pigmented epithelium that lacks myosin VIIa, the Usher syndrome 1B protein. Proc Natl Acad Sci USA 2003; 100:6481-6.

Gibbs D, Azarian SM, Lillo C, Kitamoto J, Klomp AE, Steel KP, Libby RT, Williams DS. Role of myosin VIIa and Rab27a in the motility and localization of RPE melanosomes. J Cell Sci 2004; 117:6473-83.

Goldmann T, Rebibo-Sabbah A, Overlack N, Nudelman I, Belakhov V, Baasov T, Ben-yosef T, Wolfrum U, Nagel-Wolfrum K. Designed aminoglycoside NB30 induces beneficial read-through of a USH1C nonsense mutation in the retina. Inv Ophthalmol Vis Sci 2010; 51:6671-80.

Goldmann T, Overlack N, Wolfrum U, Nagel-Wolfrum K. PTC124 mediated translational read -through of a nonsense mutation causing Usher type 1C. Hum Gene Ther 2011; 22:537-47.

Gorlin RJ, Tilsner TJ, Feinstein S, Duvall AJ 3rd. Usher's syndrome type III. Arch Otolaryngol 1979; 105:353-4.

Gouras P. Color vision. In: Kolb H, Fernandez E, Nelson R (eds). Webvision: The organization of the retina and visual system [Internet]. Salt Lake CIty (UT), University of Utah Health Sciences Center; 1995-2005, updated 2009.

von Graefe A, Arlt F, Donders FC. Exeptionelle Verhalten des Gesichtsfeldes bei Pigmententartung der Netzhaut. Graefes Arc Clin Exp Ophthalmol 1858; 4:250-3.

Gröndahl J, Mjöen S. Usher syndrome in four Norwegian counties. Clin Genet 1986; 30:14-28.

Gurnienny TL, Brugnera E, Tosello-Trampont A, Kinchen JM, Haney LB, Nishiwaki K, Walk SF, Nemergut ME, Macara IG, Francis R, Schedl T, Qin Y, Van Aelst L, Hengartner MO, Ravichandran KS. CED-12/ELMO, a novel member of the CrkII/Dock180/Rac Pathway, is required for phagocytosis and cell migration. Cell 2001; 107:27-41.

Hachmeister JE. An abbreviated history of the ear: from Renaissance to present. Yale J Biol Med 2003; 76:81-6.

Harris WA, Messersmith SL. Two cellular inductions involved in photoreceptor determination in Xenopus retina. Neuron 1992; 9:357-72.

Hashimoto T, Gibbs D, Lillo C, Azarian SM, Legacki E, Zhang XM, Yang XJ, Williams DS. Lentiviral gene replacement therapy of retinas in mouse model for Usher syndrome type 1B. Gene Ther 2007; 14:584-94.

Hasson T, Heintzelman MB, Santos-Sacchi J, Corey DP, Mooseker MS. Expression in cochlea and retina of myosin-VIIa, the gene product defective in Usher syndrome type 1B. Proc Natl Acad Sci USA 1995; 92:9815-9.

Hasson T, Gillespie PG, Garcia JA, MacDonald RB, Zhao Y, Yee AG, Mooseker MS, Corey DP. Unconventional myosins in inner-ear sensory epithelia. J Cell Biol 1997; 137:1287-307.

Hauswirth WW, Aleman TS, Kaushal S, Cideciyan AV, Schwartz SB, Wang L, Conlon TJ, Boye SL, Flotte TR, Byrne BJ, Jacobson SG. Treatment of Leber congenital amaurosis due to RPE65 mutations by ocular subretinal injection of adeno-associated virus gene vector: short-term results of a phase I trial. Hum Gene Ther 2008; 19:979-90.

Hemler ME. Tetraspanin functions and associated microdomains. Nat Rev Mol Cell Biol 2005; 6:801-11.

Herrera W, Aleman TS, Cedeciyan AV, Roman AJ, Banin E, Ben-Yosef T, Gardner LM, Sumaroka A, Windsor EAM, Schwartz SB, Stone EM, Liu XZ, Kimberling WJ, Jacobson SG. Retinal disease in Usher syndrome III caused by mutations in the Clarin-1 gene. Invest Ophthalmol Vis Sci 2008; 49:2651-60.

Hewitt SM, Fraizer GC, Wu YJ, Rauscher III FJ, Saunders GF. Differential function of Wilms' tumor gene WT1 splice isoforms in transcriptional regulation. J Biol Chem 1996; 271:8588-92.

Hmani M, Ghorbel A, Boulila-Elgaied A, Zina ZB, Kammoun W, Drira M, Chaabouni M, Petit C, Ayadi H. A novel locus for Usher syndrome type II, USH2B, maps to chromosome 3 at p23-24.2. Eur J Hum Genet 1999; 7:363-7.

Hoogenboom HR, de Bruïne AP, Hufton SE, Hoet RM, Arends J, Roovers RC. Antibody phage display technology and its applications. Immunotechnology 1998; 4:1-20.

Hoogenboom HR, Chames P. Natural and designer binding sites made by phage display technology. Immunol Today 2000; 21:371-8.

Hope CI, Bundey S, Proops D, Fielder AR. Usher syndrome in the city of Birmingham: prevalence and clinical classification. Br J Ophthalmol 1997; 81:46-53.

HUGO (International Human Genome Sequencing Consortium). Finishing the euchromatic sequence of the human genome. Nature 2004; 431:931-45.

Hunter DG, Fishman GA, Mehta RS, Kretzer FL. Abnormal sperm and photoreceptor axonemes in Usher's syndrome. Arch Ophthalmol 1986; 104:385-9.

Jacobson SG, Cideciyan AV, Aleman TS, Sumaroka A, Roman AJ, Gardner LM, Prosser HM, Mishra M, Bech-Hansen NT, Herrera W, Schwartz SB, Liu XZ, Kimberling WJ, Steel KP, Williams DS. Usher syndromes due to MYO7A, PCDH15, USH2A or GPR98 mutations share retinal disease mechanism. Hum Mol Genet 2008; 17:2405-15.

Jaijo T, Aller E, García-García G, Aparisi MJ, Bernal S, Ávila-Fernández A, Barragán I, Baiget M, Ayuso C, Antiñolo G, Díaz-Llopis M, Külm M, Beneyto M, Nájera C, Millán JM. Microarray-based mutation analysis of 183 Spanish families with Usher syndrome. Invest Ophthalmol Vis Sci 2010; 51:1311-7.

Jalkanen R, Mäntyjärvi M, Tobias R, Isosomppi J, Sankila EM, Alitalo T, Bech-Hansen NT. X linked cone-rod dystrophy, CORDX3, is caused by a mutation in the CACNA1F gene. J Med Genet 2006; 43:699-704.

Jensen AM, Walker C, Westerfield M. Mosaic eyes: a zebrafish gene required in pigmented epithelium for apical localization of retinal cell division and lamination. Development 2001; 128:95-105.

Joensuu T, Blanco G, Pakarinen L, Sistonen P, Kääriäinen H, Brown S, de la Chapelle A, Sankila EM. Refined mapping of the Usher syndrome type III locus on chromosome 3, exclusion of candidate genes, and identification of the putative mouse homologous region. Genomics 1996; 38:255-63.

Joensuu T, Hämäläinen R, Lehesjoki AE, de la Chapelle A, Sankila EM. A sequence-ready map of the Usher syndrome type III critical region on chromosome 3q. Genomics 2000; 63:409-16.

Joensuu T, Hämäläinen R, Yuan B, Johnson C, Tegelberg S, Gasparini P, Zelante L, Pirvola U, Pakarinen L, Lehesjoki AE, de la Chapelle A, Sankila EM. Mutations in a novel gene with transmembrane domains underlie Usher syndrome type 3. Am J Hum Genet 2001; 69:673-84.

Johnson JM, Castle J, Garrett-Engele P, Kan Z, Loerch PM, Armour CD, Santos R, Schadt EE, Stoughton R, Shoemaker DD. Genome-wide survey of human alternative pre-mRNA splicing with exon junction microarrays. Science 2003a; 302:2141-4.

Johnson KR, Gagnon LH, Webb LS, Peters LL, Hawes NL, Chang B, Zheng QY. Mouse models of USH1C and DFNB18: phenotypic and molecular analyses of two new spontaneous mutations of the Ush1c gene. Hum Mol Genet 2003b; 12:3075-86.

Johnston AM, Naselli G, Niwa H, Brodnicki T, Harrison LC, Gonez LJ. Harp (harmonin-interacting, ankyrin repeat-containing protein), a novel protein that interacts with harmonin in epithelial tissues. Genes Cells 2004; 9:967-82.

Kajiwara K, Berson EL, Dryja TP. Digenic retinitis pigmentosa due to mutations at the unlinked peripherin/RDS and ROM1 loci. SCIENCE 1994; 264:1604-8.

Kaplan J, Gerber S, Bonneau D, Rozet JM, Delrieu O, Briard ML, Dollfus H, Ghazi I, Dufier JL, Frezal J. A gene for Usher syndrome type I (USH1A) maps to chrosomsome 14q. Genomics 1992; 14:979-87.

Karp A, Santore F. Retinitis pigmentosa and progressive hearing loss. J Speech Hear Disord 1983; 48:308-14.

Katayama S, Tomaru Y, Kasukawa T, Waki K, Nakanishi M, Nakamura M, Nishida H, Yap CC, Suzuki M, Kawai J, Suzuki H, Carninci P, Hayashizaki Y, Wells C, Frith M, Ravasi T, Pang KC, Hallinan J, Mattick J, Huma DA, Lipovich L, Batalov S, Engström PG, Mizuno Y, Faghihi MA,

Sandelin A, Chalk AM, Mottagui-Tabar S, Liang Z, Lenhard B, Wahlestedt. Antisense transcription in the mammalian transcriptome. Science 2005; 309:1564-6.

Kazmierczak P, Sakaguchi H, Tokita J, Wilson-Kubalek EM, Milligan RA, Müller U, Kachar B. Cadherin 23 and protocadherin 15 interact to form tip-link filaments in sensory hair cells. Nature 2007; 449:87-91.

Keats BJ, Savas S. Genetic heterogeneity in Usher syndrome. Am J Med Genet A 2004; 130:13-6.

Kelley MW. Regulation of cell fate in the sensory epithelia of the inner ear. Nat Rev Neurosci 2006a; 7:837-49.

Kelley MW. Hair cell development: Commitment through differentiation. Brain Res 2006b; 1091:172-85.

Kersten FFJ, van Wijk E, van Reeuwijk J, van der Zwaag B, Märker T, Peters TA, Katsanis N, Wolfrum U, Keunen JEE, Roepman R, Kremer H. Association of whirlin with $Ca_v1.3(\alpha_{1D})$ channels in photoreceptors, defining a novel member of the Usher protein network. Inv Ophthalmol Vis Sci 2010; 51:2338-46.

Khajavi M, Inoue K, Lupski JR. Nonsense -mediated mRNA decay modulates clinical outcome of genetic disease. Eur J Hum Genet 2006; 14:1074-81.

Khan MI, Kersten FFJ, Azam M, Collin RWJ, Hussain A, Shah STA, Keunen JEE, den Hollander AI. *CLRN1* mutations cause nonsyndromic retinitis pigmentosa. Ophthalmology 2011; 118:1444-8.

Kikkawa Y, Shitara H, Wakana S, Kohara Y, Takada T, Okamoto M, Taya C, Kamiya K, Yoshikawa Y, Tokano H, Kitamura K, Shimizu K, Wakabayashi Y, Shiroishi T, Kominami R, Yonekawa H. Mutation in a new scaffold protein Sans cause deafness in Jackson shaker mice. Hum Mol Genet 2003; 12:453-61.

Kimberling WJ, Möller CG, Davenport S, Priluck IA, Beighton PH, Greenberg J, Reardon W, Weston MD, Kenyon JB, Grunkemeyer JA, Dahl SP, Overbeck LD, Blackwood DJ, Brower AM, Hoover DM, Rowland P, Smith RJH. Linkage of Usher syndrome type I gene (USH1B) to the long arm of chromosome 11. Genomics 1992; 14:988-94.

Kong L, Zhou X, Li F, Yodoi J, McGinnis J, Cao W. Neuroprotective effect of overexpression of thioredoxin on photoreceptor degeneration in Tubby mice. Neurobiol Dis 2010; 38:446-55.

Kremer H, van Wijk E, Märker T, Wolfrum U, Roepman R. Usher syndrome: molecular links of pathogenesis, proteins and pathways. Hum Mol Genet 2006; 15:R262-70.

Kretzschmar T, von Rüden T. Antibody discovery: phage display. Curr Opin Biotechnol 2002; 13:598-602.

Küssel-Andermann P, El-Amraoui A, Safieddine S, Nouaille S, Perfettini I, Lecuit M, Cossart P, Wolfrum U, Petit C. Vezatin, a novel transmembrane protein, bridges myosin VIIA to the cadherin-catenins complex. The EMBO Journal 2000; 19:6020-9.

Lagziel A, Ahmed ZM, Schultz JM, Morell RJ, Belyantseva IA, Friedman TB. Spatiotemporal pattern and isoforms of cadherin 23 in wild type and waltzer mice during inner ear hair cell development. Dev Biol 2005; 280:295-306.

Lagziel A, Overlack N, Bernstein SL, Morell RJ, Wolfrum U, Friedman TB. Expression of cadherin 23 isoforms is not conserved: implications for a mouse model of Usher syndrome type 1D. Mol Vis 2009; 15:1843-57.

Landry JR, Mager DL, Wilhelm BT. Complex controls: the role of alternative promoters in mammalian genomes. TRENDS in Genetics 2003; 19:640-8.

Lentz JJ, Gordon WC, Hamilton EF, MacDonald GH, Cunningham DE, Robbins CA, Tempel BL, Bazan NG, Rubel EW, Oesterie EC, Keats BJ. Deafness and retinal degeneration in a novel USH1C knock-in mouse model. Dev Neurobiol 2010; 70:253-67.

Libby RT, Kitamoto J, Holme RH, Williams DS, Steel KP. Cdh23 mutations in the mouse are associated with retinal dysfunction but not retinal degeneration. Exp Eye Res 2003; 77:731-9.

Lin JH, Walter P, Yen TS. Endoplasmic reticulum stress in disease pathogenesis. Annu Rev Pathol 2008; 3:399-425.

Liu X, Vansant G, Udovichenko IP, Wolfrum U, Williams DS. Myosin VIIa, the product of the Usher 1B syndrome gene, is concentrated in the connecting cilia of photoreceptor cells. Cell Motil Cytoskeleton 1997a; 37:240-52.

Liu XZ, Walsh J, Mburu P, Kendrick-Jones J, Cope MJ, Steel KP, Brown SD. Mutations in the myosin VIIA gene cause nonsyndromic recessive deafness. Nat Genet 1997b; 16:188-90.

Liu XZ, Walsh J, Tamagawa Y, Kitamura K, Nishizawa M, Steel KP, Brown SD. Autosomal dominant non-syndromic deafness caused by a mutation in the myosin VIIA gene. Nat Genet 1997c; 17:268-9.

Liu X, Ondek B, Williams DS. Mutant myosin VIIa causes defective melanosome ditribution in the RPE of shaker-1 mice. Nat Genet 1998a; 19:117-8.

Liu XZ, Hope C, Walsh J, Newton V, Ke XM, Liang CY, Xu LR, Zhou JM, Trump D, Steel KP, Bundey S, Brown SD. Mutations in the myosin VIIA gene cause a wide phenotypic spectrum, including atypical Usher syndrome. Am J Hum Genet 1998b; 63:909-12.

Liu X, Udovichenko IP, Brown SD, Steel KP, Williams DS. Myosin VIIa participates in opsin transport through the photoreceptor cilium. J Neurosci 1999a; 19:6267-74.

Liu XZ, Hope C, Liang CY, Zou JM, Xu LR, Cole T, Mueller RF, Bundey S, Nance W, Steel KP, Brown SDM. A mutation (2314delG) in the Usher syndrome type IIA gene: high prevalence and phenotypic variation. Am J Hum Genet 1999b; 64:1221-5.

Liu XZ. The clinical presentation of DFNB2. Adv Otorhinolaryngol 2002; 61:120-3.

Liu X, Bulgakov OV, Darrow KN, Pawlyk B, Adamian M, Liberman MC, Li T. Usherin is required for maintenance of retinal photoreceptors and normal development of cochlear hair cells. Proc Natl Acad Sci USA 2007; 104:4413-8.

Liu Q, Zhang Q, Pierce E. Photoreceptor sensory cilia and inherited retinal degeneration. Adv Exp Med Biol 2010; 664:223-32.

LoGiudice L, Matthews G. The role of ribbons at sensory synapses. Neuroscientist 2009; 15:380-91.

Lopes VS, Gibbs D, Libby RT, Aleman TS, Welch DL, Lillo C, Jacobson SG, Radu RA, Steel KP, Williams DS. The Usher 1B protein, MYO7A, is required for normal localization and function of the visual retinoid cycle enzyme, RPE65. Hum Mol Genet 2011; 20:2560-70.

Luijendijk MW, Van Wijk E, Bischoff AM, Krieger E, Huygen PL, Pennings RJ, Brunner HG, Cremers CW, Cremers FP, Kremer H. Identification and molecular modelling of a mutation in the motor head domain of myosin VIIA in a family with autosomal dominant hearing impairment (DFNA11). Hum Genet 2004; 115:149-56.

Maerker T, van Wijk E, Overlack N, Kersten FF, McGee J, Goldmann T, Sehn E, Roepman R, Walsh EJ, Kremer H, Wolfrum U. A novel Usher protein network at the periciliary reloading point

between molecular transport machineries in vertebrate photoreceptor cells. Hum Mol Genet 2008; 17:71-86.

Matlin AJ, Clark F, Smith CW. Understanding alternative splicing: towards a cellular code. Nat Rev Mol Cell Biol 2005; 6:386-98.

Mburu P, Mustapha M, Varela A, Weil D, El-Amraoui A, Holme RH, Rump A, Hardisty RE, Blanchard S, Coimbra RS, Perfettini I, Parkinson N, Mallon A, Glenister P, Rogers MJ, Paige AJ, Moir L, Clay J, Rosenthal A, Liu XZ, Blanco G, Steel KP, Petit C, Brown SDM. Defects in whirlin, a PDZ domain molecule involved in stereocilia elongation, cause deafness in the whirler mouse and families with DFNB31. Nat Genet 2003; 34:421-8.

McGee J, Goodyear RJ, McMillan DR, Stauffer EA, Holt JR, Locke KG, Birch DG, Legan PK, White PC, Walsch EJ, Richardson GP. The very large G-protein -coupled receptor VLGR1: a component of the ankle link complex required for the normal development of auditory hair bundles. J Neurosci 2006; 26:6543-53.

McMillan DR, Kayes-Wandover KM, Richardson JA, White PC. Very large G protein-coupled receptor-1, the largest known cell surface protein, is highly expressed in the developing central nervous system. J Biol Chem 2002; 277:785-92.

McMillan DR, White PC. Studies on the very large g protein-coupled receptor: from initial discovery to determining its role in sensorineural deafness in higher animals. Adv Exp Med Biol 2011; 706:76-86.

Merin S, Abraham FA, Auerbach E. Usher's and Hallgren's syndromes. Acta Genet Med Gemellol 1974; 23:49-55.

Michalski N, Michel V, Bahloul A, Lefevre G, Barral J, Yagi H, Chardenoux S, Weil D, Martin P, Hardelin JP, Sato M, Petit C. Molecular characterization of the ankle-link complex in cochlear hair cells and its role in the hair bundle functioning. J Neurosci 2007; 27:6478-88.

Michel V, Goodyear RJ, Weil D, Marcotti W, Perfettini I, Wolfrum U, Kros CJ, Richardson GP, Petit C. Cadherin 23 is a component of the transient lateral links in the developing hair bundles of cochlear sensory cells. Dev Biol 2005; 280:281-94.

Moore JK, Linthicum FH Jr. The human auditory system: A timeline of development. Int J Audiol 2007; 46:460-78.

Modafferi EF, Black DL. Combinatorial control of a neuron-specific exon. RNA 1999; 5:687-706.

Nawrocki L, BreMiller R, Streisinger G, Kaplan M. Larval and adult visual piments of the zebrafish, Brachydanio rerio. Vis Res 1985; 25:1569-76.

Ness SL, Ben-Yosef T, Bar-Lev A, Madeo AC, Brewer CC, Avraham KB, Kornreich R, Desnick RJ, Willner JP, Friedman TB, Griffith AJ. Genetic homogeneity and phenotypic variability among Ashkenazi Jews with Usher syndrome type III. J Med Genet 2003; 40:767-72.

Newman EA, Reichenbach A. The Müller cell: a functional element of the retina. Trends Neurosci 1996; 19:307-12.

Ng TK, Lam CY, Lam DSC, Chiang SWY, Tam POS, Wang DY, Fan BJ, Yam GHF, Fan DSP, Pang CP. AC and AG dinucleotide repeats in the PAC6 P1 promoter are associated with high myopia. Mol Vis 2009; 15:2239-48.

Nicolson T. The genetics of hearing and balance in zebrafish. Annu Rev Genet 2005; 39:9-22.

Norio R. Finnish Disease Heritage I: characteristics, causes, background. Hum Genet 2003a; 112:441-456.

Norio R. Finnish Disease Heritage II: population prehistory and genetic roots of Finns. Hum Genet 2003b; 112:457-469.

Norio R. The Finnish Disease Heritage III: the individual diseases. Hum Genet 2003c; 112:470-526.

Nuutila A. Dytrofia retinitis pigmentosa -dysacusis syndrome (DRD): A study of the Usher or Hallgren syndrome. J Hum Genet 1970; 18:57-88.

Ouyang XM, Yan D, Du LL, Hejtmancik JF, Jacobson SG, Nance WE, Li AR, Angeli S, Kaiser M, Newton V, Brown SD, Balkany T, Liu XZ. Characterization of Usher syndrome type 1 gene mutations in an Usher syndrome patient population. Hum Genet 2005; 116:292-9.

Overlack N, Maerker T, Latz M, Nagel-Wolfrum K, Wolfrum U. SANS (USH1G) expression in developing and mature mammalian retina. Vision Research 2008; 48:400-12.

Pan Q, Shai O, Lee LJ, Frey BJ, Biencowe BJ. Deep surveying of alternative splicing complexity in the human transcriptome by high-throughput sequencing. Nat Genet 2008; 40:1413-5.

Pakarinen L, Karjalainen S, Simola KO, Laippala P, Kaitalo H. Usher's syndrome type 3 in Finland. Laryngoscope 1995a; 105:613-7.

Pakarinen L, Sankila EM, Tuppurainen K, Karjalainen S, Kääriäinen H. Usher syndrome type III (USH3): the clinical manifestations in 42 patients. Scand J Log Phon 1995b; 20:141-150.

Pakarinen L, Tuppurainen K, Laippala P, Mäntyjärvi M, Puhakka H. The ophthalmological course of Usher syndrome type 3. Int Ophthalmol 1996; 19:307-11.

Pakarinen L. Usher syndrome type III (USH3). Thesis, University of Tampere, 1997, no. 574.

Peng YW, Zallocchi M, Wang WM, Delimont D, Cosgrove D. Moderate light induced degeneration of rod photoreceptors with delayed transducin translocation in shaker1 mouse. Invest Ophthalmol Vis Sci 2011; 52:6421-7.

Pennings RJE, Wagenaar M, van Aarem A, Huygen PLM, Kimberling WJ, Cremers CWRJ. Hearing impairment in Usher's syndrome. Adv Otorhinolaryngol 2002; 61:184-91.

Petit C. Usher syndrome: from genetics to pathogenesis. Annu Rev Genomics Hum Genet 2001; 2:271-97.

Phillips JB, Lentz JJ, Owens K, Khanobdee K, Sampath S, Keats BJ, Raible D, Williams DS, Westerfield M. Analysis of zebrafish Ush1c (Harmonin) in sensory cell function and synaptic integrity. Invest Ophthalmol Vis Sci 2008; 49:E-Abstract 3070.

Pieke-Dahl SA, Weston MD, Kimberling WJ. Genetics heterogeneity of the Usher syndromes. Assoc Res Otolaryngol 1997; 20:A870.

Plantinga RF, Kleemola L, Huygen PLM, Joensuu T, Sankila EM, Pennings RJE, Cremers CWRJ. Serial audiometry and speech recognition findings in Finnish Usher syndrome type III patients. Audiol Neurootol 2005; 10:79-89.

Plantinga RF, Pennings RJE, Huygen PLM, Sankila EM, Tuppurainen K, Kleemola L, Cremers CWRJ, Deutman AF. Visual impairment in Finnish Usher syndrome type III. Acta Ophthalmol Scand 2006; 84:36-41.

Ramon y Cajal SR. The Structure of the Retina. La Retine des Vertébrés. Springfield ILL Thomas Springfield. 1893.

Rapaport DH. Retinal neurogenesis. In: Sernagor E, Eglen S, Harris B and Wong R (eds) Retinal development. Cambridge University Press, New York, 2006, pp 30-58.

Rasheva VI, Domingos PM. Cellular responses to endoplasmic reticulum stress and apoptosis. Apoptosis 2009; 14:996-1007.

Ratnam K, Västinsalo H, Sundquist S, Roorda A, Sankila EM, Duncan JL. Cone structure in patients with Usher syndrome III caused by mutations in the Clarin-1 gene. Invest Ophthalmol Vis Sci 2011; 4975:ARVO E-Abstract A399.

Rattner A, Sun H, Nathans J. Molecular genetics of human retinal diseases. Annu Rev Genet 1999; 33:89-131.

Rebibo-Sabbah A, Nudelman I, Ahmed ZM, Baasov T, Ben-Yosef T. In vitro and ex vivo suppression by aminoglycosides of PCDH15 nonsense mutations underlying type 1 Usher syndrome. Hum Genet 2007; 122:373-81.

Reiners J, Reidel B, El-Amraoui A, Böeda B, Huber I, Petit C. Differential distribution of harmonin isoforms and their possible role in Usher-1 protein complexes in mammalian photoreceptor cells. Invest Ophthalmol Vis Sci 2003; 44:5006-15.

Reiners J, van Wijk E, Märker T, Zimmermann U, Jürgens K, te Brinke H, Overlack N, Roepman R, Knipper M, Kremer H, Wolfrum W. Scaffold protein harmonin (USH1C) provides molecular links between Usher syndrome type 1 and type 2. Hum Mol Genet 2005a; 14:3933-43.

Reiners J, Märker T, Jürgens K, Reidel B, Wolfrum U. Photoreceptor expression of the Usher syndrome type 1 protein protocadherin 15 (USH1F) and its interaction with the scaffold protein harmonin (USH1C). Mol Vis 2005b; 11:347-55.

Reiners J, Nagel-Wolfrum K, Jürgens K, Märker T, Wolfrum U. Molecular basis of human Usher syndrome: deciphering the meshes of the Usher protein network provides insights into the pathomechanisms of the Usher disease. Exp Eye Res 2006; 83:97-119.

Reiners J, Wolfrum U. Molecular analysis of the supramolecular usher protein complex in the retina. Harmonin as the key protein of the Usher syndrome. Adv Exp Med Biol 2006; 572:349-53.

Resendes BL, Williamson RE, Morton CC. At the Speed of Sound: Gene Discovery in the Auditory System. Am J Hum Genet 2001; 69:923-35.

Rhodes CR, Hertzano R, Fuchs H, Bell RE, de Angelis MH, Steel KP, Avraham KB. A Myo7a mutation cesegregates with stereocilia defects and low-frequency hearing impairment. Mamm Genome 2004; 15:686-97.

Richardson GP, Forge A, Kros CJ, Fleming J, Brown SD, Steel KP. Myosin VIIA is required for aminoglycoside accumulation in cochlear hair cells. J Neurosci 1997; 17:9506-19.

Sadeghi M, Cohn ES, Kimberling WJ, Tranebjaerg L, Möller C. Audiological and vestibular features in affected subjects with USH3: a genotype/phenotype correlation. Int J Audiol 2005; 44:307-16.

Saihan Z, Webster AR, Luxon L, Bitner-Glindzicz M. Update on Usher syndrome. Curr Opin Neurol 2009; 22:19-27.

Sankila EM, Pakarinen L, Kääriäinen H, Aittomäki K, Karjalainen S, Sistonen P, de la Chapelle A. Assignment of an Usher syndrome type III (USH3) gene to chromosome 3q. Hum Mol Genet 1995; 4:93-8.

Scheel H, Tomiuk S, Hofmann K. A common protein interaction domain links two recently identified epilepsy genes. Hum Mol Genet 2002; 11:1757-62.

Schneider E, Märker T, Daser A, Frey-Mahn G, Beyer V, Farcas R, Schneider-Rätzke B, Kohlschmidt N, Grossmann B, Bauss K, Napiontek U, Keilmann A, Bartsch O, Zechner U, Wolfrum U, Haaf T. Homozygous disruption of PDZD7 by reciprocal translocation in a consanguineous family: a new member of the Usher syndrome protein interactome causing congenital hearing impairment. Hum Mol Genet 2009; 18:655-66.

Schraermeyer U, Heimann K. Current understanding on the role of retinal pigment epithelium and its pigmentation. Pigment Cell Res 1999; 12:219-36.

Schug J, Schuller WP, Kappen C, Salbaum JM, Bucan M, Stoeckert CJ. Promoter features related to tissue specificity as measured by Shannon entropy. Genome Biol 2005; 6:R33.

Schwander M, Xiong W, Tokita J, Lelli A, Elledge HM, Kazmierczak P, Sczaniecka A, Kolatkar A, Wiltshire T, Kuhn P, Holt JR, Kachar B, Tarantino L, Müller U. A mouse model for nonsyndromic deafness (DFNB12) links hearing loss to defects in tip links of mechanosensory hair cells. PNAS 2009; 106:5252-7.

Senften M, Schwander M, Kazmierczak P, Lillo C, Shin J, Hasson T, Géléoc GSG, Gillespie PG, Williams D, Holt JR, Müller U. Physical and functional interaction between protocadherin 15 and myosin VIIa in mechanosensory hair cells. J Neurosci 2006; 26:2060-71.

Sernagor E. Synaptogenesis and early neural activity. In: Sernagor E, Eglen S, Harris B and Wong R (eds) Retinal development. Cambridge University Press, New York, 2006, pp 265-287.

Sheedlo HJ, Nelson TH, Lin N, Rogers TA, Roque RS, Turner JE. RPE secreted proteins and antibody influence photoreceptor cell survival and maturation. Brain Res Dev Brain Res 1998; 107:57-69.

Sheedlo HJ, Brun-Zinkernagel AM, Oakford LX, Roque RS. Rat retinal progenitor cells and a retinal pigment epithelial factor. Brain Res Dev Brain Res 2001; 127:185-7.

Siemens J, Kazmierczak P, Reynolds A, Sticker M, Littlewood-Evans A, Müller U. The Usher syndrome proteins cadherin 23 and harmonin form a complex by means of PDZ- domain interactions. Proc Natl Acad Sci USA 2002; 99:14946-51.

Skradski SL, Clark AM, Jiang H, White HS, Fu YH, Ptacek LJ. A novel gene causing a mendelian audiogenic mouse epilepsy. Neuron 2001; 31:537-44.

Smith RJ, Lee EC, Kimberling WJ, Daiger SP, Pelias MZ, Keats BJ, Jay M, Bird A, Reardon W, Guest M, Ayyagari R, Fielding J, Hejtmancik JF. Localization of two genes for Usher syndrome type I to chromosome 11. Genomics 1992; 14:995-1002.

Smith RJH, Berlin CI, Hejtmancik JF, Keats BJ, Kimberling WJ, Lewis RA, Möller CG, Palias MZ, Tranebjaerg L. Clinical diagnosis of the Usher syndromes. Usher Syndrome Consortium. Am J Med Genet 1994; 50:32-8.

Soderpalm AK, Fox DA, Karlsson JO, van Veen T. Retinoic acid produces rod photoreceptor selective apoptosis in developing mammalian retina. Invest Ophthalmol Vis Sci 2000; 41:937-47.

Soni LE, Warren CM, Bucci C, Orten DJ, Hasson T. The unconventional myosin-VIIa associates with lysosomes. Cell Motil Cytoskeleton 2005; 62:13-26.

Spandau UH, Rohrschneider K. Prevalence and geographical distribution of Usher syndrome in Germany. Graefes Arch Clin Exp Ophthalmol 2002; 240:495-8.

Staub E, Pérez-Tur J, Siebert R, Nobile C, Moschonas NK, Deloukas P, Hinzmann B. The novel EPTP repeat defines a superfamily of proteins implicated in epileptic disorders. Trends Biochem Sci 2002; 27:441-4.

Stetefeld J, Ruegg Ma. Structural and functional diversity generated by alternative mRNA splicing. Trends Biochem Sci 2005; 30:515-21.

Strauss O. The retinal pigment epithelium in visual function. Physiol Rev 2005; 85:845-81.

Strom TM, Nyakatura G, Apfelstedt-Sylla E, Hellebrand H, Lorenz B, Weber BH, Wutz K, Gutwillinger N, Ruther K, Drescher B, Sauer C, Zrenner E, Meitinger T, Rosenthal A, Meindl A. An L-type calcium-channel gene mutated in incomplete X-linked congenital stationary night blindness. Nat Genet 1998; 19:260-3.

Sullivan LS, Heckenlively JR, Bowne SJ, Zuo J, Hide WA, Gal A, Denton M, Inglehearn CF, Blanton SH, Daiger SP. Mutations in a novel retina-specific gene cause autosomal dominant retinitis pigmentosa. Nat Genet 1999; 22:255-9.

Tamagawa Y, Kitamura K, Ishida T, Ishikawa K, Tanaka H, Tsuji S, Nishizawa M. A gene for a dominant form of non-syndromic sensorineural deafness (DFNA11) maps within the region containing the DFNB2 recessive deafness gene. Hum Mol Genet 1996; 5:849-52.

Tian G, Zhou Y, Hajkova D, Miyagi M, Dinculescu A, Hauswirth WW, Palczewski K, Geng R, Alagramam KN, Isosomppi J, Sankila EM. Clarin-1, encoded by the Usher syndrome III causative gene, forms a membranous microdomain. J Biol Chem 2009; 284:18980-93.

Tian C, Liu XZ, Han F, Yu H, Longo-Guess C, Yang B, Lu C, Yan D, Zheng QY. Ush1c gene expression levels in the ear and eye suggest different roles for Ush1c in neurosensory organs in a new Ush1c knockout mouse. Brain Res 2010; 1328:57-70.

Turunen L, Takkinen K, Söderlund H, Pulli T. Automated panning and screening procedure on microplates for antibody generation from phage display libraries. J Biomol Screen 2009; 14:282-93.

Usher CH. On the inheritance of retinitis pigmentosa with notes of cases. Br J Ophthalmol 1914; 19:130-236.

Verpy E, Leibovici M, Zwaenepoel I, Liu XZ, Gal A, Salem N, Mansour A, Blanchard S, Kobayashi I, Keats BJ, Slim R, Petit C. A defect in harmonin, a PDZ domain-containing protein expressed in the inner ear sensory hair cells, underlies Usher syndrome type 1C. Nat Genet 2000; 26:51-5.

Vihtelic TS, Doro CJ, Hyde DR. Cloning and characterization of six zebrafish photoreceptor opsin cDNAs and immunolocalization of their corresponding proteins. Vis Neurosci 1999; 16:571-85.

Wang Z, Burge C. Splicing regulation: From a parts list of regulatory elements to an integrated splicing code. RNA 2008; 14:802-13.

Wang ET, Sandberg R, Luo S, Khrebtukova I, Zhang L, Mayr C, Kingsmore SF, Schroth GP, Burge CB. Alternative isoform regulation in human tissue transciptomes. Nature 2008; 456:470-6.

Wayne S, Der Kaloustian VM, Schloss M, Polomeno R, Scott DA, Hejtmancik JF, Sheffield VC, Smith RJ. Localization of the Usher syndrome type ID gene (Ush1D) to chromosome 10. Hum Mol Genet 1996; 5:1689-92.

Wayne S, Lowry RB, McLeod DR, Knaus R, Farr C, Smith RJ. Localization of the Usher syndrome type 1F (Ush1F) to chromosome 10. Am J Hum Gen 1997; 61:A300.

Webb SW, Grillet N, Andrade LR, Xiong W, Swarthout L, Della Santina CC, Kachar B, Müller U. Regulation of PCDH15 function in mechanosensory hair cells by alternative splicing of the cytoplasmic domain. Development 2011; 138:1607-17.

Weil D, Blanchard S, Kaplan J, Guilford P, Gibson F, Walsh J, Mburu P, Varela A, Levilliers J, Weston MD, Kelley PM, Kimberling WJ, Wagenaar M, Levi-Acobas F, Larget-Piet D, Munnich A, Steel KP, Brown SDM, Petit C. Defective myosin VIIA gene responsible for Usher syndrome type 1B. Nature 1995; 374:60-1.

Weil D, Lévy G, Sahly I, Lévi-Acobas F, Blanchard S, El-Amraoui A, Crozet F, Philippe H, Abitbol M, Petit C. Human myosin VIIA responsible for the Usher 1B syndrome: A predicted membrane-associated motor protein expressed in developing sensory epithelia. Proc Natl Acad Sci USA 1996; 93:3232-7.

Weil D, Küssel P, Blanchard S, Lévy G, Levi-Acobas F, Drira M, Ayadi H, Petit C. The autosomal recessive isolated deafness, DFNB2, and the Usher 1B syndrome are allelic defects of the myosin-VIIA gene. Nat Genet 1997; 16:191-3.

Weil D, El-Amraoui A, Masmoudi S, Mustapha M, Kikkawa Y, Lainé S, Delmaghani S, Adato A, Nadifi S, Zina ZB, Hamel C, Gal A, Ayadi H, Yonekawa H, Petit C. Usher syndrome type I G (USH1G) is caused by mutations in the gene encoding SANS, a protein that associates with the USH1C protein, harmonin. Hum Mol Genet 2003; 12:463-471.

Westerfield M. The zebrafish book. A guide for the laboratory use of zebrafish (Danio rerio). Eugene, OR:University of Oregon Press 2007; 5th ed.

Weston MD, Kelley PM, Overbeck LD, Wagenaar M, Orten DJ, Hasson T, Chen ZY, Corey D, Mooseker M, Sumegi J, Cremers C, Möller C, Jacobson SG, Gorin MB, Kimberling WJ. Myosin VIIA mutation screening in 189 Usher syndrome type 1 patients. Am J Hum Genet 1996; 59:1074-83.

Weston MD, Eudy JD, Fujita S, Yao SF, Usami S, Cremers C, Greenberg J, Ramesar R, Martini A, Möller C, Smith RJ, Sumegi J, Kimberling WJ. Genomic structure and identification of novel mutations in Usherin, the gene responsible for Usher syndrome type IIA. Am J Hum Genet 2000; 66:1199-1210.

Weston MD, Luijendijk MW, Humphrey KD, Müller C, Kimberling WJ. Mutations in the VLGR1 gene implicate G-protein signaling in the pathogenesis of Usher syndrome type II. Am J Hum Genet 2004; 74:357-66.

Whitfield TT, Riley BB, Chiang MY, Phillips B. Development of the zebrafish inner ear. Dev Dyn 2002a; 223:427-58.

Whitfield TT. Zebrafish as a model for hearing and deafness. J Neurobiol 2002b; 53:157-71.

van Wijk E, Pennings RJ, te Brinke H, Claassen A, Yntema HG, Hoefsloot LH. Identification of 51 novel exons of the Usher syndrome type 2A (USH2A) gene that encode multiple conserved functional domains and that are mutated in patients with Usher syndrome type II. Am J Hum Genet 2004; 74:738-44.

van Wijk E, van der Zwaag B, Peters T, Zimmermann U, Te Brinke H, Kersten FF, Märker T, Aller E, Hoefsloot LH, Cremers CW, Cremers FP, Wolfrum U, Knipper M, Roepman R, Kremer H. The DFNB31 gene product whirlin connects to the Usher protein network in the cochlea and retina by direct association with USH2A and VLGR1. Hum Mol Genet 2006; 15:751-65.

Williams DS. Usher syndrome: animal models, retinal function of Usher proteins, and prospects for gene therapy. Vision Res 2008; 48:433-41.

Williams DS, Aleman TS, Lillo C, Lopes VS, Hughes LC, Stone EM, Jacobson SG. Harmonin in the murine retina and the retinal phenotypes of Ush1c-mutant mice and human USH1C. Invest Ophthalmol Vis Sci 2009; 50: 3881-9.

Wilson SM, Householder DB, Coppola V, Tessarollo L, Fritzsch B, Lee EC, Goss D, Carlson GA< Copeland NG. Jenkins NA. Mutations in Cdh23 cause nonsyndromic hearing loss in waltzer mice. Genomics 2001; 74:228-33.

Wolfrum U, Liu X, Schmitt A, Udovichenko IP, Williams DS. Myosin VIIa as a common component of cilia and microvilli. Cell Motil Cytoskeleton 1998; 40:261-71.

Wong ROL. Introduction -from eye field to eyesight. In: Sernagor E, Eglen S, Harris B and Wong R (eds) Retinal Development. Cambridge University Press, New York, 2006, pp 1-7.

Yan D, Li F, Hall ML, Sage C, Hu WH, Giallourakis C, Upadhyay G, Ouyang XM, Du LL, Bethea JR, Chen ZY, Yajnik V, Liu XZ. An isoform of GTPase regulator DOCK4 localizes to the stereocilia in the inner ear and binds to harmonin (USH1C). J Mol Biol 2006; 357:755-64.

Yan D, Ouyang X, Patterson DM, Du LL, Jacobson SG, Liu XZ. Mutation analysis in the long isoform of *USH2A* in American patients with Usher syndrome type II. J Hum Genet 2009; 54:732-8.

Yan D, Liu XZ. Genetics and pathological mechanisms of Usher syndrome. J Hum Genet 2010; 55:327-35.

Yan D, Kamiya K, Ouyang XM, Liu XZ. Analysis of subcellular localization of Myo7a, Pcdh15 and Sans in Ush1c knockout mice. Int J Exp Path 2011; 92:66-71.

Yang J, Liu X, Zhao Y, Adamian M, Pawlyk B, Sun X, McMillan DR, Liberman MC, Li T. Ablation of Whirlin long isoform disrupts the USH2 protein complex and causes vision and hearing loss. PLOS genetics 2010; 6:e1000955.

Young JE, Vogt T, Gross KW, Khani SC. A short, highly active photoreceptor-specific enhancer/ promoter region upstream of the human rhodopsin kinase gene. Invest Ophthalmol Vis Sci 2003; 44:4076-85.

Zahs K and Esguerra M. In: Sernagor E, Eglen S, Harris B and Wong R (eds) Retinal development. Cambridge University Press, New York, 2006, pp 172-192.

Zallocchi M, Meehan DT, Delimont D, Askew C, Garige S, Gratton MA, Rothermund-Franklin CA, Cosgrove D. Localization and expression of clarin-1, the Clrn1 gene product, in auditory hair cells and photoreceptors. Hear Res 2009; 255:109-20.

Zheng QY, Yan D, Ouyang XM, Du LL, Yu H, Chang B, Johnson KR, Liu XZ. Digenic inheritance of deafness caused by mutations in genes encoding cadherin 23 and protocadherin 15 in mice and humans. Hum Mol Genet 2005; 14:103-11.

Zina ZB, Masmoudi S, Ayadi H, Chaker F, Ghorbel AM, Drira M, Petit C. From DFNB2 to Usher syndrome: variable expressivity of the same disease. Am J Med Genet 2001; 101:181-3.